THE IDENTIFICATION AND CHARACTERIZATION OF MKRP, A NOVEL KELCH RELATED PROTIEN

APPROVED BY SUPERVISORY COMMITTEE

Dr. Harold Garner

_____

Dr. Daniel Garry

_____

Dr. Robert Hammer

_____

Dr. Thomas Kodadek

_____

ACKNOWLEDGEMENTS

This work would not have been possible without the support and patience of my mentor, Dr. Daniel Garry, and the other members of the Garry lab. I would first like to thank Dr. Arianna Capriolli, Sean Goetsch, Teresa Gallardo, and Nan Jiang for teaching me the experimental techniques used in the work presented in this dissertation. I would also like to thank those individuals, and all my professors here at Southwestern for helping to develop my ability to analyze experimental data critically and my ability to design experiments to investigate specific aims.

I would like the thank the members of my committee, Dr. Harold Garner, Dr. Robert Hammer, and Dr. Thomas Kodadek for their guidance, support, and encouragement. Specifically, I would like to acknowledge Dr. Garner for his help in designing the original siRNA oligos, and for the assistance of Dr. Cristi Galindo with interpretation of the microarray data.

THE IDENTIFICATION AND CHARACTERIZATION OF MKRP, A NOVEL KELCH RELATED PROTIEN

by

LAURENCE J. EMBREE

DISSERTATION

Presented to the faculty of the Graduate School of Biomedical Sciences

The university of Texas Southwestern Medical Center at Dallas

In Partial fulfillment of the Requirements

For the Degree of

DOCTOR OF PHILOSOPHY

The University of Texas Southwestern Medical Center at Dallas

Dallas, Texas

December 2007

THE IDENTIFICATION AND CHARACTERIZATION OF MKRP, A NOVEL KELCH RELATED PROTIEN

Publication No. _____

Laurence J. Embree Ph.D.

The University of Texas Southwestern Medical Center at Dallas, 2007

Supervising Professor: Dr. Daniel J Garry M.D. Ph.D.

The cells of adult myofibers in mammals are terminally differentiated and are incapable of division and self-renewal. Regeneration of damaged skeletal muscle tissue is facilitated through the proliferation and differentiation of resident stem cells known as satellite cells . These satellite cells remain quiescent in uninjured tissue, occupying a sublaminar position between the sarcolemma and basal lamina of adult myofibers. In response to trauma, these cells become activated, and proliferate. The activated cells will reestablish the pool of resident quiescent satellite cells, while others will proliferate, migrate by chemotaxis to the area of injury, withdraw from the cell cycle, and differentiate into new myoblasts. These myoblasts will fuse with and repair the injured fibers, or align with each other and fuse to form new fibers. Genes involved in this process should exhibit

an altered pattern of expression in skeletal muscle in response to injury by cardiotoxin, and the changes in expression level can be quantified though the measurement of mRNA levels at specified time points following injury. Utilizing transcriptome analysis, we identified a completely novel transcript that is induced in the myogenic progenitor cells following cardiotoxin injury.

The novel transcript contained an open reading frame that coded for a protein belonging to the Kelch superfamily. Expression of the transcript was restricted to skeletal muscle lineages during development, and to myogenic progenitor cells and immature myotubes during injury regeneration. Because of its structural identity and restriction to skeletal muscle, the novel transcript was named the myogenic Kelch related protein (MKRP). Knockdown of MKRP expression using siRNA in C2C12 cells revealed an inhibition of both migration and differentiation in myogenic progenitor cells. A yeast two-hybrid screen identified calsarcin-2 as a potential interacting protein, indicating a possible role for MKRP in the calcineurin pathway during myogenic differentiation.

TABLE OF CONTENTS

PRIOR PUBLICATIONS

Goetsch SC, Martin CM, **Embree LJ,** Garry DJ. Myogenic progenitor cells express filamin C in developing and regenerating skeletal muscle. Stem Cells Dev. 2005 Apr;14(2):181-7.

LIST OF FIGURES

LIST OF TABLES

A historical perspective of regeneration

The study of mammalian skeletal muscle fibers and their ability to regenerate probably began with the earliest observations of Anton von Leeuwenhoek. Leeuwenhoek, whom many consider to be the father of microbiology because of his microscopic studies on a wide variety of subjects, was the first to identify the banded pattern of skeletal muscle in 1682, and was the first to observe that individual fibers were the same size across several different species, including mice, oxen, and whales (Schierbeek, 1953). Von Leeuwenhoek's microscopes were all made by hand, and were capable of magnifying objects up to 500 times, a truly remarkable accomplishment in that age. However, it would require the power of a transmission electron microscope for Alexander Mauro to identify the cell population responsible for muscle regeneration in mammals, almost 300 years after von Leeuwenhoek's initial observations (Mauro, 1961).

Other organisms are capable of much more extensive regeneration than mammals. One of the organisms von Leeuwenhoek observed when he turned his microscopes to samples of algae filled water was the Cnidarian Hydra, a microscopic organism capable of complete regeneration after losing a large

percentage of its body. When split precisely in half, a hydra is capable of regenerating fully, producing two separate and distinct but identical organisms. No vertebrate animals possess the ability to regenerate to this degree (Gierer, 1972). However, urodele amphibians are capable of regenerating completely amputated appendages (Thornton, 1968; Iten and Bryant, 1973).

This capability was first observed and studied by Lazzaro Spallanzani in 1768, and later investigators demonstrated that newts and salamanders were also capable of regenerating lost portions of their jaw, eye (lens and retina), and even signifigant portions of their heart, in addition to completely regenerating lost appendages and tails (Wolpert, 1971). Unlike mammals, the cells of these amphibians are able to dedifferentiate and return to the cell cycle to restore the lost tissue (Lo, 1993).

The process of amphibian regeneration begins with the migration of epithelial cells to cover the wound, or the formation of a clot in the case of injury to the heart. Wounds can be completely closed within two hours after amputation. The rate of closure, and the genes expressed in the early stages of wound healing are the same regardless of whether the injury involves amputation, or is merely a lateral wound. A lateral wound will close without scarring, while an amputated limb will proceed to the next stage of dedifferentiation and the outgrowth of the limb bud (Lo, 1993).

In 1993 Jeremy Brockes demonstrated that limb regeneration in amphibians required the dedifferentiation of cells adjacent to the wound, and their reentry into the cell cycle (Lo, 1993). These dedifferentiated cells proliferate and then differentiate to form new tissues. Brockes labeled cultured newt myotubes with rhodamine-dextran, a lineage tracer, and then implanted the labeled tubes beneath the wound epidermis of injured subject animals. Within a week, mononucleated labeled cells appeared in the wound area, indicating that the implanted myotoubes had dedifferentiated (Lo, 1993). The number of labeled mononucleated cells increased significantly in the following 2 weeks, indicating that the implanted cells had not only dedifferentiated, they had begun to proliferate to regenerate the amputated limb. In 2001 Karen Echeverri would use Nomarski imaging to demonstrate that labeled myotubes dedifferentiated, proliferated, and contributed to the development of the blastema, *in vivo (*Echeverri, 2001). The blastema is a mass of dedifferentiated cells, from which the regenerated limb will eventually grow.

Brockes also demonstrated that for myotubes, re-entry into the cell cycle requires phosphorylation of the retinoblastoma protein, in the presence of thrombin and serum (Tanaka, 1998). In this series of experiments, Brockes showed that serum treated with thrombin produced a ligand that acted on the urodele myotubes to return them to the cell cycle. Later experiments by Jay Schneider showed that mouse myotubes that lacked a functional retinoblastoma gene were also able to return to S-phase (Schneider, 1994).

For many years it was unknown if adult amphibian regeneration was accomplished solely by cells which had dedifferentiated from existing tissues, or if regeneration also involved a resident stem cell population and other undifferentiated cells. Andras Simon may have answered this question when he identified a population of multipotent cells that expressed Pax7, and resided within the skeletal muscle of a salamander limb (Morrison, 2006). By costaining with Pax7 and phosphorylated histone 3 (H3P) antibodies, Simon identified a population of cells residing below the basement membrane of the salamanders muscle fibers and that were restricted to skeletal muscle. These cells were quiescent in uninjured tissue, but began to express H3P after injury, indicating that they had reentered the cell cycle. After isolating this cell population and growing them in culture, Simon demonstrated that these cells could adopt adipogenic or osteogenic fates, when cultured in adipogenic or osteogenic media (Morrison, 2006). Finally, labeled satellite cells were injected into a subject's muscle prior to amputation. Labeled cells were detected within the blastema at every stage of regeneration, and in regenerated limbs, BrdU labeled cells were found not only in skeletal muscle, but also in the epidermis and cartilage as well, indicating that these cells were capable of forming multiple tissues during regeneration (Morrison, 2006).

Satellite cells were first identified by Alexander Mauro, in 1961, as he used an electron microscope to study the muscle fibers of a frog (Mauro, 1961). This was

significant because frogs did not display the same type of regenerative capacity as the urodele amphibians. Mauro observed a population of cells with very little cytoplasm, located between the basal lamina and basement membrane of the muscle fibers. Mauro noted that these cells were almost impossible to identify with a light microscope, because of their size and lack of cytoplasmic contents, giving them the appearance of a peripheral myotube nucleus. Later studies would also identify satellite cells in mammals (Mauro, 1961; Muir, Kanji, Allbrook, 1965).

Prior to Mauro's discovery, there was some debate over the extent to which adult mammalian skeletal muscle was able to regenerate, at all. Despite studies by Paul Clark (1946) and Gabriel Godman (1957) in the United States, and Anton Studitsky in the Soviet Union (1952-1959), reported in the U.S. by Bruce Carlson, (in 1968) many still did not believe in the possibility of regeneration by a resident stem cell population.

Studitsky's lab pioneered the minced muscle regeneration model, in which skeletal muscle was surgically removed from experimental animals (birds and rats in the earliest experiments) and then minced into small fragments and reimplanted into the site they had been excised from (Carlson, 1968). Studitsky observed that new muscle was able to form from the mince. This technique was later used by Bruce Carlson to demonstrate that regeneration in amphibians occurred by two pathways, one of which was independent of the formation of a

blastema, and that amphibians that were incapable of regeneration through the dedifferentiation of cells and formation of a blastema, such as frogs, were still capable of regenerating damaged muscle tissue (Carlson, 1975).

Prior to these studies, and the identification of satellite cells, many held the belief that regeneration could only occur through the epimorphic pathway. Epimorphic regeneration refers to the dedifferentiation of cells, and the formation of the blastema. Mauro's discovery in 1961 opened up new lines of research and inquiry, as well as a vigorous debate over the mechanisms of regeneration in mammals and other vertebrates. In 1970, Bruce Carlson demonstrated that formation of the blastema was independent of the musculature of the stump. To demonstrate this, Carlson used a series of experiments wherein the upper arm musculature of an axolotl was removed surgically, and then the limb was amputated through the site of muscle excision (Carlson, 1970). The excised upper arm muscle was either minced and reimplanted, or intentionally excluded. In both cases, the blastema formed normally, and regeneration below the excision site was complete, but the excised upper arm muscle only regenerated in the animals where the minced muscle had been reimplanted. This demonstrated that morphogenesis of the blastema and the epimorphically regenerated limb is independent of the mechanism of skeletal muscle regeneration (Carlson, 1970).

More compelling evidence of the role of satellite cells in tissue regeneration came from researchers working with mammals. In 1975 Carlson used the minced muscle model to demonstrate that a migrating factor was necessary for regeneration. By enclosing the muscle within a filter prior to reimplantation, Carlson demonstrated that regeneration did not occur when cells from inside the filter were unable to migrate outward (Carlson 1975). Mikel Snow followed these experiments in 1977 by labeling either satellite cells or myotube nuclei with 3H-thymidine prior to injury, and then analyzing the regenerating tissue after injury (Snow 1977). He found that after injury, nuclei from labeled satellite cells were found in regenerating myotubes.

Carlson would follow his experiments with minced muscle by grafting entire, intact muscles into the bed of another muscle. Although grafting and transplantation experiments had been performed since the early 1800's this was the first time they were used to evaluate the mechanism of skeletal muscle regeneration. What Carlson found in his experiments was the first suggestion of how important neural innervation of the muscle tissue was, for regeneration.

In Carlson's experiments, the soleus and extensor digitorus longus (EDL) muscles of rats were removed and then regrafted to the animal's contralateral leg (Carlson 1983). Half the muscle specimens were denervated for 14 days prior to reimplantation, and half were untreated. His experiments showed rapid degradation in the denervated muscle, but more rapid regeneration, accelerated

differentiation, and a higher survival rate for original myofibers (Carlson, 1983). If denervated regenerating muscle is not reinnervated, however, it will atrophy or undergo apoptosis. Also, the reinnervating nerves will determine the newly regenerated muscles fiber type. When Carlson grafted a rat's soleus muscle into the space of the EDL, and vice versa, the fast twitch EDL and slow twitch soleus were innervated by nerves of the opposite fiber type, and in response the newly regenerated fibers change their functional type.

Once studies had established the requirement of a migratory factor in the mechanism of skeletal muscle regeneration, researchers began the task of attempting to identify the cell type or types that are capable of contributing to regeneration. Studies that followed Mauro's discovery of the satellite cell suggested that other cell types, including bone marrow derived cells (BMCs) and purified hematopoetic stem cells (HSCs), are capable of contributing to the regeneration of skeletal muscle following injury (Bittner, 1999. Labarge, 2002. Camargo, 2003.). These cell types are primarily found in bone marrow, but are also constitutively present in the bloodstream at low levels, and this circulating population of cells is readily accessible for participation in the regeneration of injured tissue.

Studies investigating the contribution of circulating cells to the regeneration of injured skeletal muscle have employed various strategies, but the most recent studies involved the injection of unfractionated bone marrow or purified HSCs

extracted from β-actin/GFP-expressing donor animals, into irradiated mice that lacked endogenous bone marrow derived cells (Sherwood, 2004). After injury, donor cells that were incorporated into regenerating myofibers were visualized with flourescence microscopy. Results of the study demonstrated that both BMCs and HSCs are able to contribute donor cells to regenerating myofibers, but only after injury, and the rate of incorporation varied depending on the muscle, and fiber type (Sherwood, 2004). By repeating the experiment with transgenic mice expressing HcRed under the β-actin promoter, the researchers were also able to establish that the injected circulating cells were able to fuse with existing myofibers. Endogenous fibers that fused with injected cells expressed both HcRed, and GFP, and 100% of the fibers that expressed GFP also expressed HcRed, indicating that the circulating cells had fused with existing fibers, and not formed new fibers (Sherwood, 2004).

The phenomenon of regeneration by a living organism has captured the imagination and scrutiny of the worlds leading intellectuals and scientists since the 18th century. More importantly, their investigations into the possible mechanisms of this phenomenon began the movement away from a descriptive view of the world and our surroundings, and into an era of experimental investigation, particularly in biology. Since those original observations, some level of regenerative capacity has been demonstrated in all animal phyla, and in a diverse variety of tissue types. Different organisms have displayed multiple pathways through which regeneration is facilitated, including the dedifferentiation

or transdifferentiation of of existing tissues, as well as the contribution of a variety of adult stem cells. Although many of the mechanisms by which mammals and other organisms are able to repair and regenerate injured tissues and organs remain undefined, the initial observations of von Leeuwenhoek began the long process by which those puzzles might be solved. The answers to these questions will not only increase our knowledge of regenerative biology, but will also provide insights into possible direct applications in the treatment of disease and injury.

The role of satellite cells in development and response to injury

Injury regeneration in adult mammalian skeletal muscle is facilitated by a resident population of undifferentiated, mononuclear myogenic progenitor cells, known as satellite cells. Satellite cells were first identified in amphibian skeletal muscle and have also been described in mammalian (Muir, 1965) reptilian and avian (Armand, 1983) muscle tissue. In mouse embryos, satellite cells first appear in the limb buds at approximately E17.5. Satellite cells were first identified by Alexander Mauro in 1961 (Figure 1). These cells were identified primarily by their morphological characteristics. When quiescent, satellite cells occupy a sublaminar position between the basal lamina and sarcolemma, surrounding individual muscle fibers. Quiescent satellite cells are small, with very little cytoplasm, or cytoplasmic organelles. The nucleus of satellite cells is smaller than the nucleus of a myofiber, with increased amounts of heterochromatin, indicating that they are less active, transcriptionally. Satellite cells can also be identified immunohistochemically by staining for markers such as Pax7, c-Met, Foxk1, M-cadherin, and Cd34.

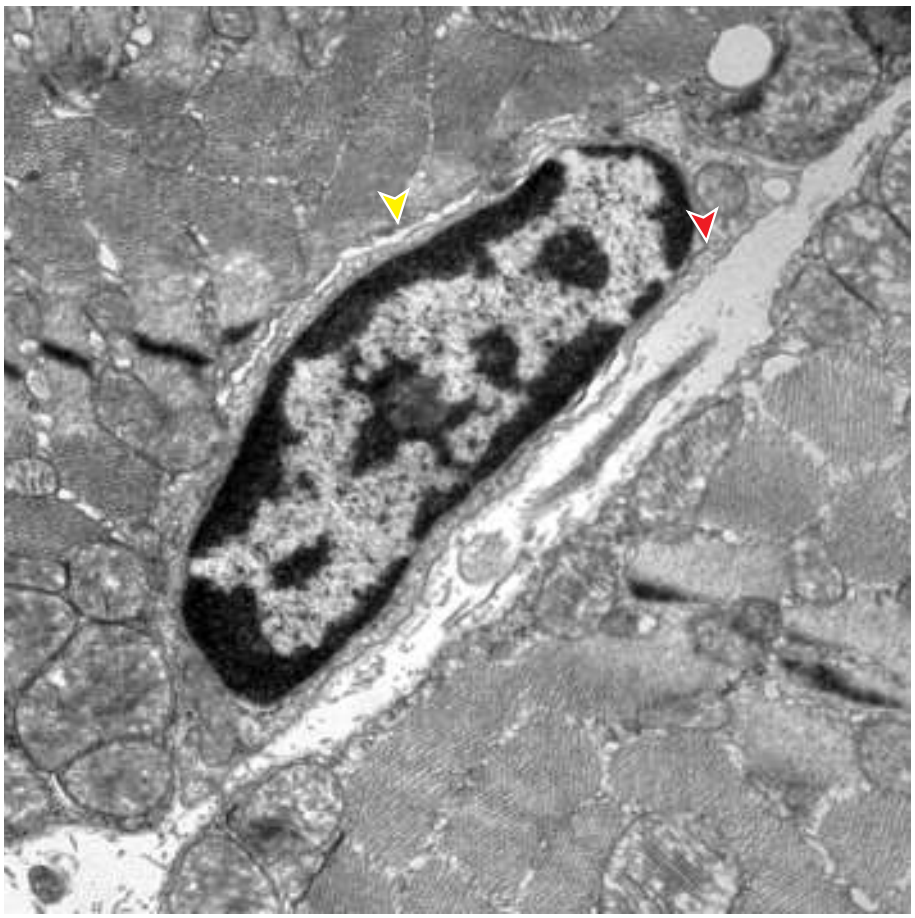

Figure 1.1 Identification of the satellite cell. The satellite cell was first identified by electron microscopy, by Andrew Mauro in 1961, This picture, taken in 2006, shows a satellite cell in its distinctive niche, located between the sarcolemma (yellow arrowhead) and the basal lamina (red arrowhead).

c-Met is a tyrosine kinase receptor that is expressed in several tissues during embryogenesis (Andermarcher, 1996). During gastrulation, c-Met and its ligand, hepatocyte growth factor (Hgf), are expressed in both the mesodermal and endodermal layers, but are absent from the ectoderm. During organogenesis, both genes are expressed in the developing heart, neural crest, and somites. Studies have demonstrated that c-Met/Hgf signaling is essential for the migration

of myogenic precursor cells from the somites to the developing limb buds (Bladt, 1995).

Although c-Met is expressed in several adult tissues, including the lung and liver, its expression in adult skeletal muscle is restricted to the satellite cell population (Andermarcher, 1996; Cornelison, 1997). Satellite cells grown in culture showed a significant increase in the rate of proliferation after treatment with exogenous Hgf (Allen, 1995). A study using multiplex single-cell RT-PCR found c-Met expression in 100% of satellite cells grown in culture from isolated myofibers, establishing c-Met as a viable marker for identification of satellite cells (Cornelison 1997). The same study demonstrated that prior to activation, M-cadherin was expressed in 20% of cells that were positive for c-Met. After activation, this number steadily increased until at 96 hours post activation (Figure 2), 100% of c-Met positive cells were also expressing M-cadherin (Cornelison, 1997).

Other markers, such as Desmin and MyoD, can identify proliferating satellite cells, but are absent in quiescent cells. Identification is also possible by staining the basal lamina and sarcolemma with laminin and dystrophin, respectively, and visualizing the cells with light microscopy.

There are currently four competing hypotheses regarding the origin of satellite cells during embryonic development. The first hypothesis involves a somitic

origin for satellite cells, and is supported by transplantation studies performed with quail and chicks (Armand, 1983). Somites from quail embryos were transplanted into chick embryos, and the chicks were allowed to develop. Cells from the implanted somites were found in the limbs of the developing chick, both in multinucleated myofibers, and satellite cells. The somitic origin theory is supported by more recent experiments that used lineage tracing to demonstrate that avian and mouse myogenic progenitor cells were derived from the central dermal myotome. The same study showed that cells occupying the satellite cell position and that express Pax7 in avian neonates which were derived from the dermal myotome (Gros, 2005).

The second hypothesis proposes an endothelial origin for satellite cells. This theory originates from studies that showed that cells expressing myogenic markers would sometimes appear in tissue that were not derived from somites. Specifically, one study (De Angelis, 1999) isolated clonable myogenic cells from the dorsal aorta of mouse embryos. These cells expressed myogenic and endothelial markers, and were morphologically very similar to satellite cells (Figure 3). The same study demonstrated that it was possible to clone myogenic cells from the limbs of c-Met-/- mice. These mutant mice had normal vasculature, but lacked appendicular muscles. After transplantation, these cloned cells were shown to fuse with endogenous satellite cells and participated in muscle regeneration and growth after injury. These studies suggest the possibility of a multipotent cell type within embryonic vasculature tissue. The

authors of the study suggested that this multipotent cell line may differentiate into the tissue that the vascular tissue perfuses, and could be the source of satellite cells in skeletal muscle.

It has also been demonstrated that bone marrow derived cells are capable of contributing to the repair of skeletal muscle injury. Initial studies used bone marrow from a transgenic mouse line, injected into chemically injured skeletal muscle (Ferrari, 1998). Immunohistochemical staining of muscle sections after regeneration showed that nuclei from the transgenic bone marrow cells had been incorporated into repaired fibers.

Further research, in which radiation was used to remove the endogenous population of satellite cells (Heslop, 2000), showed a distinct progression of bone marrow derived cells giving rise to a new satellite cell population that were capable of participating in muscle regeneration, after injury. In this study, 10 day old mice that had undergone total body irradiation received bone marrow cells from GFP+ transgenic mice, by tail vein injection. These mice were sacrificed and dissected at specific time points from two to six months post irradiation. Isolated myofibers from the TA muscle were analyzed immunohistochemically, using confocal microscopy. GFP positive cells were clearly shown occupying the same sublaminar position as that used to identify satellite cells. Sections of tissue were also stained with ToPro to mark the nucleus in myofibers, and with an antibody for the transcription factor Myf-5. Myf-5 is a member of the basic

Helix-loop-Helix family of transcription factors, and is expressed in the early stages of satellite cell differentiation (Cossu, 1996). Colocalization of GFP with ToPro and Myf-5 signal indicated that the transplanted bone marrow cells had occupied the satellite cell niche, and begun to express the myogenic gene program. GFP positive satellite cells that were isolated from dissected tissues and grown in culture continued to express muscle specific genes, including Desmin, c-Met, Myf-5, and α7-integrin, indicating that the myogenic phenotype was stable and passed on to subsequent generations as the satellite cells proliferated (Heslop, 2000).

Isolated GFP positive myoblasts from these experiments were able to form myotubes when grown in low-serum media in culture. To demonstrate that these bone marrow-derived cells could also participate in myotube formation *in vivo*, GFP+ cells were injected into the TA muscle of a group of mice, and one week later those mice were sacrificed. Dissection revealed that GFP+ fibers had been incorporated into the TA muscle (Heslop, 2000). A separate experiment, in which the mice were given an exercise wheel for six months post-transplantation, showed a 20-fold increase in the number of GFP+ positive myofibers, indicating that bone marrow derived satellite cells were able to contribute to regenerating fibers, following exercise induced damage (Heslop, 2000).

Recent studies have attempted to further define the role of bone marrow's contribution to skeletal muscle by comparing the contribution of labeled

hematopoietic stem cells (HSCs) to unfractionated bone marrow, transplanted into injured skeletal muscle (Sherwood, 2003). In these studies, irradiated mice were transplanted with either purified HSCs, or unfractionated bone marrow cells isolated from mice that expressed GFP under the control of a β-actin promoter, and then injured (Sherwood, 2003). Injuries were performed by either cardiotoxin injection or by crush injury, to the triceps surae (TS) or tibialis anterior (TA) muscle, and tissue sections were harvested 8 weeks after injury. Frozen sections were stained with antibodies to GFP, dystrophin, α-actinin, myosin, or the hematopoetic marker CD45. Expression of GFP and the muscle specific markers, in cells that did not express CD45, was used to identify the contribution of transplanted BM or HSC cells to muscle tissue. Tissue samples were harvested from both injured and uninjured animals. However, no GFP+ myofibers were observed in muscle sections taken from uninjured mice transplanted with either unfractionated bone marrow, or purified HSCs. GFP+ cells were observed in both TA and TS muscle sections after both crush and cardiotoxin induced injuries. The method of injury used, and the number of injuries performed on a single animal did not appear to significantly affect the rate of incorporation of GFP+ cells in animals transplanted with unfractionated BM, but animals transplanted with HSCs demonstrated a higher rated of GFP incorporation after multiple injury.

To identify the hematopoetic fraction that is capable of contributing to regenerating muscle fibers after injury, researchers used fluorescence-activated

cell sorting (FACS) analysis to isolate specific hematopoetic derivatives for intramuscular transplantation (Dyonnas, 2004). In these studies, bone marrow, peripheral blood and skeletal muscle cells were isolated from GFP+ mice, and stained with antibodies for CD11b, CD45, CD31, CD34, c-kit, IL7R, Gr1, and Sca-1, and sorted by FACS analysis into five distinct fractions, and then injected directly into injured skeletal muscle. Cell fractions were separated based on their expression of myeloid or lymphoid progenitor markers, and the presence of HSCs or committed precursor cells. After regeneration, tissues were harvested four weeks after injection, and GFP+ myofibers were observed only in muscle sections that had been transplanted with HSCs or myeloid progenitors, as identified by their expression of c-kit, Sca-1, CD31 and CD34. Lymphoid progenitor cells and mature cells from lymphoid and myeloid lineages, identified by their expression of CD11b, GR1, and IL7R, did not incorporate into regenerating muscle fibers.

A fourth possible origin for satellite cells was first encountered during a study using bone marrow transplantation to restore dystrophin expression in mice with Duchenne's muscular dystrophy (Gussoni, 1999). The authors of this study used Hoechst 3342 staining and FACS analysis to separate HSCs from bone marrow for their transplantations, and then used a similar technique to identify a population of cells within skeletal muscle that shared several physical characteristics with HSCs.

After isolating mononuclear cells from juvenile (3-5 weeks) mouse skeletal muscle, these cells were stained with H03342 and sorted by FACS analysis. FACS sorting separated a side population (SP) of cells that stained weakly with H03342, from a main population (MP) that demonstrated strong staining. Treatment of cells with verapamil, a drug that inhibits the efflux of Hoechst dye, resulted in the disappearance of SP cells from the FACS sorting profile, similar to the effect of verapamil on HSC cells. Main population cells were unaffected by verapamil treatment. Muscle SP cells also demonstrated an expression profile distinct from both muscle MP cells, and bone marrow SP cells. Both muscle and bone marrow SP cells expressed Sca-1, however muscle SP cells did not express c-kit, CD45, or CD43, three markers present on bone marrow SP cells. Muscle MP cells expressed CD43, CD11, and Gr1, all of which were absent in muscle SP cells. Muscle SP cells were also morphologically distinct from muscle MP cells, when grown in culture (Gussoni, 1999). MP cells adhered to the culture dish immediately, and differentiated to myoblasts within a week. SP cells, conversely, failed to adhere to the plate, and did not differentiate for 2 weeks, at which point they produced a mixture of myoblasts and fibroblasts.

To investigate the ability of muscle SP cells to participate in muscle regeneration, SP cells isolated from male C57BL/10 mice were injected into the tail veins of lethally irradiated female *mdx* mice (Gussoni, 1999). Animals were sacrificed at 30 days post-injection, and cells analyzed by fluorescence *in situ* hybridization (FISH) to detect engraftment of donor cells. Cells positive for the Y chromosome

were found in both the bone marrow and spleen of the irradiated mice, indicating that muscle SP cells were capable of repopulating the haematopoeitic compartment of irradiated subjects (Gussoni, 1999). FISH and immunohistochemical analysis of skeletal muscle tissue sections identified nuclei from donor cells in dystrophin expressing myofibers (Figure 4). Donor nuclei were also identified in a position peripheral to, but not fused with, myofibers, occupying locations similar to the niche populated by satellite cells. These results indicate the existence of a population of adult stem cells resident in muscle tissue, capable of adopting a myogenic fate, and occupying the same niche populated by satellite cells.

Even though there may still be some questions regarding the origin of satellite cells, one gene playing a key role in the maintenance of the population of satellite cell fate has been identified as Pax7 (Seale, 2000). Pax7 is a transcription factor from the Paired Box family, and is closely related to Pax3. Expression of Pax7 and Pax3 overlaps during embryonic development (Jostes 1990). Pax7 is expressed in both proliferating and quiescent satellite cells, but is downregulated sharply at the onset of differentiation. Centrally nucleated cells within existing myofibers also express Pax7, indicating that satellite cells that have recently fused with existing myofibers still express the gene. In adult tissues, Pax7 expression is restricted to skeletal muscle.

Pax7-/- mutant mice are viable and appear normal at birth, but do not develop, postnatally, usually dying within 2 weeks of birth (Mansouri, 1996). Mutant

Pax7-/- mice are 50% smaller than their wild-type littermates 7 days after birth, and dissection shows a marked decrease in skeletal muscle fiber size, although no significant difference in the number of fibers. Also, the skeletal muscle fibers of Pax7-/- mutants are devoid of satellite cells. Cultures of primary cells taken from mutant skeletal muscle failed to produce myoblasts. Taken together, these data strongly suggest a key role for Pax7 in the production of satellite cells.

During embryogenesis, Pax3 and Pax1 serve as markers for the formation of the somites, segmented epithelial structures from which the vertebrate skeleton and skeletal muscle arise (Brand-Saberi, 1993). Somites are derived from the mesodermal layer, which is divided into four segments, the lateral, axial, paraxial and intermediate mesoderm. Somites are formed from the paraxial mesoderm, in bilateral, symmetric pairs on each side of the neural tube. Myogenic precursor cells migrate into the limb buds from the hypaxial segment of the somites, while the muscles of the back arise from the epaxial segment, which lies alongside the neural tube (Gamel, 1995). Myogenic progenitor cells separate from the epithelium of the somites and migrate into the limb buds.

As previously noted, the migration of myogenic progenitor cells from the somites into the limb buds requires the functional interaction of c-met and its ligand, HGF. Studies have demonstrated that myogenic precursor cells only delaminate from the somites when in proximity to cells expressing HGF (Dietrich, 1999) and that

HGF is also expressed by cells along the route of migration into the limb buds. Mutant mice that lack functional c-Met or HGF genes do not form muscles of the limbs during embryogenesis (Bladt, 1995).

Pax3 is a transcriptional activator of c-Met (Epstein, 1996), and was expressed normally in mutant mice lacking c-Met and HGF, but cells expressing Pax3 failed to migrate in the mutant embryos, as they did in the wild-type embryos. Instead the Pax3 expressing cells attached to adjacent somites, creating a connection between the previously segregated structures.

Migrating precursor cells also express the homeobox gene Lbx1, and myogenic precursor cells in mutant mice lacking Lbx1 migrate less efficiently (Brohmann, 2000). Mutant embryos lacking c-Met or HGF also expressed Lbx1 in the somites at day E10.5, but Lbx1 expressing cells failed to delaminate from the somites (Dietrich, 1999). The expression of both Pax3 and Lbx1 indicated that precursor cells were specified in c-Met and HGF mutant embryos, but were unable to migrate.

Expression of Lbx1 was used as a marker for migrating cells in *in situ* hybridization studies comparing the localization of cells in wild-type and c-Met mutant embryos (Dietrich, 1999). These studies showed that Lbx1 expressing cells co-localized with HGF expressing cells in wild-type embryos, along migratory pathways leading from the occipital somites to the tongue, and from

the cervical somites to the diaphragm. In embryos mutant for c-Met there was similar expression of Lbx1 in the dermomyotome at day E10.5, but Lbx1 cells did not migrate outward. HGF was expressed in the same spatial pattern in both wild-type and c-Met-/- embryos, but Lbx1 expressing cells failed to colocalize with HGF expressing cells in the c-Met-/- embryos (Dietrich, 1999).

Unlike the c-Met mutants, myogenic precursor cells in mutant mice that did not express Lbx1 were able to delaminate from the somite, but failed to migrate (Schafer and Braun 1999). These mice lacked forelimb musculature, but development of skeletal muscle in the tongue and diaphragm appeared unaffected. Myogenic progenitor cells that were unable to migrate to the limb buds would adopt other fates, or underwent apoptotic cell death.

Embryos lacking Pax3, the transcriptional activator of c-Met, also fail to develop limb muscles, and precursor cells fail to separate from the somites. In most cases the Pax3 mutation is lethal in embryogenesis, but surviving neonates are born without limb muscles (Bober, 1994). Embryos expressing a constitutively active Pax3 gene produced greater numbers of myogenic precursor cells.

Recent studies involving the disruption of the Pax3 locus have shown that most functions of this gene, with the exception of skeletal muscle development, can be replaced by its paralog, Pax7 (Relaix, 2004). Using a gene targeting strategy to splice out the Pax3 gene, and replace it with Pax7, the study authors

demonstrated that neural crest development and somitogenesis proceeded normally in the development of mutant mice, including somite segmentation and the development of hypaxial dermomyotome (Relaix, 2004). However, mutant mice in which Pax3 was replaced by Pax7 developed no limb muscles, indicating that myogenic precursor cells were unable to migrate to the limb buds in these mice, and that Pax7 is inadequate to replace the function of Pax3 in limb musculature development (Relaix, 2004). Mutant mice lacking Pax7 showed no limb muscle defects (Mansouri, 1996).

Migrating precursor cells do not express the myogenic determination gene program until they reach their destination, and studies have shown that these migrating cells can differentiate into other lineages in the absence of transcription factors MyoD and Myf5 (Kablar, 1999.) The genetic program that drives determination of precursor cells into the myogenic fate is controlled by members of the basic-helix-loop-helix (bHLH) family of transcription factors, including MyoD and Myf5, as well as myogenin (Myf4) and Myf6 (Mrf4). These transcription factors often form heterodimeric DNA-binding complexes with other bHLH proteins, and regulate a cascade of genes during embryogenesis and muscle regeneration. Binding partners for MyoD include members of the E2 gene family, including E47 and E12. The interaction of MyoD and E47 was first demonstrated in a mobility shift assay that identified complexes of MyoD and E47 bound to the MEF1 binding site (Lassar and Weintraub, 1991). In that same

study, co-transfection of MyoD and E47 was shown to synergistically enhance expression of a reporter gene that contained a MyoD binding site. MyoD and Myogenin both form complexes with E12, and these complexes have been shown to bind to the canonical E-box DNA sequence, CANNTG (Braun, 1991).

Gene disruption strategies have demonstrated that expression of MyoD and Myf5 occurs independently of each other during embryogenesis. Induction of either MyoD or Myf5 is sufficient to initiate the myogenic gene program in myoblasts (Rudnicki 1992, Braun 1992), and expression of MyoD in other cell types can induce the production of muscle specific proteins (Weintraub, 1989). Both genes are downregulated at the onset of differentiation.

Mice lacking Myf5 develop their limb muscles normally, but development of the intercostal muscles is delayed until the initiation of MyoD expression (Braun, 1994). In mice lacking MyoD, Myf5 expression remains elevated past E12, when it would normally be downregulated (Rudnicki, 1992). In MyoD-/- mice the trunk and intercostal muscles develop at the same rate as their wild-type littermates (Kablar, 1997), but development of the limb musculature is delayed. During embryogenesis, Myf5 expression is first observed in the dorsal-medial segment of the dermomyotome, in cells that will form the epaxial muscles. MyoD expression occurs initially in the ventral-lateral segment of the dermomyotome, in cells that will give rise to the hypaxial muscles. Mice lacking either MyoD or Myf5 were viable and developed normal muscle structure, although development was

delayed. Mice lacking both genes, however, were born without skeletal muscle, and died soon after birth (Rudnicki, 1993). These data suggest the possibility of redundant functions between MyoD and Myf5.

Mutant mice lacking MyoD and Myf5 were bred with transgenic mice carrying a construct that attached the MyoD promoter region to LacZ (Kablar, 1999). *In situ* hybridization analysis showed Pax3 expressing cells migrating to the limb buds in embryos that lacked both MyoD and Myf5, and LacZ expression was observed in the somites and limb buds. Skeletal muscle was completely absent in embryos lacking MyoD and Myf5, but at day E11.5 LacZ expressing cells were observed in the vertebral, humeral and rib cartilage. These observations indicate that MyoD and Myf5 are not required for the migration of precursor cells, but are required for the determination of myoblasts, and that in the absence of these factors precursor cells remain multipotent and capable of adopting other fates.

Similar experiments using a LacZ reporter to investigate Myf5 expression has shown that Myf5 is the first gene of the basic-helix-loop-helix (bHLH) family expressed in the limb buds during embryogenesis (Tajbakshs and Buckingham, 1994). Myf5 expression was detected in the somites at E9.0, and in the forelimb buds at E9.5. MyoD and Myogenin (Myf4) are not detected in the limb buds until E11.5 (Buckingham, 1989). Cells expressing Myf5 and MyoD in the limb buds did not show expression of Myosin Heavy Chain (MHC), indicating that they had not yet begun terminal differentiation. These data indicate that MyoD and Myf5

may not be required for migration or differentiation of myoblasts, but may play a role in proliferation (Figure 2).

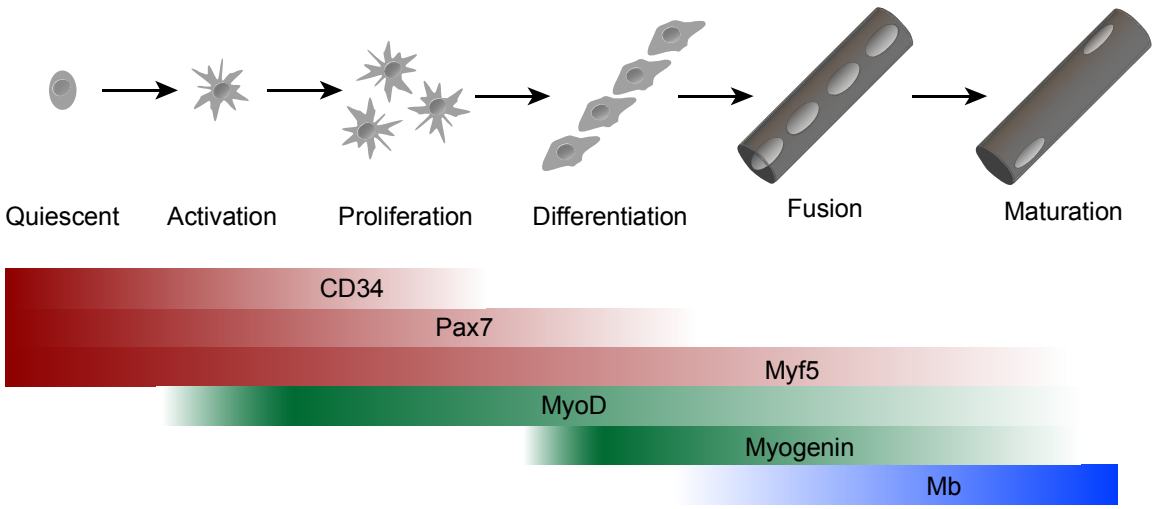

Figure 2. Schematic of the pathway of satellite cell myogenesis. Satellite cells are quiescent in uninjured skeletal muscle, but will activate in response to injury and begin to proliferate. A segment of the proliferating cells will return to quiescence to restablish the resident satellite cell pool, and the remainder will migrate to the site of injury and fuse with damaged fibers to repair the injury. Specifice marker can identify each stage, CD34 is present in quiescent satellite cells and is downregulated during proliferation. Pax7 is present in quiescent cells, bu expression drops prior to fusion. Myf5 is expressed in undifferentiated cells, but dissapears in mature myofibers. myogenin and myoglobin are absent in quiescent cells, but are upregulated at the onset of differentiation. Myoglobin expression is highest in mature myofibers.

Myod and Myf5 expression has been observed in proliferating undifferentiated myoblasts (Tapscott, 1988; Braun, 1989), and their possible role in the proliferation of myoblasts was first suggested by studies performed in mice that lacked dystrophin (mdx, Duchennes muscular dystrophy). Mdx mice were interbred with mice lacking MyoD, and the resulting progeny that lacked both dystrophin and MyoD showed a pronounced impairment in their capacity to

regenerate skeletal muscle after injury (Megeney, 1996), and a reduction in the proliferation of myogenic precursor cells. These animals also demonstrated severe cardiomyopathy (Megeney, 1999) and premature death, dying at approximately 1 year of age.

The homeo-box transcription factor msx1 has also been observed in migrating progenitor cells (Houzelstein, 1999), and may play a role in myoblast proliferation. Myoblasts transfected with an msx1 overexpression vector failed to form myotubes after serum withdrawal, and continued to proliferate (Song, 1992). Cells transfected with an empty vector, or an anti-sense msx1 construct resulted in growth arrest and the formation of myotubes when cultured in low serum conditions. Msx1 transfected cells failed to form myotubes, and did not express myosin heavy chain (MHC), a marker of differentiation. Mice injected subcutaneously with msx1 developed visible tumors at the injection site within 2.5 months. Expression of myoD was also downregulated in cells overexpressing msx1 (Song, 1992).

Additional studies demonstrated that Msx1 is capable of binding to the MyoD enhancer element (Woloshin, 1995), and that expression of a human MyoD construct was inhibited by over expression of Msx1, when co-transfected into 10T1/2 fibroblasts. These data strongly suggested a role for Msx1 as a negative regulator of MyoD (Woloshin, 1995). Mutant mouse embryos that lacked Msx1 demonstrated no visible phenotype in skeletal muscle (Satokata, 1994;

Houzelstein, 1997). However, the authors speculated that Msx2, which is co-expressed with Msx1 in several locations, could perform redundant functions in the mice lacking Msx1 (Houzelstein, 1997).

Many of the same regulatory factors that drive the embryonic development of skeletal muscle are also present in adult muscle. However, in adult tissue some studies have shown that Pax7 may have a more important role than its limited participation during embryogenesis. Researchers first observed by *in situ* hybridization analyses that Pax7 appeared to be expressed in proliferating satellite cells (Seale, 2000). They also observed that mutant mice deficient in Pax7 demonstrated postnatal growth defects and reduced lifespan, an indicator of a possible defect in satellite cell function (Mansouri, 1996). Pax7 mutant mice were significantly smaller than wild type littermates, and individual muscle fibers were smaller in diameter (Seale, 2000).

When primary cells were isolated from the skeletal muscle of 7-10 day old Pax7-/- mice, and wild type littermates, immunohistochemical staining with antibodies recognizing desmin and c-Met was used to identify myoblasts derived from satellite cells. Although desmin and c-Met immunohistochemically positive cells were abundant in the primary cells derived from wild-type animals, none were observed in the cultures isolated from Pax7-/- mice (Seale, 2000). The study authors further cultured isolated myofibers in media that promoted the proliferation and migration of satellite cells. Within 48 hours, clusters of desmin

positive staining cells were observed in the cultures of fibers obtained from wild type animals. However, no desmin positive cells and no single mononuclear cells were observed in cultures of fibers taken from Pax7-/- animals. Within 2 weeks, myotubes that stained positive for myosin heavy chain proteins were observed in the wild type cultures, but no myotubes ever formed in the Pax7-/- cultures. These observations would suggest that satellite cells were either completely absent, or present only in small number in Pax7-/- animals, and were unable to proliferate further. When researchers examined biopsies of gastrocnemius muscle taken from 7-10 day old Pax7-/- mutant mice and wild type littermates, satellite cells were readily identified in the wild type tissue by their characteristic position beneath the basal lamina, but no such cells were observed in the Pax7-/- tissue, another indication that mice lacking Pax7 may not be able to form satellite cells (Seale, 2000).

Muscle SP cells, identified by their ability to exclude Hoechst dye 33342 were observed in both wild type and Pax7-/- cell cultures. However, when these cells were grown in methylcellusoe media which promotes the formation of both myogenic and hematopoetic cells, the cells isolated from Pax7-/- animals were 10-fold more likely to adopt a hematopoetic fate, suggesting that Pax7 may be required for adoption of the muscle lineage, and that muscle SP cells may be a progenitor of satellite cells (Seale, 2000).

Later studies showed that Pax7 was required for the maintenance of the satellite cell population and renewal of the satellite cell pool after injury regeneration, but was not necessary for specification of satellite cells (Oustanina, 2004). Utilizing a Pax7-/- mouse in which the the Pax7 gene was deleted by insertion of a β-galactosidase gene into the first exon of Pax7, researchers showed that lacZ positive cells increased in skeletal muscle after injury, indicating the proliferation of myoblasts derived from satellite cells. Electron microscopy revealed that satellite cell number was reduced in Pax7-lacZ mice, in comparison to wild type littermates, but these data showed that satellite cells were still able to divide, and respond to injury (Oustanina, 2004).

Immunohistochemical staining of skeletal muscle sections and isolated myofibers from Pax7-lacZ mice at different stages of postnatal development showed a steady reduction in satellite cell number as development progressed (Oustanina (2004). Double staining with antibodies directed at CD34, an established marker for satellite cells, and lacZ showed a dramatic reduction in satellite cells between days P11 and P60. Flourescence microscopy also revealed that at P60 the remaining cells that expressed CD34 were morphologically distinct from satellite cells.

To investigate the ability of Pax7-/- mice, primary myoblasts were isolated from both Pax7-/- and Pax7 +/- mice at P8 and P60. Cells in both cultures expressed MyoD, a marker for activated satellite cells, however there was a significant

decrease in the number of MyoD positive cells in the cultures grown from fibers taken from Pax7-/- animals. Cells from Pax7-/- were still able to form myotubes, and immunohistochemical staining showed the newly formed myotubes expressed myosin heavy chain (MHC) a marker for differentiated myofibers (Oustanina, 2004).

When primary myoblasts isolated from the myofibers of Pax7-/- and Pax7+/- mice were plated in equal numbers and allowed to proliferate, there was a significant reduction in the number and size of differentiated myotubes in the Pax7-/- cultures. Immunohistochemical staining showed no significant reduction in the number of MyoD and desmin expressing cells in the Pax7-/- culture after 4 days growth. However, after 7 days of growth there was a significant reduction in bother myotubes staining positive for MyoD and desmin, as well as in the number of myotubes expressing MHC. These data indicate that Pax7 is necessary for the maintenance and proliferation of satellite cells in post-natal development, but not necessary for their initial specification (Oustinina, 2004).

Pax3 and Pax7 are structurally very similar, and have almost identical DNA binding domains (Schafer, 1994), suggesting that they may regulate similar sets of genes. However, their temporal expression patterns indicate separate roles in developing and adult muscle. Studies have demonstrated the possibility of some overlap of function (Relaix, 2004), but Pax7 cannot completely replace the

function of Pax3. These data suggest that, although similar, Pax3 plays a more important role in migration of satellite cells during development, while Pax7 is required for the specification of new satellite cells in adult tissue. Pax7 may play an important role in satellite cell's ability to self-renew after a round of activation and proliferation.

The capacity for self-renewal is a key element in the ability of the satellite cell population to regenerate muscle tissue in response to injury. Satellite cells become activated within 6 hours after injury, and begin to express MyoD and Myf6 as they re-enter the cell cycle (Nicolas 1996, Garry 2000, and Goetsch 2003). Satellite cells will continue to proliferate through the fifth day post-injury, but then will either begin to differentiate into new myofibers, or achieve a quiescent state and re-establish the resident pool of satellite cells (Garry, 2000). It has been observed that expression of the winged helix transcription factor myocyte nuclear factor (MNF) undergoes a reciprocal change in isoforms during this process (Garry, 2000). RT-PCR analysis demonstrates that the β- isoform of MNF is primarily expressed in quiescent satellite cells, but is down regulated in activated cells, while the α- isoform is upregulated after activation, and then down regulated again when cells return to quiescence (Garry, 2000). This expression pattern suggests the possibility of an important role for MNF in the process of regeneration in a pathway independent of the mechanisms associated with embryonic development.

MNF-/- mice are viable, but significantly smaller than wild type and heterozygous littermates. They have a greatly diminished skeletal muscle regenerative capacity in response to injury. After injury by cardiotoxin, muscle architecture in wild type mice is largely restored within 10 days, but in MNF-/- littermates muscle tissue is characterized by interstitial edema and necrotic cell death for as long as 3 weeks post-injury, and even after regeneration, much of the tissue previously occupied by muscle has been replaced by fat deposits (Garry, 2000). Expression of myogenic specific genes MyoD, Myogenin, and c-Myc are delayed during regeneration of the MNF mutant mouse. Satellite cells still proliferate in MNF-/- cells in response to injury, but have impaired cell cycle kinetics. (Garry, 2000).

The kelch protein family

The members of the kelch protein superfamily have many diverse functions, but share a common domain, the kelch beta propeller, in their tertiary structure. The kelch domain is characterized by a series of repeating four-stranded antiparallel β-sheets that form a propeller shaped tertiary structure, with the “blades” of the propeller tilted inward toward a central axis (Figure 1). Each individual sheet will contain between 44 and 56 amino acids, and 90% of all known kelch proteins are characterized by two glycine residues, a tyrosine, and a tryptophan residue in conserved positions in the β-sheets (Xue and Cooley, 1993; Bork, 1994). These conserved residues distinguish a kelch protein from other β-propeller forming proteins. More than 30 members of this family have been identified, and the known kelch proteins have shown a wide diversity in the number of kelch motifs within the propeller, and the position of the propeller within the protein’s tertiary structure.

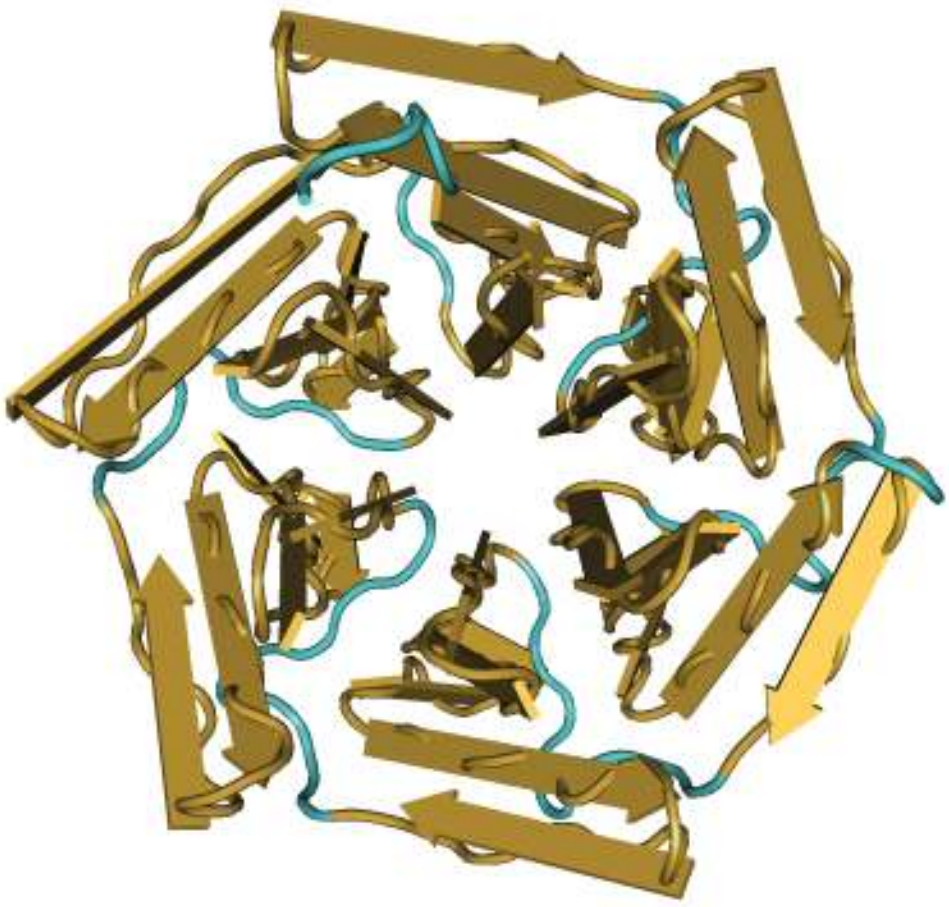

Figure 1.3 The tertiary structure of the Kelch motif. The kelch beta propeller is composed of a series of beta sheets, each blade consisting of 44-56 amino acids. Each kelch motif forms a four-stranded beta sheet, comprising one blade of the propeller, with each blade tilting inward toward a central axis. This image was generated from the crystal structure of the Kelch domain of Keap1, file 1U6DX2 in the NCBI database, using Cn3D 4.1 software.

The Drosophila *kelch* gene was first identified in a screen for recessive mutations on chromosome 2 of *D. melanogaster* that caused sterility, but not mortality, in homozygous females (Schupbac, 1991). The screen was carried out by inducing a mutation in isogenized males with ethane methyl sulfonate (EMS), and then evaluating the F3 generation for fertility (Schupbac, 1991). 528 mutant lines were identified in which homozygous females were viable, but also sterile. Their mutations were mapped to specific loci, and the mutations were grouped into

three phenotypic categories, determined by the stage of embryogenesis affected by the mutation. Of the 62 mutant lines that caused abnormalities in early stages of oogenesis, eight mutations interfered with the migration of follicle cells. The *kelch* gene fell into this category, mutations within its loci resulted in open ended or “cup shaped” chorion, and a failure to form dorsal appendages (Schupbac, 1991). Dorsal appendage material was found within the egg shell, indicating that a number of follicle cells had differentiated into dorsal appendages, but had failed to migrate (Schupbac, 1991).

When the *kelch* gene was cloned, the gene produced a 6 kb mRNA transcript that contained 2 open reading frames separated by a UGA stop codon. Monoclonal antibodies raised against a fusion protein from ORF1 recognized an 80 kd protein in Western blots of purified adult *D. Melanogaster* protein, but also produced a less prominent band at 180 kd (Xue and Cooley, 1993). Both proteins were absent from protein extracts taken from drosophila with a *kelch* null mutation. The larger protein was determined to be a full length protein translated from both ORF1 and ORF2, caused by suppression of the UGA stop codon, while the smaller protein was the product of ORF1. No separate protein corresponding to ORF2 alone was detected.

Suppression of a stop-codon is unusual, but not unprecedented. The first documented observation of a stop codon read through occurred in the coat protein of coliphage Qβ (Weiner and Weber, 1973). Similar to *kelch,* the mRNA

was able to be translated into 2 proteins, with a tryptophan incorporated into the protein at the UGA codon position. Although the larger protein represented only a 2% of the protein translated from the coliphage mRNA (Weiner and Weber, 1973), it was shown to be required for infectivity. The read through of a UGA codon has since been observed in several viral species (Strauss, 1983; Feng, 1989; Jones, 1989), as well as in Drosophila (Lee, 1990) and E. coli bacteria (Schon, 1989). In eukaryotes, UGA codon read through has resulted in the incorporation of a selenocysteine residue in the UGA position (Berry, 1991).

The predicted secondary structure of the ORF1 protein product was primarily α-helical at the N-terminus, and primarily β-sheets at the C-terminus. The predicted structure for the product of ORF2 was predominantly β-sheets (Wieschaus, 1991). When translated, ORF1 would produce a protein with a full kelch beta-propeller, but the read through into ORF2 would attach 2 additional kelch motifs to the protein. A database search revealed several known genes amongst Drosophila and poxviruses with strong homology to the N-terminus of ORF1. These genes encoded a set of zinc finger transcription factors, including the Drosphila proteins *tramtrack* and *Broad Complex,* both of which function as transcriptional repressors during Drosophila embryogenesis (DiBello, 1991; Harrison and Travers, 1991). The BTB domain (Broad Complex, tramtrac and Bric-a-brac) would be found in several Kelch family proteins, and is the most common motif found associated with Kelch related proteins (Adams, 2000). The

BTB domain has also been shown to act as a protein binding domain, and can be involved in homo or heterodimerization (Chen, 1995).

Drosophila *kelch* was shown to colocalize with actin in ring canals, during oogenesis (Xue and Cooley, 1993). Ring canals are intercellular bridges connecting nurse cells to each other in the egg chamber, and to the oocyte, and they are rich in actin (Warn, 1985). Immunohistochemical analysis using a monoclonal antibody directed at ORF1 of *kelch* showed that expression of the protein was restricted to the ring canals, and that *kelch* colocalized with the actin filaments. During oogenesis, *kelch* is necessary for the organization of the actin skeleton inside the ring canal (Robinson, 1997). Protein binding experiments demonstrated that the β-propeller of *kelch* would bind directly to the actin filaments, and that the BTB domains would dimerize to form crosslinks between actin filaments.

Other Kelch family members including α-Scruin (Schmid, 1994), intracisternal A particle-promoted polypeptide (IPP) (Kim, 1999), and Mayven (Soltysik-Espanola, 1999), have been shown to bind directly to actin. During sperm activation in *Limulus polyphemus*, α-scruin forms crosslinks between adjacent actin filaments, in a binding complex similar to *kelch* (Sanders, 1996). α-scruin lacks a BTB domain, but has kelch motifs at both its N and C termini, and those domains are capable of binding to both actin and to the corresponding kelch domain of other α-scruin molecules, creating a homodimer. Crosslinking by α-

scruin increases the rigidity and stability of the actin bundle of the acrosomal process (Sanders, 1996).

Actin-fragmin kinase (AFK) is a kelch family protein that interacts with actin, but does not bind directly to it. AFK contains six kelch repeat motifs at its C-terminus, but no BTB domain, and its primary sequence showed no similarity to other known protein kinases in a database search (Eichinger 1996). Expression of a construct containing the N-terminal 360 residues of AFK was sufficient to catalyze the phosphorylation of actin in the actin-fragmin complex at residues Thr202 and Thr203, although at a rate significantly lower than in lysates from cells transfected with a full length AFK construct (Eichinger, 1996). Expression of a construct containing the C-terminal 340 residues of AFK failed to phosphorylate the actin-fragmin complex, and co-expression of both N-terminal and C-terminal constructs did not increase kinase activity above that seen in lysates from cells transfected with the N-terminal construct alone. To determine if the N-terminus of AFK interacted with ATP, cell lysates containing the N-terminal construct were incubated with the ATP analogue 5'-p-flourosulfonyl-benzoyl-adenosine (FSO2BzAdo). Incubation with the ATP analogue resulted in a dose dependant inhibition of actin phosphorylation by the N-terminal construct, indicating that FSO2BzAdo was competing with ATP for a binding site on the N-terminus of AFK (Eichinger, 1996).

Although the primary sequence of AFK did not share homology with any other known protein kinases, when the crystal structure of the protein was solved, it revealed a tertiary structure similar to the catalytic subunit of eukaryotic protein kinases. This region was 160 kd in length, and contained a nucleotide binding site, and five conserved residues necessary for phosphoryl transfer in other eukaryotic protein kinases (Steinbacher, 1999).

A database search identified three AFK homologues that showed strong similarity to the predicted nucleotide binding site of AFK (T'Jampens, 2002). All three homologues, CKR, Mayven and Keap1, were kelch related proteins containing a BTB/POZ domain at their amino terminus, and multiple kelch repeats at the carboxyl terminus. None of the AFK homologues had demonstrated kinase activity in a previous analysis. Mayven was first identified in mouse brain and neural cells, where it colocalized with the actin cytoskeleton of astrocytes and neurons (Soltysik-Espanola, 1999). Mayven localization was strongest at the retracting end of the cell and in the lamellipodia, which suggests a possible role in actin organization and remodeling. Coimmunoprecipitation analysis showed an increased association of Mayven to actin when cultured neurons were depolarized by the addition of KCL. Immunohistochemical studies showed that Mayven was redistributed along the neuronal process, immediately after depolarization. The hypothesis that Mayven played a role in cytoskeletal remodeling was supported by later studies, in which overexpression of Mayven

was shown to promote process elongation in oligodendrocytes (Jiang, 2005; Williams, 2005).

Keap1 was first identified in a yeast two-hybrid screen for proteins that interacted with Nrf2 (Itoh, 1999). Nrf2 is a transcription factor that regulates the expression of phase II detoxifying enzymes and oxidative stress inducible proteins (Itoh, 1997). Keap1 is expressed ubiquitously, but it's expression is strongest in hematopoeitic cell lineages. Expression of the Keap1 protein is restricted to the cytoplasm, where it functions as a negative regulator of Nrf2 regulatory target genes. Keap1 sequesters Nrf2 in the cytoplasm, preventing transcription of genes regulated by Nrf2. In response to oxidative stress, Nrf2 disassociates from Keap1 and translocates to the nucleus, where it can initiate transcription of its target genes (Itoh, 1999). Later studies would demonstrate that Keap1 not only sequesters Nrf2, but also plays a role in the degradation of the protein by acting as a ubiquitin ligase (Figure 2) (Kobayashi, 2004).

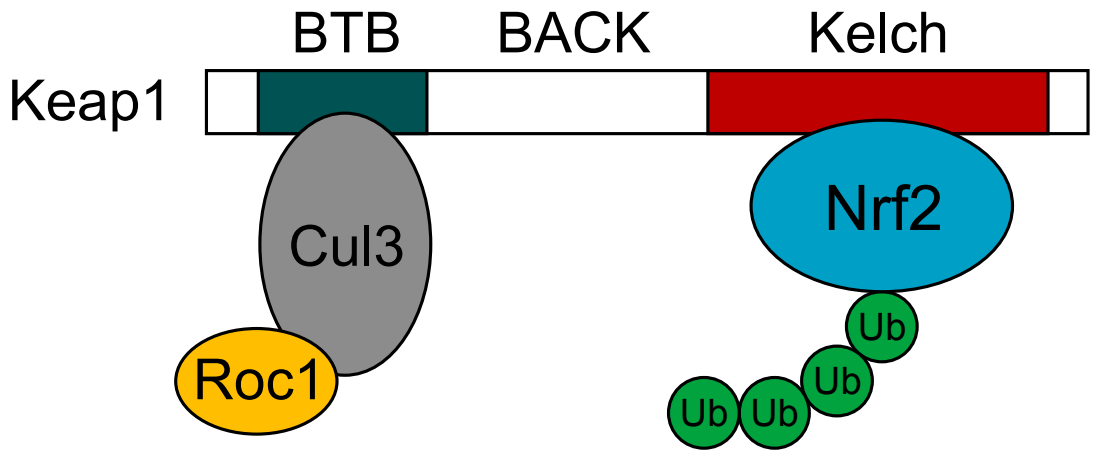

Figure 1.4. Keap1 acting as a ubiquitin ligase. Schematic representation of Keap1 interacting with NRF2 and acting as a ubiquitin ligase to regulate the degradation of NRF2. In the absence of oxidative stress, Keap1 binds to the actin cytoskeleton, and keeps Nrf2 sequestered in the cytoplasm, and also mediates the conjugation of ubiquitin residues to Nrf2 to regulate its degradation by the proteasome.

CKR is a BTB-Kelch protein found in *C. elegans*, whose function remains undescribed. None of the three homologues of AFK identified in the database search have demonstrated kinase activity in functional assays. Both Keap1 and Mayven have been shown to bind directly to actin.

To determine if these three proteins were able to interact with ATP at the predicted binding sites, each gene was expressed as a fusion construct with glutathione-s-transferase (GST) and incubated with ATP-sepharose and GTP-sepharose. Western blotting with a GST antibody showed that all three proteins had bound to ATP. Competition assays with the covalently binding ATP analog FSBA showed that FSBA was able to bind to all 3 proteins, but that binding was inhibited in a concentration dependant manner when ATP was added to the

reaction (T'jampens, 2002). No kinase activity has been observed in these three proteins, and the role of their ATP-binding domain remains undescribed.

The BACK domain is another feature of BTB-Kelch proteins that is highly conserved, but whose functional role is not clear (Stogios and Prive 2004). The BTB/POZ domain occurs in several proteins that do not contain Kelch motifs, and the distance between BTB and other domains can vary greatly (Chen, 1995; Horlein, 1995, Jackson, 1997). The intervening region is usually disordered with little to no regular secondary structure. However, in all known BTB-Kelch proteins, the BTB domain is located at the amino terminus of the protein and the Kelch repeats are located closer to the carboxyl terminus. The intervening region is approximately 130 amino acid residues in length, and computer modeling by Jpred secondary structure prediction server, a stand-alone computer program from: http://barton.ebi.ac.uk/ (Cuff and Barton, 2000), predicts an entirely α-helical structure. The primary sequence in this region shows strong homology within the BTB/Kelch family, particularly in the first 70 residues immediately following the BTB domain. Conserved residues include an Asn-Cys-Leu-Gly-Ile sequence at the N-terminus of the domain, and a Val-Arg-{Met/Leu/Phe}-Pro-Leu-Leu sequence beginning at residue 91 within the BTB domain. A highly conserved phenylalanine residue at position 38 is often flanked by two glutamic acid residues upstream on its amino terminal side, and by three leucine residues on its carboxyl side. The first leucine is the least conserved, but it is replaced in the sequence by other non-polar residues such as isoleucine or

valine (Stogios and Prive 2004). The most highly conserved residues are predominantly non-polar, suggesting the possible existence of a hydrophobic core in the proteins tertiary structure. A glutamic acid residue at position 60 and a tryptophan at residue 70 are also highly conserved throughout different BTB/Kelch proteins. BLAST searches of the Protein Databank found no significant matches between the BACK domain and other previously described protein motifs.

To identify proteins with possible BACK domains, the study authors created a hidden Markov model, a statistical model used to determine hidden parameters of a system, by using the observable parameters (Stogios and Prive 2004),. The computer model was trained using the putative BACK sequences from 20 known BTB/Kelch proteins, and was used to search the NCBI non-redundant database, which contains genomic sequences of 165,000 organisms (Benson, 2004), and the SWISS-PROT protein database. Most of the potential BACK proteins identified in this search were also BTB/Kelch proteins, but there were examples of possible BTB-BACK proteins identified in the *Arabadopsis* and *Drosophila* genomes. In vertebrates and *C. elegans,* the majority of the identified proteins followed the BTB-BACK-Kelch structure. In *Drosophila* there were also eight proteins identified as possible BACK proteins that contained neither BTB nor Kelch domains.

Although no functional assays or binding studies were performed to complement the database searches, the authors of the study speculated that the BACK domain could play a role in the ubiquitination of proteins, targeting them for degradation in the proteosome (Stogios and Prive 2004). Keap1, a BTB/Kelch protein, has been shown to catalyze the ubiquitination of Nrf2 (Furukawa 2005), and other BTB proteins have been shown to interact with Cullin3, a component of E3 ubiquitin ligase complexes (Furukawa 2003). Strong structural similarities between the BTB domain and two components of the E3 complex, Skp1 and F box, first suggested the possibility of a role for BTB/Kelch proteins in ubiquitination. In this model, the Kelch domain would function as the substrate recognition motif, a role played by WD40 in the E3 complex. WD40 family members are also β-propeller proteins with diverse functions and are often involved in protein binding. The most extensively characterized member of the WD40 family is the Gβ subunit of G-protein coupled receptors. These structural similarities lead to the hypothesis that BTB/Kelch proteins could be single molecules capable of performing the same function as the Skp1-Cullin-F box (SCF) E3 complex. In the proposed model, the BTB domain would be equivalent to the N-terminal half of Skp1, and the BACK domain would perform the functions of the F-box and the C-terminal region of Skp1. In BTB-BACK-Kelch proteins, the BTB domain is separated from the first α-helix of the BACK domain by only two amino acids, and the 2 helices could possibly be continuous (Stogios and Prive, 2004). The kelch motif would be equivalent to the β-propeller of WD40.

In cells undergoing oxidative stress, Nrf2 disassociates from Keap1, but is still degraded in a proteosome independent manner (McMahon, 2004). Under homeostatic conditions, when Nrf2 is still sequestered by Keap1, the protein undergoes a much higher turnover rate as it is ubiquitinated and targeted for degradation by the 26S proteosome (McMahon, 2004). When the oxidative stressor isothiocyanate Sul was added to rat RL34 cells in culture, Nrf2 protein translocated from the cytoplasm to the nucleus, and high levels of the protein accumulated within the first 2 hours. Real time PCR showed no significant change in Nrf2 mRNA levels during this time period, suggesting that the change in expression levels was due to an inhibition of degradation. Three different proteosomal inhibitors were added to RL34 cells under homeostatic conditions, resulting in accumulation of Nrf2 in the cytoplasm, but still excluded from the nucleus. When media containing the proteosomal inhibitors was replaced with media containing CHX, protein levels dropped rapidly. When media containing proteosomal inhibitors was replaced with media containing Sul, protein degradation was inhibited again. These data indicate that Nrf2 is degraded in a proteosome dependant manner both under homeostatic conditions, and under oxidative stress. However, degradation is noticeably decreased during periods of oxidative stress. When Nrf2 was overexpressed in COS1 cells, protein levels did not respond significantly to oxidative stress. Only when Nrf2 and Keap1 were cotransfected in cells was the degradation mechanism restored, indicating that a

direct interaction between Nrf2 and Keap1 was necessary for degradation under homeostatic conditions.

To determine if this proteosomal degradation was mediated by ubiqitination of Nrf2, proteins were extracted from Nrf2 transfected COS1 cells that had been treated with proteosome inhibitors. This was done with two sets of cells, one that was treated with Sul, and a sample that was left untreated. Western blotting produced a smear, indicating ubiquitination of the Nrf2 protein, in both the Sul treated and untreated cells. The study concluded that Keap1 could be ubiquitinated independent of Keap1, but association with Keap1 lead to a more rapid ubiquitination and degradation of the Nrf2 protein (McMahon, 2003).

When an HA-tagged Nrf2 construct was co-expressed with Keap1 proteins carrying mutations in the BTB domain or the cytoplasmic tail, the ability of Keap1 to interact with Nrf2 was not impaired. However, a mutant construct that lacked the 142 amino acid stretch separating the BTB domain from the kelch domain was unable to sequester Nrf2 in the cytoplasm, and mislocalized to the nucleus (Zhang and Hanninnck, 2003). This region of the protein corresponds to what is now known as the BACK domain, but at the time of these assays, the BACK domain had not been identified. A mutated Keap1 protein that lacked the kelch domain was unable to bind to Nrf2, and was also unable to sequester Nrf2 in the cytoplasm, although it did not localize to the nucleus with Nrf2. Because Keap1-Nrf2 binding is affected by oxidative stress, it was hypothesized that the oxidation

state of one or more of the cysteine residues on Keap1 could affect the ability of the protein to bind its substrate. Seven mutant constructs that contained serine codons in place of individual cysteine codons located within the BTB and BACK domain were constructed, and expressed in NIH 3T3 cells. RNA was extracted from transfected cells under both homeostatic and oxidative stress conditions, and RT-PCR was used to evaluate the expression level of Nrf2 target genes. Four of the mutant constructs showed no difference in gene expression from cells transfected with a wild-type Keap1 construct. One construct, with a mutation at C151, acted as a constitutive repressor of Nrf2 target genes, under both basal and stress conditions. Two mutations, C273 and C288, resulted in an increase in the expression of Nrf2 target genes under basal conditions, and no change under oxidative stress, indicating that their ability to sequester Nrf2 had been impaired. A construct in which both C151 and C273 were mutated to serine codons restored the transcriptional activity of Nrf2 targets, indicating that the C273 may play a more important role in the interaction of Keap1 with Nrf2. C151 is located within the BTB domain of Keap1, while C273 and C288 are both located in the BACK domain.

Coimmunoprecipitation assays demonstrated that the C273 and C288 mutants were still able to bind Nrf2. However, pulse chase assays showed that the half-life of Nrf2 increased from 2.6 hours when co-expressed with wild-type Keap1, to over 5 hours when co-expressed with either the C273 or C288 mutants in COS1 cells. Nrf2 was also detected in the nucleus of cells transfected with the two

mutant Keap1 constructs, but was restricted to the cytoplasm in cells transfected with wild-type Keap1.

Prior studies had already demonstrated that Keap1 bound to Nrf2 through an interaction between the Kelch repeat region of Keap1, and the Neh2 domain of Nrf2 (Itoh, 2003). Immunohistochemistry showed Keap1 colocalizing with the actin filaments in transgenic mice overexpressing Keap1. Immunoprecipitation studies using an actin anti-serum and full length Keap1 and deletion constructs lacking the BTB domain, BACK domain, Kelch repeat region, or C-terminal tail, showed that full length Keap1 and all the deletion mutants with the exception of the construct lacking a kelch domain were able to co-precipitate with actin.

Disruption of the actin cytoskeleton in NIH 3T3 cells with cytochalasin B, a reagent that inhibits polymerization of actin filaments, resulted in the translocation of Nrf2 from the cytoplasm to the nucleus within 1 hour of treatment (Itoh, 2003). Keap1 remained localized to the cytoplasm, indicating that disruption of the actin cytoskeleton inhibited the binding of Keap1 to Nrf2. These observations support the hypothesis that the actin cytoskeleton played a role in the sequestering of Nrf2, by Keap1 under homeostatic conditions.

Immunostaining and microscopic analysis showed that all of the deletion mutants used in the binding studies localized to the cytoplasm in NIH 3T3 cells. Wild type Keap1, and the BTB and BACK domain deletion mutants also colocalized with a

fusion construct linking the Neh2 domain of Nrf2 to GFP, and the Neh2-GFP construct was excluded from the nucleus when co-transfected with these proteins (Itoh, 2003). Deletion mutants lacking the Kelch repeat domain or the C-terminal tail failed to colocalize with Neh2-GFP, and Neh2-GFP expression was observed predominantly in the nucleus. This suggests that the C-terminal tail of Keap1 may play a role in Keap1-Nrf2 binding, even though it does not directly interact with Nrf2 (Itoh, 2003). Immunoprecipitation with cell extracts from 293T cells cotransfected with a flag-tagged full length Nrf2 and the series of Keap1 deletion mutants demonstrated that Keap1 lacking the C-terminal tail was still able to interact with Nrf2, but Keap1 lacking its kelch domain failed to associate with Nrf2. These data suggest that the Kelch domain is required for Keap1 binding to both Nrf2 and to the actin cytoskeleton, but that the C-terminal tail of Keap1 may play a role in regulating Keap1 binding activity, possibly by causing a conformational change under conditions of oxidative stress (Itoh, 2003). The C-terminal region of Keap1 does contain a cysteine residue that became biotinylated when incubated with BIA, C613, indicating that it could be a reactive residue under oxidative stress conditions (Eggler, 2005).

Prior studies had identified several BTB proteins without Kelch domains that were able to function as ubiquitin ligases by binding to Cullin3, a component of the E3 Skp1-Cullin-F box (SCF) complex (Furukawa, 2003; Geyer, 2003; Pintard, 2003; and Xu, 2003). A yeast two-hybrid screen using full length Keap1 and the Keap1 BTB domain as baits failed to identify interacting proteins that might affect

ubiquitination (Kobayashi, 2004). Immuprecipitation with a Keap1 antibody indicated a potential interaction between endogenous Keap1 and Cul3 in 293T cells. To investigate this interaction further, 293T cells were cotransfected with plasmids expressing an HA-tagged Keap1 protein, and FLAG-tagged Cul3. Cell extracts were initially filtered through a column containing beads conjugated to an anti-Flag antibody. Immunoblot analysis of the precipitates utilizing an anti-HA antibody demonstrated that Keap1 had co-precipitated with Cul3. Other Cullin proteins were also analysed for interaction with Keap1 in similar immunoprecipitation assays, but no association with any Cullin protein other than Cul3 was observed (Kobayashi, 2004). Similar immunoprecipitation experiments performed later in COS1 cells indicated an association between Keap1 and Cul2, as well as Cul3 (Zhang and Hanninnk, 2004).

To identify the specific region of Keap1 that interacted with Cul3, additional immunoprecipitation studies were performed, using Keap1 deletion mutants conjugated to HA. In these experiments, deletion of the BTB domain did not affect the ability of Keap1 ability to associate with Cul3. The Keap1 mutant lacking a BACK domain was the only construct that failed to interact with Cul3. A full length Keap1 protein, in which cysteine residues C273 and C288 were mutated to serines, retained its ability to bind Cul3 (Kobayashi, 2004). Mutations at those positions in the BACK domain had previously been shown to impair the ability of Keap1 to ubiquitinate Nrf2 (Wakabayashi, 2004). These studies indicate that Cul3 binding to Keap1 is not dependant upon these residues. A

Cul3 deletion mutant lacking the N-terminal 280 residues of the protein was unable to interact with full length Keap1.

A protein containing only the N-terminal 280 residues did associate with Keap1, indicating that the interaction site for the two proteins was within this domain (Kobayashi, 2004). This is significant, because the N-terminal 280 residues of Cul3 contain the binding site that interacts with Skp1, the adaptor protein in the SCF complex (Zheng, 2002).

To investigate the role of a Keap1-Cul3 complex in the ubiquitination of Nrf2, 293T cells expressing histidine tagged ubiquitin were transfected with plasmids expressing Keap1, Cul3, and Nrf2. Twenty-four hours post transfection, cells were treated with the proteosome inhibitor MG132 for 12 hours. Cell lysates were filtered through columns containing nickel affinity beads, which would interact with proteins bound to the histidine tagged ubiquitin molecules. Immunostaining with an Nrf2 antibody showed multiple bands and a smeared trail of migration in the gel, indicating that Nrf2 had been ubiquitinated (Kobayashi, 2004). Co-transfection of Keap1 increased ubiquitination of Nrf2, and the co-expression of Cul3 and Keap1 produced an increase in ubiqitination, over expression of Keap1 alone. Transfection of Cul3 in the absence of Keap1 did not produce any change in ubiquitination over what was observed in cells transfected only with Nrf2. This indicated that Nrf2 ubiquitination was dependant

on Keap1 and could be enhanced by Cul3, but Cul3 was not required for efficient ubiquitination (Kobayashi, 2004).

These data were supported by assays using only the Neh2 domain of Nrf2, bound to Gal4 (Zhang and Hannink, 2004). The Neh2-Gal4 construct was expressed in MDA-MB-231 cells that had been co-transfected with HA conjugated ubiquitin, Keap1, and each of the five known cullin proteins. Immunoprecipitation with and anti-Gal4 antibody and immunostaining with an anti-HA antibody showed that the Neh2 domain was ubiquitinated in cells transfected with Keap1, and that the level of ubiquitination was dose dependant. Co-expression of Cul3 with Keap1 increased ubiquitination of the Neh2 domain, but expression of the other Cullin proteins did not affect ubiquitination. Cotransfection of a dominant negative truncated Cul3 protein, in which the C-terminal binding site of Cul3 was deleted, effectively inhibited ubiquitination of Neh2, and the full length Nrf2 protein (Zhang and Hannink 2004).

Crystal structure of the BTB domain of the *C. elegans* protein MEI-26, a BTB protein that had been shown to bind Cul3, predicted that eight amino acids were essential for interaction with Cul3 (Li, 2004). These residues corresponded to positions 123-127 and 160-164 in the BTB domain of Keap1. Keap1 proteins with alanine mutations at those specific sites were constructed, and analyzed for their ability to interact with Nrf2, and to regulate its ubiquitination. When the mutant proteins were expressed in COS1 cells, they were still able to bind

efficiently to Nrf2, and to Cul3. The mutant proteins were unable to ubiquitinate the Neh2-Gal4 construct or full length Nrf2. An unexpected result of the mutations was a marked increase in ubiquitination of the mutant Keap1 proteins, in comparison to the wild-type Keap1 (Zhang and Hannink, 2004).

The Neh2 domain of Nrf2 contains seven lysine residues that are potential targets for ubiquitination (Zhang and Hannink, 2004). Mutation of all 7 lysine residues to arginine did not impair the ability of a mutant Neh2 domain to bind to Keap1 after co-transfection in COS1 cells. Pulse-chase experiments indicated that the half-life of the Neh2-R7 mutant was greater than 3 hours, indicating a much lower rate of degradation than the wild-type Hrf2 protein with a half-life of 1 hour. Further pulse chase experiments performed in mutant Neh2 constructs, in which one of the seven mutated residues was restored to lysine, resulted in an increase in ubiquitination for each of the restored proteins (Zhang and Hannink, 2004). Ubiquitination was strongest in constructs where L52 and L53 were restored. These findings suggest that several lysine residues in the Neh2 domain of Nrf2 are targeted for ubiquitination by Keap1 (Zhang and Hannink, 2004).

Mutant Keap1 proteins that contained alanine mutations in their BTB domains demonstrated lower steady state levels of expression due to more rapid rates of degradation, corresponding to an increase in ubquitination. However, treatment of cells with MG132, a proteosome inhibitor, failed to increase steady state levels

of the protein. Experiments with other proteosome inhibitors produced similar results, indicating that degradation of Keap1 occurred by a proteosome independent pathway (Zhang and Hannink, 2005).

Exposing cells to oxidative stress conditions by incubating them with tBHQ resulted in an increase in ubiquitination and degradation of wild-type Keap1. To identify the lysine residues involved in ubiquitination of Keap1, plasmids expressing deletion mutant Keap1 proteins were transfected into COS1 cells and these cells were exposed to tBHQ. Ubiquitination and degradation increased the mutant proteins lacking either the BTB or kelch domains, both prior to and after exposure to tBHQ (Zhang and Hannink, 2005). A deletion mutant lacking the BACK domain of Keap1 demonstrated a decrease in ubiquitination under both basal and oxidative stress conditions, indicating that one or more of the lysine residues within the BACK domain is involved in the ubiquitination of the protein (Zhang and Hannink, 2005).

Taken together, these data suggest a complex pathway regulating the expression of Nrf2 target genes in response to oxidative stress. Under homeostatic conditions, Nrf2 is primarily localized to the cytoplasm, where it is sequestered by Keap1, which is bound to both Nrf2 and to the actin cytoskeleton. Interaction with Keap1 also regulates the ubiquitination of Nrf2, leading to a rapid degradation of the protein, resulting in low steady state levels of Nrf2 under basal conditions. In response to oxidative stress, Nrf2 is released from binding to

Keap1 and translocates to the nucleus, enhancing transcription of its target genes. Keap1 is also ubiquitinated and degraded under stress conditions, leading to a rapid rise in the level of Nrf2 protein, and an attenuation of the expression of its downstream target genes. This allows cells to rapidly respond to changes under stress conditions, as Nrf2 protein levels are upregulated rapidly without any change in the rate of its transcription or translation.

Several close homologues of Keap1 also underwent an increase in ubiquitination under oxidative stress (Zhang and Hannink, 2004). The BTB-Kelch proteins Sarcosin, ENC1 and GAN1 were expressed in GCS-2 cells, and the cells were treated with tBHQ. Sarcosin and ENC1 underwent rapid ubiquitination after exposure to tBHQ and steady-state levels of the proteins dropped measurably. GAN1 remained unaffected, and its protein levels remained unchanged after tBHQ treatment. These observations suggest the possibility of a conserved function in some BTB-Kelch proteins to act as both adaptor proteins in a Cul3 ubiquitin ligase complex, and as sensors of oxidative stress.

Due to the observation of this novel mechanism, Keap1 has been one of the most thoroughly characterized kelch family proteins. Mice lacking Keap1 appeared identical to wild type and heterozygous littermates at birth, but post-natal development was severely impaired (Wakabayashi and Yamamoto, 2003). Growth deficiencies were visibly apparent in Keap1-/- mice at postnatal day 4 and pups began do develop scales on day 5, which eventually covered their

bodies. No Keap1-/- pups survived beyond day 21. Sections of the internal organs of day 7 Keap-/- pups showed no visible differences between null and wild-type littermates with the exception of several layers of cornified epithelial cells lining the interior walls of the stomach and esophagus, similar to the scales appearing on their skin. The stomachs of Keap1-/- mice were significantly smaller than their wild-type littermates, and filled with milk, suggesting the possibility that their premature deaths could be caused by gastric obstruction (Wakabayashi and Yamamoto, 2003).

Immunohistochemical analysis showed distinct differences in expression levels of several proteins used as markers for proliferation and differentiation, including four members of the cytokeratin gene family, and loricrin, a marker for terminal differentiation. Loricrin and keratin K6 were upregulated in Keap1-/- mice, while cytokeratin K13 and involucrin were inhibited, indicating that Keap1 played a role in the terminal differentiation of epithelial cells in the esophagus and stomach (Wakabayashi and Yamamoto, 2003). Using the promoter regions of loricrin and K6 fused to a luciferase reporter, researchers demonstrated that cotransfection of Nrf2 with these constructs was sufficient to induce expression of these genes, indicating that Nrf2 could be a specific transcriptional regulator of these epithelial cell differentiation genes, during embryogenesis. RT-PCR analysis revealed that previously identified Nrf2 target genes, NQO1 and GSTΠ, are also upregulated in both Keap1-/- E10.5 embryos, and neonates (Wakabayashi and Yamamoto, 2003).

Mutant mice deficient in Nrf2 were viable and fertile (Itoh, 1997), so it was possible to breed compound mutant mice lacking both Keap1 and Nrf2. This cross breeding effectively reversed the phenotype observed in the Keap1-/- neonates. The homozygous compound mutant mice lacked the scaling skin and growth retardation phenotype of Keap1-/- mice, and were indistinguishable from their wild type littermates. The hyperkeratonic esophagi and stomach observed in the Keap1-/- mutants was also not observed the compound mutant neonates, and compound mutants remained viable for over 60 days. All Keap1-/- littermates died prior to day P21 (Wakabayashi and Yamamoto, 2003).

The tertiary structure of the Kelch domain of Keap1 has also been characterized by radio crystallography (Li, 2004: Padmanabhan, 2005). The crystal structure of Keap1 indicates that the conserved residues that identify a Kelch repeat protein play important roles in maintaining the beta-propeller structure. The crystal structure also identified a single amino acid that is required for binding of Nrf2 (Li, 2004).

The most recently identified member of the Kelch family appears to plays a significant role in the migration and differentiation of myoblasts. The gene mKlhdc2 was identified in a microarray analysis of the expression profile of cells extracted from embryos deficient in Lbx1, a protein required for migration and differentiation of myoblasts (Schafer, 1999). Lbx1 is a homeobox transcription

factor constitutively expressed in myogenic progenitor cells, and homozygous mutation of the Lbx1 gene resulted in embryonic lethality and a severe reduction in appendicular muscle formation during embryogenesis (Gross, 2000). To perform the microarray, mRNA was extracted from tissues dissected from E10.5 Lbx1 null embryos, and wild-type littermates (Neuhaus, 2006).

The kelch protein mKlhdc2 is expressed ubiquitously in adult tissues, and at all stages of embryogenesis after E10.5, but is downregulated in muscle tissue extracted from Lbx1 null embryos. The expression pattern described by the microarray was confirmed by RT-PCR (Neuhaus, 2006).

Overexpression of mKlhdc2 in 10T1/2 fibroblast cells, and C2C12 myoblasts, a myogenic progenitor cell line that expresses mKlhdc2 only after differentiation, resulted in the induction of transcription of LZIP, a leucine zipper transcription factor that is also modified post translationally by mKlhdc2 (Zhou 2001). C2C12 cells overexpressing mKlhdc2 were also unable to differentiate after the removal of serum from their media, while wild-type cells formed myotubes and expressed myogenic markers rapidly after serum depletion (Neuhaus, 2006).

RT-PCR analysis demonstrated that wild-type cells downregulated MyoD and Myf5 after serum depletion, and upregulated myogenin (Neuhaus, 2006). Myogenin was never induced in mKlhdc2 overexpressing cells, and Myf5 expression remained consistent. Myotubes never formed in cells overexpressing

mKlhdc2. Some elongation and parallel orientation of cells was observed, but mKlhdc2 overexpressing cells were unable to fuse into mature myotubes (Neuhaus 2006).

The inihibition of fusion in mKlhdc2 cells was reversed when overexpressing cells were grown in coculture with wild-type cells (Neuhaus, 2006). When mKlhdc2 overexpressing cells were grown labeled with DiI and grown in culture with wildtype cells, after serum depletion and myotube formation, DiI labeled nuclei were observed within the newly formed myotubes. The total number of labeled cells able to participate in myotube formation was directly proportionate to the ration of wild-type cells in the culture (Neuhaus, 2006). These data seemed to indicate that overexpression of mKlhdc2 did not prevent cells from participating in fusion, but inhibited differentiation at an earlier stage.

The migration capability of mKlhdc2 cells was tested using a Boyden chamber assay, in which cells were grown in the upper chamber of a well divided by a polycarbonate membrane, and the lower chamber was filled with a chemoattractant (Neuhaus, 2006). The assay was run using either IGF, HGF, or no attractant in the lower chamber. After incubation for 16 hours, cells were stained with Hoechst dye, and the number of migrants was determined by microscopy. The assay found no difference in migration between wild-type and mKlhdc2 overexpressing cells in the wells containing no attractant or IGF. However, migration was drastically decreased in wells containing HGF and

mKlhdc2 overexpressing cells, in comparison to wild-type cells. 10T1/2 fibroblasts that overexpressed mKlhdc2 were also unable to respond when grown in wells with HGF, indicating that the overexpression of mKlhdc2 caused a loss of HGF-directed migration (Neuhaus, 2006).

In the same study, researchers utilized an RNAi strategy to knockdown expression of mKlhdc2, but the reduction of mKlhdc2 expression had no visible affect on the cells ability to differentiate (Neuhaus, 2006). The study authors used three different RNAi oligos, all of which were effective in silencing mKlhdc2 expression, but silencing of the gene did not result in impaired differentiation, in comparison with untransfected cells (Neuhaus, 2006).

Kelch proteins represent a large family of proteins with strong structural homology, but diverse functions. The most recently identified member of this family has been shown to play an important role in both the migration and differentiation of C2C12 myoblasts grown in culture. Several other kelch proteins have been shown to regulate migration in other cell types, and many kelch family members are involved in cytoskeletal remodeling through their interaction with actin.

Calsarcin proteins mediate the effects of Calcineurin in skeletal muscle

The three known member of the Calsarcin protein family are expressed in different tissue types, but all three are regulators of the calcium and calmodulin-dependant protein phosphatase Calcineurin (Frey and Olson, 2000; Frey and Olson, 2002; Faulkner, 2000; Takada, 2001) . The first of the Calsarcin proteins was identified in a yeast two-hybrid screen, using the calcineurin catalytic subunit as bait to screen a human cardiac cDNA library. One of the positive interactions identified in the screen was a sequence 2,422 base pairs in length with an open reading frame that coded for a protein of 264 amino acids. This protein was named calcineurin-associated sarcomeric protein-1, or Calsarcin-1 (Frey and Olson, 2000).

Calcineurin is a calmodulin-dependant phosphatase that responds to calcium signaling in variety of tissue types. When Calcineurin is activated in skeletal muscle by an increase in calcium concentration, Calcineurin will dephosphorylate and activate the nuclear factor of activated T cell (NFAT) and myocyte enhancement factor-2 (MEF2) transcriptional pathways (Beals, 1997; Chin, 1998; Mao, 1999). Dephosphorylation by Calcineurin allows NFATs to translocate from cytoplasm to nucleus, and initiate transcription of its target genes (Beal 1997). Mammalian skeletal muscle expresses three forms of NFAT

at different stages of differentiation, NFATc3 in myotubes, NFATc2 in newly fused, immature myotubes, and NFATc1 in mature myotubes (Abbott, 1998) and each isoform is translocated to the nucleus at the appropriate stage of differentiation. Forced expression of calcineurin in C2C12 myoblasts also resulted in the translocation of NFATc3 to the nucleus, but did not affect the localization of NFATc2 or NFATc3 (Delling 2000).

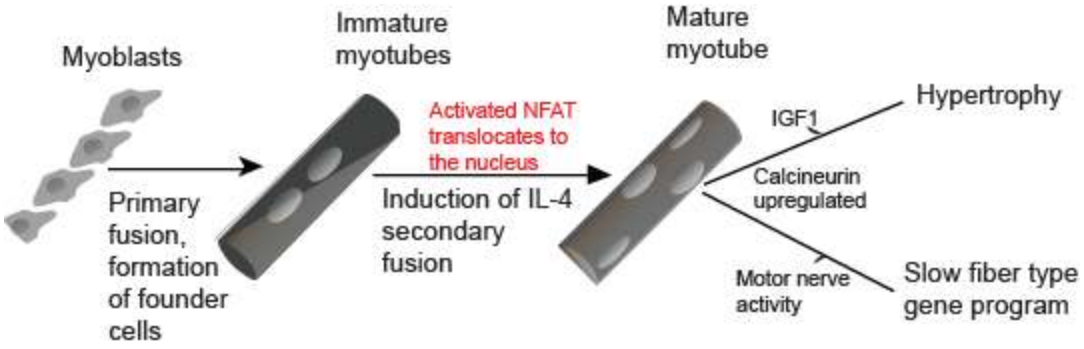

Figure 1.5 NFAT signaling, activated by Calcineurin, regulates skeletal muscle hypertrophy and fiber-type switching. Translocation of NFAT family proteins to the nucleus in the early stages of differentiation and fusion induces the transcription of IL-4 (Horsley, 2003), which acts as a chemoattractant to direct myoblasts to newly formed myotubes (founder cells). The induction of IGF-1 expression raises intracellular calcium concentration, driving the upregulation of Calcineurin. Expression of NFAT with MEF-2C will direct newly formed myofibers to express the slow twitch muscle fiber expression profile.

Studies utilizing the Calcineurin inhibitor cyclosporine A (CsA) have demonstrated that Calcineurin signaling is required for differentiation of myoblasts into myotubes (Abbott, 1998). Confluent human myoblasts that were treated with CsA failed to form myotubes, and did not express the myosin heavy chain protein. Creatine kinase activity was also inhibited in a dose dependant manner in cells treated with CsA (Abbott, 1998). In the same study, the authors

caused a localized injury in the hindlimb of mice to demonstrate the effect of Calcineurin inhibition on regeneration after injury. Mice were anesthetized while a 3 mm incision was made in their hindlimbs, and dry ice was applied directly to the exposed muscle tissue. The mice were then injected with either an empty vehicle or 45mg/kg of CsA. Mice that received the empty vehicle regenerated completely in 12-14 days (Abbott, 1998). At 10 days, the mice were sacrificed and analyzed, and the CsA treated animals showed very few centrally nucleated myofibers, an indication of ongoing regeneration, indicating that Calcineurin signaling was required for skeletal muscle regeneration, and myoblast differentiation (Abbott, 1998).

The ability of CsA to inhibit Calcineurin signaling and affect regeneration was dose dependant (Serrano, 2001). 25mg/kg administered twice daily was necessary to impair regeneration, and lower doses were insufficient to prevent muscle hypertrophy after overload (Bodine, 2001), or regeneration after injury (Serrano, 2001). This has led researchers to hypothesize the possible existence of a parallel compensatory pathway, possibly regulated by IGF-1 (Musaro, 1999). IGF-1 protein was upregulated in experiments when Calcineurin activity was repressed, and there was a corresponding upregulation in IGF-1 target genes such as myogenin (Adi, 2000) and GATA-2 (Musaro 2001). At the transcriptional level, it has also been demonstrated that CsA inhibition of Calcineurin during muscle overload leads to an increase in the upregulation of IGF-1 (Figure 2.) as well as its target genes, myogenin and Myf5 (Michel 2004). Expression of

myostatin, a protein that inhibits muscle hypertrophy, was downregulated during overload in untreated cells, but treatment with CsA restored myostatin expression, suggesting that Calcineurin and NFAT may play a regulatory role in myostatin expression during hypertrophy (Michel, 2004).

Calcineurin signaling also plays a regulatory role in muscle fiber-type determination. Upregulation of calcineurin signaling during myogenesis will drive newly formed myotubes towards a slow-twitch fiber fate (Chin, 1998). Forced expression of a constitutively active calcineurin in C2C12 cells resulted in an upregulation of slow tropinin-1 (TnIs) and myoglobin (Mb), markers for slow twitch fibers. There was no corresponding upregulation in muscle creatine kinase (MCK), a marker for fast twitch fibers (Chin, 1998). In the same study, when CsA was added to culture media, the opposite effect was observed. MCK was upregulated and expression of Mb and TnIs were both repressed. This was followed by *in vivo* analyses of mice that were given intraperitoneal injections of CsA for 6 weeks. Administration of the calcineurin inhibitor lead to a significant increase in the percentage of fast twitch muscle fibers, as measured by immunohistochemical staining for the fast myosin protein. The NFAT pathway was linked to the fiber switching mechanism as outlined in a study demonstrating that in cells expressing a constitutively active calcineurin mutant, the MHC-slow transcript was upregulated, and MHC-fast was inhibited (McCullagh, 2004). Regenerating soleus and EDL muscle tissue, both of which are primarily fast twitch fibers, were transfected with the constitutively active

form of NFAT, and within 7 days the regenerating muscles were expressing the MHC-slow transcript, and not expressingt he MHC-fast transcript (McCullagh, 2004).

In cardiac and skeletal muscle, calcineurin is bound to α-actin at the z-line of the sarcomere, by a family of proteins known as Calsarcins (calcineurin associated sarcomeric protein) (Frey, 2000). Sequestered in this way, calcineurin is unable to dephosphorylate NFAT, which prevents NFAT from translocating to the nucleus, and the genes regulated by NFAT remain transcriptionally dormant (Frey, 2004).

The Calsarcin family of proteins was first described by two different groups, at Univ. of Texas-Southwestern Medical Center (Frey, 2000), and Harvard University (Takada, 2001). The UT-Southwestern study was submitted and published first, but the two papers were published just two months apart.

The authors of the first study were attempting to identify cardiac specific proteins that interacted with calcineurin (Frey 2000), utilizing the catalytic A subunit of calcineurin as the bait in a yeast-two hybrid screen. The catalytic A subunit (CnA) was selected as bait because it contains binding sites for calmodulin and an autoinhibitory domain. A fusion construct of the CnA and the Gal4 DNA binding domain was generated, and used as the bait to screen a Clontech human heart cDNA library. One of the clones identified in the screen consisted of a

2,422 bp cDNA, containing an open reading frame of 792 bp encoding a previously undescribed protein of 264-aa. This protein was named calcineurin-associated sarcomeric protein-1, or calsarcin-1. A database search identified a homolog of calsarcin-1 in *mus musculus,* with an 88% amino acid similarity to human calsarcin-1. The database search also identified a second protein with strong homology to calsarcin-1 at both the amino and carboxyl termini, but little similarity in the central region (Figure 3). This second protein was named calsarcin-2 (Frey, 2000).

```
 5′-
CAATTCCCTGCCACTCCACAACATTCCGTTTCTGTCTAAGAGGATTTCCAGGTTATTGGACGGTGGGGTT
AAGAAGTTCTAGGTACTGCAGAAGGTCTTGGACAGACACTTAGTCCTCCGAAGCTGCTGGACCCCGGGGA
GAGCCGACCACCAACTGAGCAGCTGGTCAGATCCACCTCCACCATGCCACTCTCAGGAACCCCGGCCCCT
AACAAGAGGAGGAAGTCAAGCAAACTGATTATGGAGCTCACTGGAGGTGGCCGGGAGAGCTCAGGCCTGA
ACCTGGGCAAGAAGATCAGTGTCCCAAGGGATGTGATGTTGGAGGAGCTGTCCCTTCTTACCAACCGAGG
CTCCAAGATGTTCAAGCTACGGCAGATGCGGGTGGAGAAATTTATCTATGAGAATCACCCCGATGTTTTC
TCTGACAGCTCAATGGATCACTTCCAGAAGTTTCTTCCCACAGTGGGAGGACAGCTGGAGACAGCTGGTC
AGGGCTTCTCATATGGCAAGGGCAGCAGTGGAGGCCAGGCTGGCAGCAGTGGCTCTGCTGGACAGTATGG
CTCTGACCGTCATCAGCAGGGCTCTGGGTTTGGAGCTGGGGGTTCAGGTGGTCCTGGGGGCCAGGCTGGT
GGAGGAGGAGCTCCTGGCACAGTAGGGCTTGGAGAGCCCGGATCAGGTGACCAGGCAGGTGGAGATGGAA
AACATGTCACTGTGTTCAAGACTTATATTTCCCCATGGGATCGGGCCATGGGGGTTGATCCTCAGCAAAA
AGTGGAACTTGGCATTGACCTACTGGCATACGGTGCCAAAGCTGAACTCCCCAAATATAAGTCCTTCAAC
AGGACAGCAATGCCCTACGGTGGATATGAGAAGGCCTCCAAACGCATGACCTTCCAGATGCCCAAGTTTG
ACCTGGGGCCTCTGCTGAGTGAACCCCTGGTCCTCTACAACCAGAACCTCTCCAACAGGCCTTCTTTCAA
TCGAACCCCTATTCCCTGGTTGAGCTCTGGGGAGCATGTAGACTACAACGTGGATGTTGGTATCCCCTTG
GATGGAGAGACAGAGGAGCTGTGAAGTGCCTCCTCCTGTCATGTGCATCATTTCCCTTCTCTGGTTCCAA
TTTGAGAGTGGATGCTGGACAGGATGCCCCAACTGTTAATCCAGTATTCTTGTGGCAATGGAGGGTAAAG
GGTGGGGTCCGTTGCCTTTCCACCCTTCAAGTTCCTGCTCCGAAGCATCCCTCCTCACCAGCTCAGAGCT
CCCATCCTGCTGTACCATATGGAATCTGCTCTTTTATGGAATTTTCTCTGCCACCGGTAACAGTCAATAA
ACTTCAAGGAAATGAAAAAAAAAAAAAAAAAAAA -3′
```

Figure 1.6 mRNA sequence of calsarcin-1. Sequence homology between the three calsarcin proteins was strongest at the 5' and 3' regions. The central region of the three transcripts shared little sequence homology.

Northern blot analysis was performed using RNA extracted from human and mouse tissues, and from C2C12 cells grown in culture. Expression of both

calsarcin-1 and calsarcin-2 was restricted to striated muscle. Calsarcin-1 was expressed only in the heart and skeletal muscle in both humans and mice (Frey, 2000). In humans, two distinct mRNA's were identified by Northern blotting of calsarcin-1, one of 1.3 kb, and one of 2.6 kb. Mouse calsarcin-1 had only a single transcript of 1.3 kb. Calsarcin-2 expression was limited to skeletal muscle, the human calsarcin-1 expressed a mRNA of 1.6 kb, and in mice the mRNA was 1.3 kb in length (Frey, 2000).

To evaluate the embryonic expression of calsarcin-1 and calsarcin-2, the study employed *in situ* hybridization analysis of sections taken from mouse embryos. Low levels of calsarcin-1 expression was first observed in the embryonic heart at day E9.5, and stronger expression was observed in both heart and skeletal muscle tissue at days E12.5 and E15.5 (Frey, 2000). Expression of calsarcin-2 showed an inverse pattern to calsarcin-1 expression, calsarcin-2 was strongly expressed in cardiac muscle at day E9.5, and expression was still visible, but weaker at day E12.5. Faint expression of calsarcin-2 was also observed in the tongue at day E12.5. Expression was upregulated in skeletal muscle at day E15.5, but was downregulated in the heart (Frey, 2000). Calsarcin-1 expression was still robust in cardiac muscle into adulthood, and also present in slow-twitch skeletal muscle. In the early stages of embryogenesis, calsarcin-2 was transiently expressed in cardiac muscle, but became restricted to skeletal muscle in later stages and into adulthood. (Frey, 2000)

Further analysis by *in situ* hybridization showed that calsarcin-1 and calsarcin-2 were expressed preferentially in different fiber types (Frey, 2000). Sections of adult mouse hindlimb were hybridized with probes specific for either calsarcin-1 or calsarcin-2, and showed that expression of calsarcin-1 was restricted to the soleus and plantaris muscles, consisting primarily of slow-twitch fibers. The *in situ* studies were confirmed by western blotting, using proteins extracted from adult tissues. Calsarcin-1 protein was detected in the heart and soleus muscle, but was absent from the gastrocnemius, and other non-muscle tissues (Frey, 2000).

To analyze the expression of the calsarcin genes in C2C12 myoblasts grown in culture, RNA was extracted from myoblasts and from cells after the onset of differentiation. Calsarcin-2 expression was not detected at any stage by RT-PCR. Calsarcin-1 expression was absent in myoblasts, but was upregulated at day 2 post-differentiation (Frey, 2000).

A second two-hybrid screen was utilized to identify possible interacting proteins with the calsarcins (Frey, 2000). Full length calsarcin-1 and calsarcin-2 proteins were expressed as fusions with the Gal4 DNA binding domain, and used as bait to screen the same adult human heart library that was used in the original screen. The screen identified 2 possible binding partners for calsarcin-1, α-actinin-2 and α-actinin-3. Filamin-C, the muscle specific isoform of filamin, and α-actinin-2 were identified as interacting partners with calsarcin-2 (Frey, 2000).

These interactions, as well as the interaction of calsarcin-1 and calsarcin-2 with CnA were confirmed by co-immunoprecipitation. Immunohistochemical analysis also demonstrated that α-actinin-2 was only able to co-precipitate with calcineurin in the presence of calsarcin-1, indicating the presence of a complex (Frey, 2000).

A similar strategy of a yeast two-hybrid screen, followed by co-immunoprecipitation, was used to map the interacting domains between calsarcin-1, calcineurin, and α-actinin (Frey, 2000). The two-hybrid screen demonstrated that amino acids 153-200 of either calsarcin protein was necessary for binding with α-actinin-2 (Figure 4). This area of the protein is highly conserved between calsarcin-1 and calsarcin-2, and between the human and mouse homologues of each gene. A calsarcin-1 mutant lacking its carboxy terminus, amino acids 217-264, was unable to bind to CnA, indicating that the calcineurin interaction domain was contained in that region (Frey, 2000).

The second group to identify the calsarcin proteins also employed a yeast two-hybrid strategy, but they began by using α-actinin and filamin-c as bait to screen a human skeletal muscle cDNA library (Takada, 2001). The screen identified 10 clones that interacted with both α-actinin and filamin-c, containing the coding sequence of three distinct possible binding partners. Two of the proteins identified in the screen were previously characterized actin binding proteins, myopodin/genethonin-2 and synaptopodin (Takada, 2001). The third protein was not listed in any database at the time of the screen, except as ESTs. This

protein was later named calsarcin-2 by its discoverers at UT-Southwestern, but the Harvard group referred to it as myozenin (Takada, 2001).

Sequence analysis of the identified clones revealed a transcript of 1,266 bp, containing an open reading frame of of 900 bp. Northern blot analysis identified a 1.5 bp transcript present in human skeletal muscle, and expressed at much lower levels in the heart and in placenta (Takada, 2001). The predicted protein would weigh approximately 32 kd, and contained 2 alpha-helical domains connected by a glycine rich loop, and a C-terminal tail (Takada, 2001). The C-terminal tail was present in all the clones identified in both yeast two-hybrid screens. A mapping strategy employing truncated versions of the myozenin protein as bait identified amino acids 163-299 as necessary for binding with α-actinin, which would be consistent with the mapping data from the previous study (Frey, 2000; Takada, 2001).

Immunohistochemical analysis was utilized to observe the subcellular localization of myozenin. Transverse and longitudinal sections of human skeletal muscle were stained with four different antibodies specific for myozenin, and all four gave similar results (Takada, 2001). In transverse sections, the myozenin protein was expressed in all fibers. In longitudinal sections, myozenin appeared localized to the sarcomere, in a striped pattern consistent with sarcomeric localization (Figure 5). Co-staining with antibodies for myosin or tropmyosin indicate that myozenin localization was restricted to the middle of the I bands.

Immunogold staining and transmission electroscopy demonstrated that myozenin localized to the periphery of the Z-lines (Takada, 2001).

Concurrent with these two studies, Calsarcin-2 was also discovered by a laboratory in Italy utilizing a different strategy (Faulkner, 2000). The transcript of calsarcin-2 was identified in a project to sequence human skeletal muscle EST's undertaken by Centro di Ricerca Interdepartimentale per le Biotecnologie Innovative, of Padova Italy. After identifying the transcript, their experimental approach included a yeast two-hybrid assay which identified filamin-c, α-actinin, and telethonin as interacting proteins (Faulkner, 2000). Expression analysis and subcellular localization assays produced data that supported the previous findings, that FATZ was restricted to skeletal muscle, and that it localized to the Z line. The study authors named it FATZ for its binding partners, filamin, actinin and telethonin. The genes referred to as FATZ, myozenin, and calsarcin-2 are all the same transcript, which can be mapped to human chromosome 10q22.1 (Frey, 2000; Takada, 2001, Faulkner, 2000). Calsarcin-1 is located on human chromosome 4q26 (Frey, 2000).

A database search using the calsarcin-1 sequence and the tBLASTN algorithm identified a possible third member of the calsarcin family, on human chromosome 5 (Frey, 2002). Two sequences with strong homology to calsarcin-1 were amplified by PCR, and those sequences were used to screen a human skeletal muscle cDNA library. A 1 kb clone was identified from this screen and

sequenced. The open reading frame coded for a predicted protein of 251 amino acids. A close homologue found in mice had a predicted protein of 245 amino acids (Frey, 2002).

Similar to the characterization of calsarcin-1 and calsarcin-2, Northern blot analysis was utilized to investigate the expression of calsarcin-3. Northern blot analysis of adult tissues revealed that calsarcin-3 was restricted to skeletal muscle in both humans and mice. Probes revealed multiple different sizes of transcripts for calsarcin-3 in both humans and mice, suggesting the possibility of different isoforms and splice variants (Frey, 2002).

Similar to the previously described calsarcin proteins, calsarcin-3 co-immunoprecipitated with calcineurin and several Z-disc related proteins, including filamin-c, α-actinin-2, and telethonin. Co-immunoprecipitation with several deletion mutants of calsarcin-3 was also utilized to map the interacting domains of the protein with its binding partners (Frey, 2002).

In calsarcin-1 and 2, the carboxyl region is important for binding, but deletion of the C-terminal 141 amino acids of calsarcin 3 did not disrupt is ability to bind to any of its interacting partners (Frey, 2002). Deletion of the N-terminal 109 amino acids left calsarcin-3 unable to bind to calcineurin, filamin-c and telethonin, but still able to interact with α-actinin. Binding to α-actinin was disrupted by deletion

of amino acids 186-207, indicating that there may be two distinct and separate binding sites for α-actinin (Frey, 2002).

To identify novel interacting partners with the calsarcin proteins, a calsarcin-1 fusion protein was used as bait to screen a human skeletal muscle library in a yeast two-hybrid assay (Frey, 2002). This screen identified several clones related to ZASP/Cypher/Oracle, a PDZ domain protein expressed only in striated muscle. In a reverse screen, using a ZASP fusion construct as bait, the ZASP protein was able to interact with all three calsarcin proteins (Frey, 2002).

Immunohistochemical analysis demonstrated that calsarcin-3 was localized to the Z disc, in a pattern similar to the other calsarcin proteins, and that it was expressed predominantly in fast-twitch skeletal muscle (Frey, 2002) (Figure 6). Immunostaining in longitudinal sections of mouse hindlimbs showed the striated pattern associated with sarcomeric proteins. Co-staining with a myosin antibody demonstrated that calsarcin colocalized with fast myosin in fast twitch fibers.

Another recently described Z-disc protein, myotilin (Salmikangas 1999), was also found to interact with calsarcin-2 (Gontier, 2005). Similar to the discovery of the calsarcin family proteins, myotilin was identified using a yeast two-hybrid screen that employed the spectrin-like repeat domains of α-actinin as the bait to screen a human skeletal muscle library (Salmakingas 1999). The myotilin cDNA contained an open reading frame of 498 amino acids, coding for a 57 kd protein

that was expressed primarily in striated muscle. The α-actinin binding site was located in the N-terminal segment of the protein, and the C-terminus contained a domain capable of interacting with filamin-c, the muscle specific isoform of filamin, and another Z-disc related protein (Salmikangas, 1999). Myotilin plays an important role in the assembly of the sarcomere by crosslinking actin filaments, and a mutation in the myotilin gene has been linked to the occurrence of limb-girdle muscular dystrophy (Hauser, 2000).

Because myotilin and calsarcin-2 shared 2 known binding partners in α-actinin and filamin-c, researchers examined the possibility that these two Z-disc proteins could also interact with each other (Salmikangas, 1999). Immunohistochemical co-staining with antibodies for calsarcin-2 and mytotilin in sections of human skeletal muscle demonstrated that the two proteins co-localized to the Z-discs along the striations of myofibers. When the two proteins were overexpressed in CHO cells, the 2 proteins again co-localized along the actin filaments. When transfected separately, myotilin again localized to the actin cytoskeleton, but calsarcin-2 showed a more dispersed and punctuated expression pattern, indicating that myotilin was able to interact with the actin cytoskeleton, and the distribution of calsarcin-2 was directed by a possible interaction with myotilin (Gontier 2005).

To further investigate the interaction between myotilin and the calsarcin proteins, fusion constructs expressing either the C-terminal or N-terminal segments of

myotilin fused to GST were generated, and incubated with glutathione-agarose beads for a GST-pulldown assay. Full length calsarcin-1 and calsarcin-2 were expressed, fused to HA, and overexpressed in CHO cells. After cell lysates were incubated with the myotilin-GST constructs, western blot analysis revealed that both calsarsin-1 and calsarcin-2 were able to interact with constructs containing full length myotilin. However, both calsarcin proteins had only weak interactions with either the C-terminal (amino acids 1-250) or N-terminal (amino acids 215-498) myotilin constructs. The C- and N- terminal constructs were capable of binding α-actinin and actin, as had been shown in previous studies, so these data seemed to indicate that the full length of the myotilin protein was necessary for strong interaction with proteins from the calsarcin family. Further studies using GST-myotilin and HA-tagged myotilin demonstrated that the protein would form homodimers, and that this dimerization was necessary for interaction with the calsarcin proteins (Gontier, 2005).

Several more fusion constructs were generated, in an effort to map the binding domains of myotilin and the calsarcin proteins. A second yeast two-hybrid assay was performed, confirming that myotilin was able to homodimerize, and identifying the Ig domains in the proteins C-terminal region as necessary for binding. Truncated constructs of myotilin were unable to bind either of the calsarcin proteins, similar to the results of the GST-pulldowns. These results suggest that the full length of myotilin may be required for efficient binding with

calsarcin proteins, or that truncation may alter the protein's tertiary structure in a way that weakens their binding with calsarcins (Gontier, 2005).

Full length calsarcin-1 and calsarcin-2 were able to associate with myotilin in the yeast two-hybrid assay. However, when specific domains of calsarcin-1 were tested for binding, only the CD2 domain, composed of amino acids 163-299, yielded a positive result from the two-hybrid assay, indicating that this region is required for interaction with myotilin, and that other regions of the protein did not play an essential role.

Because myotilin and calsarcin-2 had both previously been shown to bind to filamin-c (Van der Ven, 2000 and Faulkner, 2001), researchers also investigated their interactions with the other filamin proteins. Another GST-pulldown assay was performed, using GST-myotilin and GST-calsarcin-2 constructs immobilized on glutathione-agarose beads. Results indicated that all three full length filamin proteins were able to interact with both myotilin and calsarcin-2. A recently identied splice variant of filamin-b, lacking a 41 amino acid segment between repeats 19 and 20, also was able to interact with both myotilin and calsarcin-2. In a separate assay, it was also demonstrated that filamin-c and both filamin-b variants were able to bind to the β1A subunit of integrin, but filamin-A was unable to interact with β1A (Gontier 2005). This interaction with integrin suggests that filamin-c may connect the other Z-disc proteins to the sarcolemma, through an interaction with β1A-integrin subunit.

Taken together, these data demonstrating a common ability to bind other Z-disc proteins suggest the possibility of overlapping functions amongst members of the calsarcin family, and the filamin family of proteins. The association of calsarcin proteins with myotilin also indicates a possible role for calsarcin-2 in limb-girdle muscular dystrophy, the first indication that the calsarcin proteins could be involved in a specific pathological condition. The interaction between calsarcin-2 and filamin-c was previously established (Frey, 2002), but the demonstration of an interaction of calsarcin-2 and other Z-disc proteins with the other members of the filamin family suggests the possibility of another functional role for the filamin proteins.

Filamin-c is the largest of the filamin proteins, containing an 81 amino acid hinge region between its 23rd and 24th Ig-like repeat domain, and raising its molecular mass to 300 kd. Unlike filamin-a and filamin-b, which are expressed ubiquitously (Takafuta 1998, and Hock 1990), filamin-c expression is restricted to skeletal and cardiac muscle (Thompson, 2000 and van der Ven 2000). Specifically, immunohistochemical assays and microscopy have shown that filamin-c dimerizes to form a complex at the myotendinous junctions in skeletal muscle, and the intercalated discs in cardiac tissue (van der Ven, 2000).

The localization of filamin-c to the Z-disc and its interaction with calsarcin-2 connect it to the calcineurin signaling pathway. However filamin-c also has been

shown to interact with the kelch family protein Krp1, one of the closest homologues to MKRP (Lu, 2003). This interaction was observed during a yeast two-hybrid screen to identify possible interacting partners with the actin binding protein N-RAP. N-RAP is found at the Z-disc, consistent with other calsarcin and filamin interacting proteins, as well as binding to the actin filaments (Carroll, 2001). Both filamin-c and Krp1 were identified as N-RAP binding partners in the two-hybrid screen, and confirmed by GST-pulldown assay. The authors of this study proposed a mechanism by which N-RAP, filamin-c, and Krp1 would all play a role in myofibril assembly, a mechanism that involved the ability of filamin proteins to bind to integrins (Pfaff, 1998) and sarcoglycans (Thompson, 2000), and the interaction of N-RAP with β-integrins, through its binding to talin (Luo, 1999). The authors observed that Krp-1 localized to the periphery of fusing myofibrils and it specifically binds to the same regions of N-RAP that interact with actin and α-actinin (Carroll, 2001), all suggesting that Krp-1 could play a significant role in the final stages of myofiber assembly. The authors proposed that the interaction of Krp-1 with both N-RAP and actin would mediate the dissociation of N-RAP, thus allowing lateral fusion of myofibers to proceed. The proposed model of N-RAP's role in myofibril assembly was supported by later studies using siRNA to transiently inhibit expression of N-RAP (Dhume, 2006). Knockdown of N-RAP by SiRNA resulted in a reduction in myofibril assembly, and changes in the organization of α-actinin. The protein levels of N-RAP binding partners α-actinin, Krp1, and muscle LIM domain proteins was unaffected by the inhibition of N-RAP.

Krp-1 is a BTB/Kelch-domain protein (Spence, 2000) and the closest known homologue of MKRP. The mRNA sequence of MKRP shows greater than 50% homology with the sequences of human and rat Krp-1. Krp-1 was first identified in a subtractive hybridization assay screening for genes that were upregulated in malignant tumors (Spence, 2000). Overexpression of Krp-1 resulted in the growth of pseudopodia, and the authors of the study speculated that Krp-1 could play a role in the migration and invasive mechanism of malignant cells.

These data taken together suggest a role for MKRP and calsarcin-2 in the calcineurin signaling pathway during myoblast differentiation, and also a possible role for MKRP in myoblast migration during development, and skeletal muscle regeneration after injury.

Models of Injury

Researchers have utilized several different models or methods of injury to study the mechanism of skeletal muscle regeneration, including the injection of chemical toxins, as well as crush and freeze injuries. Several different chemical toxins have demonstrated the ability to create a reproducible injury in mammalian skeletal muscle, including cardiotoxin, notexin, and barium chloride.

Cardiotoxins (CTXs), derived from cobra venom, are small polypeptide molecules, approximately 60 amino acids in length, and 6.5-7.0 Kda in weight. The venoms of different species of cobras, genus *naja,* will usually contain five different but homologous cardiotoxin molecules. Cardiotoxins comprise approximately 45-55% of the volume of cobra venom (Bougis, 1986) which will also include various neurotoxins, and phospholipase A2. Their secondary structure consists of four beta sheets connected by three extended loops (Figure 1), that are linked by four disulfide bridges, and create a finger-like tertiary structure (Kumar, 1997). In all cardiotoxins the N-terminal beta-sheet will be double stranded and the third sheet, between loops 2 and 3, will be triple stranded. All cardiotoxins are highly basic, and share 90% amino acid sequence homology (Dufton and Hider, 1983).

Two distinct forms of cardiotoxin have been identified distinguished by their mode of binding to membrane phospholipids, and the presence or absence

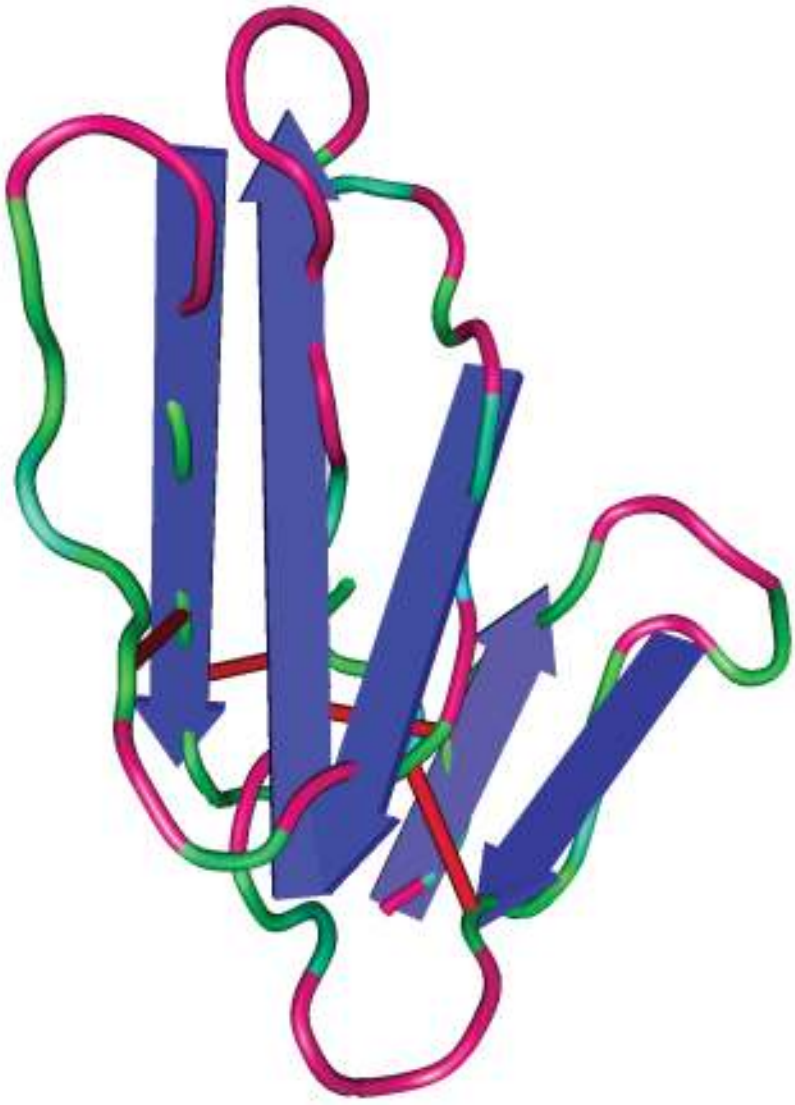

Figure 1.7 Tertiary structure of CTX II. The five beta sheets and three loops form a fingerlike structure that plays an important role in the binding of cardiotoxin molecules to zwitterionic membrane phospholipids. The hydrophobic regions, highlighted in red, allow the protein to penetrate the lipid membrane. This image was generated from the crystal structure of cardiotoxin IV, from the Tawain cobra (*Naja atra*), file 1UG4A0 in the NCBI database, using Cn3D 4.1 software.

of two conserved amino acid residues (Chien, 1994). A proline residue at AA 31 identifies P-type cardiotoxins, and is required for the binding of loop 2 with phospholipids. S-type cardiotoxins interact with phospholipids only through a binding site on loop 1. S-type cardiotoxins lack the proline residue at Pro-31, but all contain a conserved Serine residue at AA 29. P-type cardiotoxins demonstrate stronger binding and fusion with the lipid membrane, due to the additional phospholipid binding site in loop 2 (Chien, 1994).

After binding with zwitterionic phospholipids, a P-type cardiotoxin will begin the insertion phase, as the three hydrophobic loops are inserted into the membrane bilayer, and the tips of the loops come together to form a single column (Dubovskii, 2003). CTX insertion leads to the fusion of membrane lipids into aggregates, and the lysis of the cell. Cardiotoxins also have been shown to block the function of the inward rectifying K^+ channel, while simultaneously inducing the formation of new outward rectifying non-specific ion channels, leading to the depolarization of the membrane (Fletcher, 1991). S-type cardiotoxins have been shown to demonstrate stronger depolarization activity in muscle cells, while P-type cardiotoxins have shown stronger hemolytic properties (Dufton and Hider 1983, Chien 1994).

Cardiotoxin has also been shown to inhibit the signaling of Protein Kinase C (PKC) (Chiou, 1993). PKC is a membrane bound protein involved in signal transduction. Cardiotoxins with the highest Hydrophobic Index are the strongest

inhibitors of PKC, but also demonstrate the weakest hemolytic activity (Chiou 1995).

Notexin is another toxin purified from snake venom, taken from the Australian Tiger Snake, *Notechis scutatus scutatus (*Karlsson, 1972*).* In addition to directly causing the necrosis of muscle cells, notexin also has been shown to interfere with nerve signal transmission at the neuromuscular junctions by inhibiting the release of acetylcholine (Harris 1973). The notexin molecule has a similar secondary structure to Phospholipase A2, found in cobra venom, and their primary sequences differ in only seven positions (Karlsson, 1972; Halpert, 1975; Carredano 1998). The notexin protein is 120 amino acids in length with a weight of approximately 14 KDa (Karlsson 1972). Its secondary structure forms 3 large alpha-helices and a single two-stranded beta sheet. The tertiary structure is stabilized by seven disulfide bridges.

Phospholipase A2 catalyzes the hydrolysis of 3-sn-phosphoglycerides in the plasma membrane (Van den Bosch, 1965; Waite, 1967). By hydrolyzing the lipids of the sarcolemma, notexin causes degradation and depolarization of the membrane. The basil lamina is unaffected by the toxin, and remains intact. During regeneration, the basement membrane serves as a scaffold for regenerating cells, and re-innervation by neurons (Sanes 1978). Influx of Ca^{2+} during the disruption of the membrane causes the activation of Ca^{2+} proteases.

Barium Chloride is another chemical that is used to create a reproducible injury in myofibers. Similar to cardiotoxin, $BaCl_2$ depolarizes the cell membrane by inhibiting the inwardly rectifying potassium channel. Injuries induced by $BaCl_2$ leave the basement membrane undamaged, and full regeneration is achieved in 10-15 days, consistent with other injury models (Table 1). Regenerated, centrally nucleated myofibers are observed by day 5 post injury, and muscle architecture is primarily restored by day 15 post injury (Caldwell, 1990)

Crush injuries have also been used to study the regeneration of damaged myofibers. Instruments have been developed to create injury with a reproducible amount of force, with the intention of creating a standard injury (Jarvinen and Sorvari, 1975). However, unlike the injection of myotoxins, the crush injury will often cause disruption to the basement membrane, and damage both the vascular supply and nerve structure in the injured tissue, which has been shown to delay regeneration (Vrako and Benditt 1972). Recent studies comparing crush injury to notexin injection in the soleus muscle of rats demonstrated that Myosin Heavy Chain (MHC) fast type isoforms were still present in crush injured soleus at 56 days post injury, but had disappeared in notexin injured soleus by day 28 (Fink 2003). In the same study, citrate synthase activity was also markedly lower in crush injured muscle, compared to notexin injured tissue Creatine kinase levels were also lower in crush injured muscle, but levels were restored in the late stages of regeneration, and were equal with notexin injured and control tissues by day 42. Lactate dehydrogenase levels in

crush injured muscle were also much lower than notexin injured samples, and were still depressed after 56 days.

Injury	Source	Structure	Mechanism	Notable.
Cardiotoxin	Cobra venom	62 AA polypeptide, 3 loops and 4 beta sheets	Inserts into membrane, causing lipids to aggregate. Causes depolarization of membrane.	No damage to basement membrane. Reproducible injury.
Notexin	Snake venom	120 AA polypeptide, 3 alpha helices and 1 beta sheet.	Hydrolyzes membrane lipids. Inhibits acetylcholine release.	Inhibits nerve signal transmission at neuromuscular junctions.
$BaCl_2$	Chemical synthesis	Small molecule.	Blocks the inwardly rectifying K+ channel. Causes membrane depolarization.	Used less frequently than cardiotoxin or notexin.
Crush	Variable	N/A	Mechanical disruption of cells.	Also damages vascular and nerve tissue.

Table 1.1 Injury models. A comparison of the various models used to indue injury for regeneration studies.

Materials and Methods

Cardiotoxin-induced skeletal muscle injury

Adult male C57BL/6 or calsarcin-2 null mice were bred according to the guidelines of the NIH and the Institutional Animal Care and Use Committee at UT Southwestern Medical Center. For the microarray and *in situ* hybridization analyses, the gastrocnemius muscle of twenty-one adult male C57BL/6 mice 2–6 months of age were injured by the intramuscular injection of 150 µl cardiotoxin (10 µM, *Naja nigricollis*; Calbiochem, La Jolla, CA) (Garry, 1997). Injured (n= 3) and uninjured mice (n=3) were sacrificed at specific time points, and the gastrocnemius muscles were harvested at 6 hours, 12 hours, 24 hours, 2 days, 5 days, 7 days or 14 days postinjury. Tissue samples were either snap frozen in liquid nitrogen and stored at -80°C or fixed overnight in a 4% paraformaldehyde/DEPC-PBS solution following Avertin-induced anesthesia and transcardiac perfusion with 10 ml of 4% paraformaldehyde/DEPC-PBS. Fixed tissues were washed three times for 5 minutes in phosphate buffered saline (PBS) at 4°C and then paraffin embedded for sectioning by rotary microtomy. 5 µm-thick sections of each sample were cut and mounted on slides treated with

Vectabond (Vector Labs, Burlingame, CA). Total RNA was isolated from frozen, unfixed tissues with TriPure isolation reagent (Roche, Basel, Switzerland) and processed for the microarray and RT-PCR analyses, as described below.

For the first injury regeneration assay in calsarcin2-/- mice, two adult male calsarcin2-/- mice two months of age, and two wild type littermates were injured by the injection of 150 µl cardiotoxin (10 µM, *Naja nigricollis*; Calbiochem, La Jolla, CA) into the gastrocnemius muscle of both hindlimbs. One calsarcin2-/- and one wild type mouse were sacrificed at 7 days post injury, and at 14 days post injury, and the gastrocnemius muscles were harvested after transcardiac perfusion with 10 ml of 4% paraformaldehyde/DEPC-PBS. Tissues were post fixed in 10 ml of 4% paraformaldehyde/DEPC-PBS overnight at 4°C, then washed 3 times in PBS for five minutes at 4°C. After washing, tissues were paraffin embedded for sectioning by rotary microtomy.

For the second calsarcin2-/- injury regeneration assay, a two month old adult male calsarcin2-/- mouse and a wild type littermate were injured by the intramuscular injection of 250 µl of cardiotoxin into the gastrocnemius muscle of both hindlimbs. Both mice were sacrificed at 14 days post injury after Avertin anesthesia, and transcardiac perfusion by 10 ml of 4% paraformaldehyde/DEPC-PBS. The gastrocnemius muscles were harvested and incubated overnight in 4% paraformaldehyde/DEPC-PBS at 4°C. Tissues were washed three times in

PBS for 5 minutes at 4°C, and then paraffin embedded for sectioning by rotary microtomy.

Riboprobe synthesis

I.M.A.G.E. Clone 138815 was sequence-verified and prepared for in vitro transcription following restriction enzyme digestion and gel isolation using the Qiaquick Gel extraction kit (Qiagen, Valencia, CA). The DNA fragment was visualized in a 1% agarose gel by ultraviolet light. The DNA was then excised from the gel and the gel was melted in a high salt buffer. DNA was precipitated by the addition of isopropanol, and the solution was decanted into a QIAquick filtration column and centrifuged to bind the DNA to the membrane. DNA was eluted from the membrane by the addition of 50 µl of RNAse-free H_2O and centrifugation for a minute.

500 ng of linearized template was transcribed using the T7 RNA polymerase (Ambion, Austin, TX) with 7.0 µM [α-35S]UTP (1,000 Ci/mmol; Amersham, Piscataway, NJ) to produce the 366-bp sense and antisense riboprobes. The probes were purified with MicroSpin G-50 Columns (Amersham, Piscataway, NJ), and stored at -80°C (Shelton, 2000; Goetsch 2003).

In situ hybridization

Prior to hybridization, slides were preheated at 58°C for 30 min. Slides were then deparaffinized in xylene and hydrated through a series of graded ethanol/DEPC-saline rinses from 95% ethanol to 85%, 60%, 30% and then DEPC-saline. The slides were then transferred to upright plastic racks and immersed in DEPC-1X Antigen Retrieval Citra pH 6.0 (Biogenex, San Ramon, CA). The slides were then heated in a 750 watt microwave at 90% power for 5 minutes. Evaporated retrieval solution was replaced with additional DEPC-H_2O, and the slides were heated at 60% power for 5 minutes. The slides were cooled for 20 min, then washed twice in DEPC-PBS, pH 7.4, for 5 minutes each in metal racks, at room temperature. The slides were fixed for 20 min in 4% paraformaldehyde/DEPC-PBS, pH 7.4, and washed twice in DEPC-PBS, pH 7.4, for 5 minutes. The slides were permeabilized for 7 minutes with 20 µg/ml pronase-E in 50 mM Tris-HCl, pH 8.0/5 mM EDTA, pH 8.0/DEPC-H_2O and then washed for 5 minutes in DEPC-PBS, pH 7.4, to remove excess. The sections were then fixed in 4% paraformaldehyde/ DEPC-PBS, pH 7.4, for 5 minutes and then washed in DEPC-PBS, pH 7.4, for 3 min. After refixing, the slides were acetylated by incubation in 0.25% acetic anhydride/0.1 M triethanolamine–HCl, pH 7.5, for 5 minutes, and repeated. The slides were then equilibrated in 1X SSC, pH 7.0, for 5 minutes, followed by incubation in 50 mM n-ethylmaleimide/1X SSC, pH 7.0, for 20 minutes. After incubation, the slides were again washed in DEPC-PBS, pH 7.4, for 5 minutes, and DEPC-saline for 5 minutes. The slides were then dehydrated through graded ethanol/DEPC-saline rinses inverse to the hydration step, 30% ethanol to 60%,

85%, 95%, and finally absolute ethanol. The slides were allowed dry under vacuum for 2 hours.

Riboprobes were diluted in aliquots of hybridization mixture containing 50% formamide, 0.3 M NaCl, 20 mM Tris-HCl, pH 8.0, 5 mM EDTA, pH 8.0, 10 mM $NaPO_4$, pH 8.0, 10% dextran sulfate, 1 x Denhardt's, and 0.5 mg/ml tRNA in sufficient volume to achieve 7.5 x 10^3 cpm/µl and the mixture heated to 95°C for 5 min. The diluted probes were cooled to 55°C and 1M DTT was then added to reach a final concentration of 10 mM DTT. The riboprobe was applied directly to the sections, and the slides were then placed in a Nalgene utility box lined with gel blot paper, soaked in 5X SSC/50% formamide. The slides were covered with parafilm, and the box was sealed. The slides were allowed to hybridize for 14 hours at 55°C.

After hybridization, the parafilm was removed and the slides were washed in 5X SSC/10 mM DTT at 55°C for 40 minutes in plastic racks. The slides received a second wash for 30 minutes in HS (2 x SSC/50% formamide/100 mM DTT), at 65°C. This was followed by three 10 minute washes in NTE (0.5 M NaCl/10 mM Tris-HCl, pH 8.0/5 mM EDTA, pH 8.0), at 37°C. After the third wash, the slides were placed in an NTE wash containing RNase-A (2 µg/ml) and incubated for 30 minutes at 37°C. The slides were then washed in NTE for 15 minutes at 37°C, to remove RNase-A, and incubated in HS for another 30 minutes at 65°C. After HS treatment, the slides were washed for 15 minutes at 37°C in 2X SSC followed by 15 minutes in 0.1x SSC. The slides were then dehydrated in graded ethanol

rinses (30%, 60%, 85%, 95%) to absolute ethanol, and allowed to dry under vacuum.

While the slides were allowed to dry, Ilford K.5 nuclear emulsion (Polysciences, Warrington, PA) was prewarmed to 42°C, in a darkroom. After drying, the slides were dipped in the nuclear emulsion, and then hung vertically to dry at room temperature and 75% humidity, for 3 hours. The slides were placed into slide storage boxes with desiccant, and the boxes were then sealed with tape, wrapped in foil, and stored at 4°C for 14-21 days. After 2-3 weeks of autoradiographic exposure, the slides were developed in Kodak D19® Film Developer (Eastman Kodak, Rochester, NY) at 14°C. Latent images were fixed with Kodak Fixer. The slides were then rinsed, counterstained with hematoxylin (Richard-Allen, Kalamazoo, MI), dehydrated, and coverslipped with permanent mounting media (Shelton, 2000).

Cell culture studies

C2C12 myoblasts (derived from myogenic progenitor satellite cells) were cultured as monolayers in Dulbecco's modified Eagle's medium (DMEM), supplemented with 20% fetal bovine serum (FBS), and 100 U/ml penicillin/100 µg/ml streptomycin. Media was made in 500 ml aliquots by adding 100 ml of FBS to 400 ml DMEM, with 5 ml of 1X penicillin/streptomycin, and filtered through a 0.22 µm GP membrane (Millipore, Billerica Mass.) (Goetsch, 2003; Martin, 2004). The

induction of differentiation was initiated by switching 80% confluent cells to differentiation media (DMEM, 2% heat-inactivated horse serum, 10 µg of insulin [GIBCO/BRL, Gaithersburg, Md.] per ml, and 10 µg of transferrin [GIBCO/BRL] per ml) (Bassel-Duby, 1992). Both myotubes and myoblasts were grown under normoxic conditions (21% oxygen, 5% CO_2) (Goetsch 2003, Martin, 2004). Differentiation was assessed morphologically by confocal microscopy, based on the appearance of multinucleated myotubes.

For RT-PCR analysis, medium was aspirated from the cells at specific time points, the monolayer of cells were rinsed with PBS, and RNA was harvested with TriPure isolation reagent (Roche, Basel, Switzerland), then stored at -80°C overnight.

For visualization by microscopy, cells were grown on glass coverslips then stained with Hoechst 33342 dye. Before staining, media was aspirated by pipet, and then the cells were washed twice with PBS for 2 minutes. PBS was removed by aspiration, and 0.5ml of 4% paraformaldehyde (PFA) was added to each well, and incubated on ice for 5 minutes. After incubation, cells were rinsed twice with PBS+ for 2 minutes. 10 µl of Hoechst dye 3342 was diluted 50:1 in 490 µl of PBS+, and 50 µl was used applied to each coverslip. The coverslips were incubated in the dark for 2 minutes, then rinsed twice with PBS+, and twice with distilled water. After staining, the coverslips were transferred to microscope slides treated with Vectabond (Vector Laboratories, Burlingame, CA).

Reverse transcription, real-time, and semi-quantitative PCR.

Total RNA was isolated with TriPure isolation reagent (Roche, Basel, Switzerland) and reverse transcribed with SuperScript II (Invitrogen, Carlsbad, CA) to cDNA in accordance with the manufacturers protocol, summarized as follows: Combine 1 µl of oligo(dT) 20 (50 µM) *or* 50 ng of random primers with 5 µg total RNA, 1 µl 10 mM dNTP Mix (10 mM each dATP, dGTP, dCTP and dTTP) and distilled water to a final volume of 13 µl, in a sterile microcentrifuge tube. Samples were heated at 65°C for 5 minutes, then incubated on ice for at least 1 minute. Samples were centrifuged and 4 µl 5X First-Strand Buffer, 1 µl 0.1 M DTT, 1 µl RNaseOUT (Invitrogen, Carslbad CA.) Recombinant RNase Inhibitor (Cat. no. 10777-019, 40 units/µl), and 1 µl of SuperScript™ III RT was added to each. Samples were mixed by pipetting, then incubated at 50°C for 45 minutes. After incubating the reaction was inactivated by heating at 70°C for 15 minutes.

RT-PCR was performed by established protocol (Garry, 1997), summarized as follows: 2 µl of each cDNA samples was combined with 11.04 µl of distilled water, 2 µl of 10X PCR buffer, 1.20 µl of 25mM MgCl, 0.40 µl of 10mM dNTP, 0.25 µl of the appropriate forward primer, 0.25 µl of the appropriate reverse primer, 2.76 µl of loading dye, and 0.10 µl of 5Units/ml Taq polymerase (GIBCO/BRL Gaithersburg, Md). Samples were heated to 94°C for 1.5 minutes,

then underwent 30 cycles of 94°C for 15 seconds to denature, 55°C for 15 seconds to anneal, and 72°C for 15 seconds to extend, and then a final 2 minutes at 72°C. Bands were visualized in a 1% agarose gel. Primer sets included: MKRP, forward TCCTTGTTGTCCTCATTGTAAGAAG -3', and reverse 5'- GTTCCTTCAGGATCTCATCTTCAT -3'.

18S rRNA, forward 5'- GGACCAGAGCGAAAGCATTTA -3' and reverse 5'-TGCCAGAGTCTCGTTCGTTAT -3'.

Myoglobin, forward, 5'- ACCATGGGGCTCAGTGATGGGGAG -3'; and reverse, 5'-CAGGTACTTGACCGGGATCTTGTGC -3'.

Myf5, forward, 5'- CTGTCTGGTCCCGAAAGAAC -3' and reverse 5'-AAGCAATCCAAGCTGGACAC -3'.

Myf6, forward, 5'- AATTCTTGAGGGTGCGGATT -3', and reverse 5'-ATGGAAGAAAGGCGCTGAAG -3'.

Myogenin, forward, 5'- GTGCCCAGTGAATGCAACTC -3' and reverse 5'-GCTGTCCACGATGGACGTAA -3'.

Realtime PCR was performed with the iCycler iQ real-time PCR detection system (Bio-Rad Laboratories, Hercules, CA) and the QuantiTect SYBR Green PCR kit (Qiagen, Valencia, CA) (Garry 1997, Garry, 2000) according to the manufacturers protocol, summarized as follows. The reaction was performed with 1µl SYBR Green PCR master mix, 0.3 µM each primer, 20 ng cDNA and distilled water to a final volume of 25 µl. The samples were incubated for 50 cycles of 20 seconds at 94°C, 20 seconds at 60°C, and 30 seconds at 72°C. The 75- to 100-

bp extension product was detected following each cycle and analyzed with the iCycler iQ software (Bio-Rad) for specificity, using melting curve, and threshold cycle (CT). Data are expressed with comparative CT method as an estimate of mRNA of target to reference control (Goetsch, 2003).

Northern Blot Analysis

The MKRP probe was synthesized using the Strip-EZ DNA Probe Synthesis Kit (Ambion; Austin, TX) in accordance with the manufacturers protocol, summarized as follows. Fifty nanograms of linearized W34362 cDNA and 5 µl of [^{32}P]dATP (1000 Ci/mmol; Amersham Biosciences, Piscataway, NJ) were combined with 2.5 µl of 10X Decamer solution, 5 µl of 5X Buffer –dATP/-dCTP, 2.5 µl dCTP 1 µl exonuclease free Klenow, and distilled water to a final volume of 25 µl. The probe was then diluted 1:50 in EDTA, and incubated at 95°C for 10 minutes. A commercially purchased Northern blot membrane (MTN blot; Clontech, Palo Alto, CA) containing full-length transcripts extracted from whole embryos at four specific stages of embryogenesis was incubated with the W34362 radioactive probe in 10 ml of Ultrahyb solution (Ambion; Austin, TX) in an 8 inch hybridization bottle at 42°C, with rotation, overnight. Hybridized membranes were washed twice in 2x SSC, 0.1% SDS at 42°C for 5 minutes at 42°C, and then twice for 15 minutes in 0.1X SSC and 0.1% SDS at 42°C. The membranes were then exposed to radiographic film at –80°C for 16 hours. A probe synthesized with ß-

actin cDNA, that was provided with the Northern blot membrane was used as a control, to demonstrate that all lanes were loaded equally with mRNA.

Vector Constructs

The full length of the MKRP open reading frame was amplified from 5 day injured skeletal muscle cDNA (prepared as described above) and the primer pair 5'-GAAGATCTTCCCTCGATACACAGACTTG-3' (forward), and 5'-CGGAATTCGCACTTGGTCAGGGCGAAG -3' (reverse) to amplify the 1820 bp mRNA. The kelch domain of MKRP was amplified using the primers 5'-GAAGATCTTCATGAGTGCTTACTTCCTGC-3' (forward) and 5'-CGGAATTCGCACTTGGTCAGGGCGAAG-3' (reverse). The BTB domain of MKRP was amplified using the primers 5'-GAAGATCTTCCCTCGATACACAGACTTG-3' (forward), and BTB-ECO 5'-GGAATTCCCAAGCACAGGCGCTTCTG -3'. The nuclear localization sequence was amplified with the primers 5'-GAAGATCTTCATGGTGAAGGATGCACATGAG -3' (forward) and 5'-GGAATTCCTGGCCCGAGCTGTCTGCTCACC -3' (reverse).

After gel extraction and restriction digest, the fragments were ligated into the Clontech pEGFP-N1 expression vector (Clontech, Mountain View, CA) by incubating 1 µl of 10 µg/ml of insert with 2 µl of 25 µg/ml vector in 5 µl of distilled water, 1 µl of 10X ligation buffer and 1 µl of T4 DNA ligase at 14°C overnight. After incubation, the ligation product was transformed into INVαF competent cells by adding 2 µl of each ligation mixture to a tube of cells thawed on ice, and

allowed to incubate on ice for 30 minutes. After incubation on ice, the cells were heatshocked in a 42°C water bath for 30 seconds. After heatshock, the cells were again placed on ice, and 250 µl of SOC media was added to each tube. The tubes were shaken at 200 rpm for 1 hour, while incubating at 37°C. 200 µl and 20 µl of each culture spread on plates inoculated with kanamycin, and incubated at 37°C overnight. Colonies were selected and grown in 5 ml of LB media inoculated with kanamycin, and incubated at 37°C overnight. DNA was extracted using the Qiagen miniprep kit (Qiagen, Valencia CA).

C2C12 cells (cultured as described above) were transfected at 60-80% confluency with the MKRP-GFP constructs, using Lipofectamine Plus (GIBCO/BRL; Gaithersburg, Md) utilizing the manufacturers protocol, as summarized here. For each well of a 6 well culture plate, 1 µl of 1 µg/ml plasmid DNA was pre-complexed with 6 µl of Plus Reagent (GIBCO/BRL; Gaithersburg, Md) and 100 µl of DMEM without serum, and allowed to incubate at room temperature for 15 minutes. In a separate tube, 4 µl of Lipofectamine Plus (Gibco BRL) was diluted into 0.8 ml of DMEM, without serum. The two solutions were then combined and allowed to incubate at room temperature for 15 minutes. 1 ml of transfection solution was added to each well, and allowed to incubate for 6 hours at 37°C. After incubation, the transfection media was removed by aspiration, and the cells were returned to growth media.

Preperation and transfection of siRNAs

siRNAs targeting MKRP were designed by established guidelines (Elbashir, 2000) and tested utilizing the BLAST local alignment search tool of GenBank (National Center for Biotechnology Information database) to ensure that only MKRP was targeted by the oligos. RNA oligonucleotides were processed by the core facility at University of Texas Southwestern Medical Center, and Ambion Biotechnologies (Applied Biosystems, Foster City CA). The oligo 5'-GUGGACCUCCUUUGAGGCCUU-3" and its complement strand were synthesized by the UT-Southwestern core facility, and were annealed by combining 40 µl of 50 µM sense oligo with 40 µl of 50 µM anti-sense oligo in 10 µl of 10X annealing buffer and 10 µl of RNAse-free water. The solution was heated at 90°C for 2 minutes to ensure the primers were linear, and then centrifuged for 15 seconds at 14,000 RPM. After centrifugation, the primers were incubated at 37°C for 1 hour to anneal the sense and antisense strands. Primers were stored at -20°C after annealing. The annealing buffer was composed of 5 ml 2M KOAc, 3ml 1M HEPES-KOH (pH 7.4), 0.2ml 1M MgOAc, and 1.8 ml of RNAse-free water, for a total volume of 10 ml (Suzuki, 2004).The oligos 5'-cgggatcccgtatctcatgtggccactcctg-3' and 5"- cgggatcccgttgcagaaaggtgggcag-3' were ordered from Ambion (Applied Biosystems, Foster City CA), and were synthesized pre-annealed with their anti-sense strands.

One day before transfection, cells were plated so that they were 30–50% confluent the following day. Cells were transfected with 100 nM of siRNA using Oligofectamine transfection reagent (Invitrogen) according to the manufacturers

protocol, and summarized as follows. For a 6-well plate, 60 pmol of siRNA oligo was diluted into Opti-MEM I reduced serum medium (Invitrogen) and mixed by pipetting, for 5 minutes. For each reaction, 3 µl of Oligofectamine was mixed with 12 µl of Opti-MEM and allowed to incubate at room temperature for 5 minutes, in the dark. The diluted DNA was added to the Oligofectamine/Opti-MEM solution, and incubated at room temperature for 20 minutes, in the dark. 60 µl of the siRNA solution was added to each well, and incubated at 37°C for 6 hours, then returned to growth media. For the differentiation assay, cells were changed to low serum media as described above, 24 hours after transfection.

Wound Assay

C2C12 cells were grown to 40% confluency and transfected with an siRNA oligo specific for MKRP as described above. Eighteen hours after transfection, a 1mm wide scrape was made at the center of a marked plate, with a sterilized pipet tip. Photomicrographs of the wounded area, using the markings on the bottom of the plate as guidelines, were taken immediately after the wound was created, and then 24 hours, 36 hours, and 40 hours later. The wounded area was visualized with a Leitz Laborlux-S microscope (Leitz; Wetzler, Germany) equipped with plan-apochromatic optics, standard bright-field condenser, and a Mears low-magnification dark-field condenser (MearsCorp; Waltham, MA). Photomicrographs were captured with an Optronics VI-470 CCD camera and Scion Image 1.62 software on a Power Macintosh G4.

TUNEL assay

Cells grown on coverslips were washed with PBS and fixed with 4% paraformaldehyde/PBS (pH 7.4) for 15 minutes. Degraded DNA was labeled with the Promega DeadEnd Flourometric TUNEL system (Promega, Madison, Wi) according to the manufacturers protocol. After fixation, cells were washed in PBS twice for 5 minutes, and 100 µl of Equilibration Buffer was applied to each coverslip, and allowed to incubate for 10 minutes in a humid chamber at room temperature. While the coverslips incubated in buffer, 5 µl of nucleotide mix and 1 µl of TdT enzyme were diluted in 45 µl of Equilibration Buffer for a total volume of 50 µl per slide. After 50 µl of TdT Reaction Mix was applied to each coverslip, the slides were allowed to incubate in a dark, humid chamber at 37°C for one hour. After incubation, the coverslips were washed with 2X SSC in a dark, humid chamber for 15 minutes, then washed twice with PBS for 5 minutes. Cells were counterstained with Hoechst 33342 dye as described, 10 µl of Hoechst dye 33342 was diluted 50:1 in 490 µl of PBS+, and 50 µl was applied to each coverslip. The coverslips were incubated in the dark for 2 minutes, then rinsed twice with PBS, and twice with distilled water. After staining, the coverslips were transferred to microscope slides treated with Vectabond (Vector Laboratories, Burlingame, CA).

Animals

Adult male C57BL/6 mice 2–6 months of age were used in these studies, in accordance with our institutional animal care guidelines. Genotyping of the calsarcin2-/- mice was done with two primer sets. The forward primer 5'-GTGACCAGGCAGGTGGAGATGG -3', located in the first intron, and the reverse primer R1: 5' GTATGGTCCTCATGCCTGCACGTGC 3', located in the second exon, produced a 400 bp band, indicating the presence of the wild type gene. The forward primer 5'- CCACCGTAGGGCATTGCTGTC -3', located inside the neomycin cassette, and the same reverse primer used in the wild type reaction would yield a 200 bp band indicating the presence of the mutation.

Photomicroscopy

MKRP expression, MKRP-GFP overexpression, morphological analysis of differentiation and injury regeneration, immunohistochemical staining, migration of siRNA transfected cells, and the TUNEL assay were visualized with a Leitz Laborlux-S microscope (Leitz; Wetzler, Germany) equipped with pan-apochromatic optics, standard bright-field condenser, and a Mears low-magnification dark-field condenser (MearsCorp; Waltham, MA). Photomicrographs were captured with an Optronics VI-470 CCD camera and Scion Image 1.62 software on a Power Macintosh G4 (Shelton, 2000; Goetsch 2003).

Immunohistochemistry

Tissue sections were co-stained with mouse monoclonal anti-BrdU serum (1:25, Roche) and rabbit anti-troponin I (1:500, Chemicon). The secondary antisera included a FITC conjugated goat anti-rabbit serum (1:50, Jackson ImmunoResearch), rhodamine goat antirabbit serum (1:50, Jackson ImmunoResearch) and FITC conjugated goat anti-mouse serum (1:50, Jackson ImmunoResearch) by an established protocol (Garry, 2000; Goetsch, 2003) summarized here.

Slides were preheated at 58°C for 30 minutes and then deparaffinized as described above. 1N HCL in PBS was preheated to 50°C in a coplin jar and the deparaffinized slides were immersed in HCL for 10 minutes at 50°C. After immersion, the slides were neutralized in a 0.1 M boric acid buffer (pH 8.5) for three minutes, and repeated twice. Slides were then rinsed in cold PBS for three minutes, repeated twice. The slides were blocked with 5% Normal goat serum/1%Bovine Serum Albumin/01% Cold fish skin gelatin/0.1% Triton X-1000.05% Tween-20 for 60 minutes at room temperature. After blocking, the slides were incubated in the monoclonal anti-BrdU serum, overnight at 4°C in a humid chamber. The following day the sections were washed with PBS for three minutes, three times, then incubated with the indicated fluorophore conjugated secondary antisera for 30 minutes at room temperature. After incubation the slides were washed with PBS/0.1% NP-40 for three minutes, three times, and coverslipped with Vectashield.

Identification of MKRP in regeneration and development

Introduction

The regeneration of adult mammalian skeletal muscle following injury is facilitated by a resident population of undifferentiated, mononuclear myogenic progenitor cells, known as satellite cells. One model successfully utilized to investigate the mechanisms regulating this regenerative process is the intentional production of a controlled injury by the injection of cardiotoxin (Nicolas, 1996. Garry, 2000). Injection of 100 µl of 10 µM cardiotoxin results in disruption of 80-90% of the muscle tissue in the hindlimb of a mouse. The physiological response to cardiotoxin injury has been well documented (Figure 1), however the molecular mechanisms of the regenerative process remain ill defined.

After cardiotoxin injury, satellite cells become activated within 6 hours (Grounds, 1992; Hawke and Garry, 2001). The first 24-48 hours post injury is characterized by the necrotic death of injured cells, and by the proliferation of the satellite cells (Garry 1997, Garry 2000). Between 48 hours and 5 days post injury, the satellite cells will cease proliferating and withdraw from the cell cycle. Some satellite cells will reassume the quiescent state, and re-establish the

resident pool of cells, while the rest will migrate by chemotaxis to the point of injury. At the site of injury, satellite cells will undergo fusion with injured fibers and terminally differentiate into myofibers.

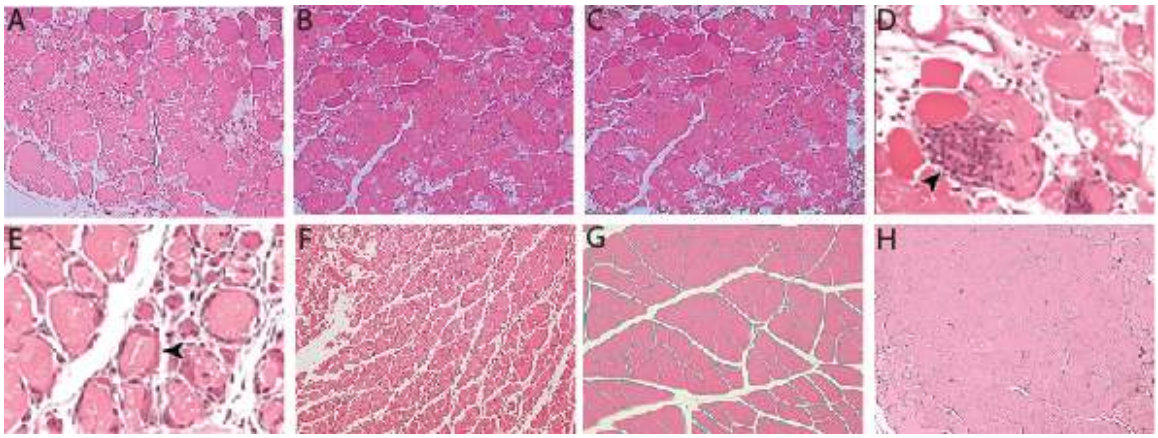

Figure 3.1 Skeletal muscle regeneration after cardiotoxin injury. A) 6 hours post injury, injured tissue shows severe edema. B) 12 hours post injury, injured tissue is characterized by myonecrotic cell death (arrowhead). C and D) 24 hours post injury, necrotic fibers lyse and the PMN response (arrowhead) is observed. E) 48 hours post injury, activated satellite cells (arrowhead) have proliferated and have migrated to the injured fibers. F) 5 days post injury, newly regenerated, mononuclear fibers (arrowhead) are observed. G) 7 days post injury, regeneration continues as new fibers mature. H) 14 days post injury, the architecture of the skeletal muscle is primarily restored.showing the temporal pattern of satellite cell activation, proliferation, and differentiation, after injury.

The mammalian regenerative response to skeletal muscle injury is a complex process that involves not only satellite cells and myogenic specific transcription factors, but also the immune response, growth factors, and proteins of the extracellular matrix (Martin, 1997. Reddi, 1998. Goetsch, 2003). Prior studies have utilized the cardiotoxin injury model to investigate the molecular mechanisms of this process (Goetsch, 2003). This study employed a microarray assay to compare gene expression in RNA extracted from injured and regenerating skeletal muscle at specific time points. Expression of selected candidate genes was confirmed by RT-PCR.

As expected, genes involved in the immune response peaked early in regenerative process, and cell cycle genes were more highly expressed in the first two days post-injury, as satellite cells went through their proliferative phase. Transcription factors known to play a role in myogenesis, such as MyoD and Myf6, were also upregulated in the early stages of regeneration, corresponding to the activation stage of satellite cells, and were downregulated as regeneration proceeded, and satellite cells differentiated into mature fibers. After the fifth day post-injury, genes involved in the formation of the extracellular matrix were upregulated, as newly formed satellite cells began to fuse with injured fibers and terminally differentiate into myotubes (Goetsch, 2003).

Utilizing this well established model, we sought to investigate the molecular mechanisms regulating skeletal muscle regeneration. To accomplish this goal,

we utilized a gene expression strategy, by examining the changes in expression of genes during the regenerative process. By extracting RNA from tissues harvested at specific points during regeneration, and using microarray technology to compare levels of expression between genes at these time points, we were able to identify possible candidate genes for further characterization.

The criteria used to select candidates for further study included a changing pattern of regulation during regeneration, the presence of structural domains similar to known transcription factors, or other proteins known to play a role in myogenesis, and no previous characterization work published on them. These novel candidate genes would be characterized through expression profiling by *In situ* hybridization, RT-PCR and Northern Blot analysis, subcloning and overexpression in C2C12 myoblasts to observe subcellular localization and the effects of overexpression, Yeast two-hybrid assay and other binding studies to identify interacting proteins, RNAi treatment, to observe the effects of loss of expression, and generation of a knockout animal, to study loss of function *In vivo*.

The goal of these studies was to identify and characterize novel genes that played a role in the regulation of satellite cell activity during myogenesis, both during regeneration, and development. Through characterization of their function and the identification of interacting partners through binding assays, we sought to further outline the pathways and mechanism by which satellite cells were able to repair and regenerate skeletal muscle.

Results

Microarray analysis

To develp an increased understanding of the molecular mechanisms regulating the myogenic progenitor cell population that is resident in adult skeletal muscle, we undertook transcriptome analysis of regenerating skeletal muscle to identify transcripts that demonstrated an altered pattern of regulation during sequential stages of skeletal muscle injury and regeneration (Goetsch, 2003). To investigate this process, we utilized the cardiotoxin injury model, a system that has produced efficient and reproducible skeletal muscle injury in prior assays (Garry, 1997; Garry, 2000; Goetsch, 2003). The gastrocnemius muscles of twenty-one adult male C57/B6 mice between the ages of 2-6 months were injured by the intramuscular injection of 150 µl cardiotoxin (10 µM, *Naja nigricollis*; Calbiochem, La Jolla, CA). Following cardiotoxin-induced muscle injury, the mice were sacrificed at 8 defined time points, 0 hours or uninjured, 6 hours post injury, 12 hours, 24 hours, 48 hours, 5 days, 7 days, and 14 days. For each time period, 3 mice were sacrificed, and the gastrocnemius muscle harvested for RNA extraction (n = 3). After extraction, RNA was labeled and hybridized to the Affymetrix high-density oligonucleotide array.

Two transcripts that were upregulated during the acute phase of muscle regeneration were identified and selected for further study (Figure 1). A search utilizing the BLAST local alignment search tool of GenBank (National Center for Biotechnology Information database) identified one transcript, W09925, as filamin-C, the skeletal muscle specific isoform of the filamin gene. The second transcript, W34362, aligned with a predicted, but previously uncharacterized gene in the BLAST program (Figure 2). The novel and uncharacterized gene is located on chromosome 9, its genomic sequence is 5924 bp in length and contains 5 introns (Figure 3). The mRNA contains an open reading frame coding for a predicted protein 603 amino acids in length (Accession# NM_028202), containing predicted BTB/POZ (Albagli, 1995), BACK (Stogios, 2004), nuclear localization (Kalderon, 1984), and Kelch (Xue, 1993; Bork, 1994) domains, with strong homology to other known members of the Kelch protein superfamily. We named this predicted protein myogenic kelch related protein (MKRP).

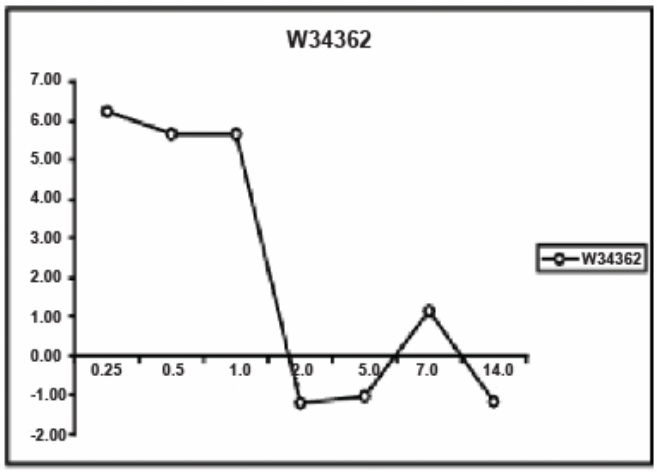

Figure 1. MKRP is upregulated early in regeneration after injury. MKRP was upregulated within 6 hours post injury, and expression remained high until 48 hours post injury. MKRP expression returned to baseline levels at 5 days post injury

Figure 3.2 MKRP mRNA sequence. The mRNA sequence for MKRP contains an open reading frame 600 bp in length, coding for a protein of approximately 70 kd. ATG start codon is shown in green, and the TGA stop codon is highlighted in red.

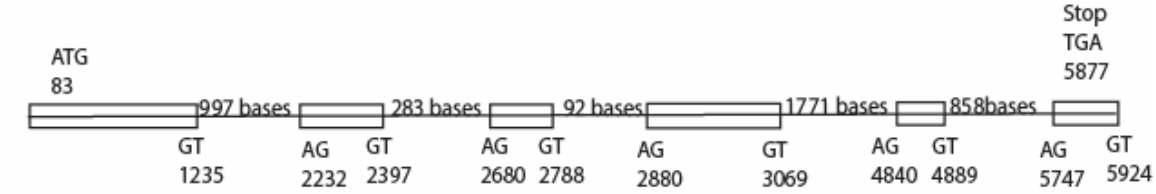

Figure 3.3 MKRP Genomic structure, with introns. MKRP is located on chromosome 9, and its genomic sequence is approximately 6kb in length with five introns, the largest of which is 1,771 base pairs in length.

RT-PCR performed with cDNA generated from mRNA extracted from regenerating skeletal muscle at the same time points as those used in the microarray, also indicated that MKRP expression was upregulated during the early stages of skeletal muscle regeneration (Figure 4).

Northern blot analysis, using a probe generated from I.M.A.G.E. Clone 138815 was utilized to probe a Clontech mouse embryonic blot, identified a 2.4 kb transcript that was upregulated in the late stages of embryogenesis. The transcript identified by the Northern Blot was consistent in size with the mRNA predicted by the BLAST database search. Expression was not observed at embryonic days E7.0 or E11.0, but was upregulated at day E15.0 and remained high at day E17.0 (Figure 5).

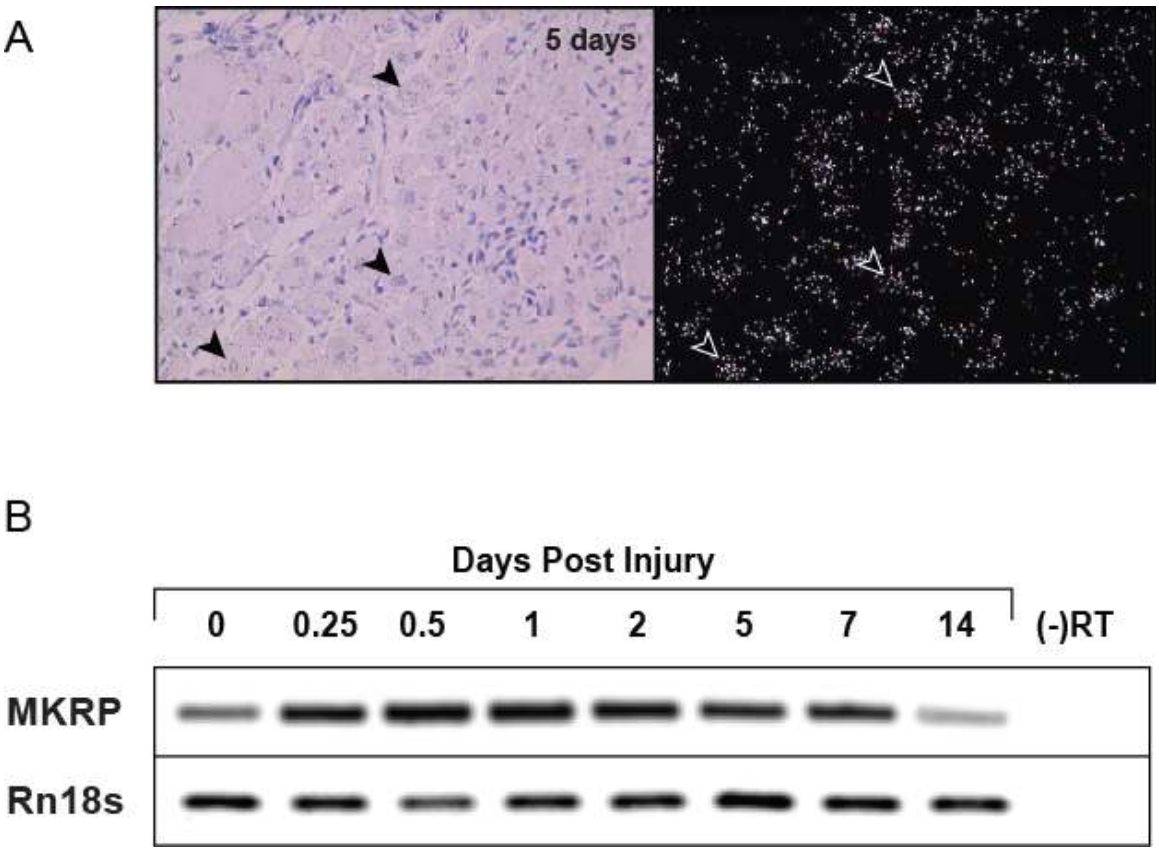

Figure 3.4 MKRP is dynamically regulated during the latter stages of muscle regeneration. A) Brightfield and darkfield images of skeletal muscle five days following injury reveals robust MKRP expression in newly regenerated (i.e. centronucleated) myofibers. Expression by 14 days was undetectable (data not shown). B) Semiquantitative RT-PCR analysis of RNA isolated from regenerating skeletal muscle following cardiotoxin induced muscle injury reveals robust MKRP expression that is decreased by 14 days. RN18s is used as a loading control

.

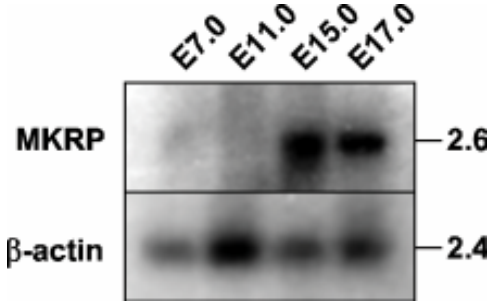

Figure 3.5 MKRP is expressed in the later stages of development. Northern blot analysis of RNA isolated from stage specific embryos reveals MKRP transcript (2.6 kb) expression at E15.5 and E17.5. β-actin was used as a loading control.

Further characterization of MKRP expression was undertaken by utilizing *in situ* hybridization analysis in injured skeletal muscle and murine embryogenesis. MKRP expression was first observed in the somites at day E11.5, and in the tongue, intercostals muscles and diaphragm on day E15.5. No expression was observed in the embryonic heart, or other tissues outside of skeletal muscle (Figure 6).

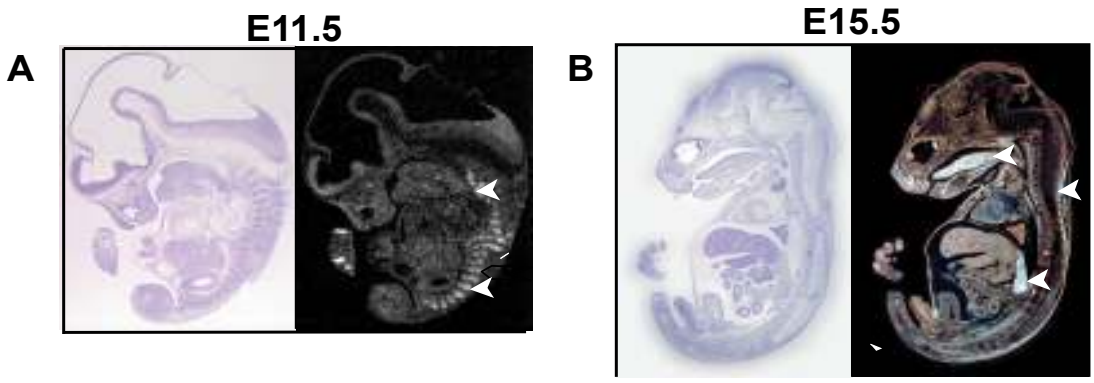

Figure 3.6 MKRP is restricted to developing muscle during murine embryogenesis. Using in situ hybridization, we examined MKRP transcript expression at defined developmental stages. (A) Brightfield and darkfield parasagittal sections reveal MKRP expression in the developing somites (white arrows) of the E11.5 mouse embryo. (B) Brightfield and darkfield parasagittal sections reveal MKRP expression in developing skeletal muscle of the tongue, somites, and diaphragm (white arrows) of the E15.5 embryo.

RT-PCR performed with cDNA generated from RNA extracted from adult tissues shows that MKRP expression is highest in skeletal muscle, but weak expression was also observed in the adult heart and brain (Figure 7).

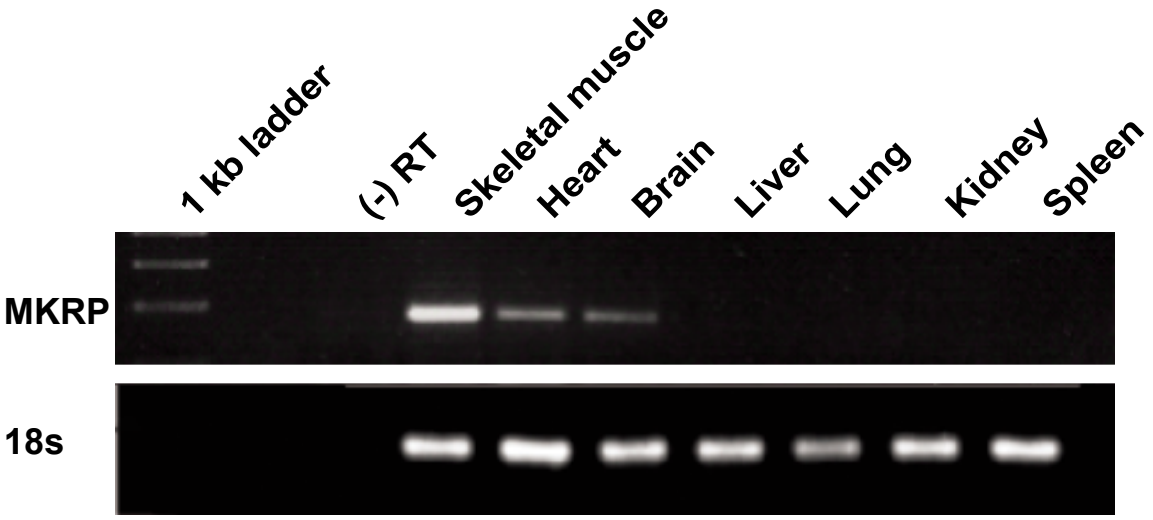

Figure 3.7 MKRP expression in adult tissues is restricted to skeletal muscle and heart. Expression of MKRP is highest in skeletal muscle, but present in lower levels in heart and brain. Expression is absent from other adult tissues, including liver, lung, kidney and spleen. 18s expression was used as a loading control.

Having demonstrated that MKRP expression is restricted to skeletal muscle lineages during murine embryonic development, we utilized *in situ* hybridization to investigate the spatial and temoral expression of MKRP during skeletal muscle regeneration following cardiotoxin-induced injury. Adult male mice were injured by the intramuscular injection of cardiotoxin to the gastrocnemius muscles, and the gastrocnemius tissue was harvested at specific time points following injury. The harvest times selected corresponded to the times utilized during the microarray, 0 hours or uninjured, 6 hours post injury, 12 hours, 24 hours, 48 hours, 5 days, 7 days and 14 days.

Within 6 hours post injury, MKRP expression was robustly upregulated in myogenic progenitor cells localized to the perimeter of the myotubes (Figure 8). Abundant MKRP expression was restricted to the region occupied by intact

myofibers, and was noticeably absent in the adjacent myonecrotic region. These data suggest the possibility of a role for MKRP in satellite cell migration, consistent with previous studies that demonstrated that satellite cells from adjacent regions will migrate to the point of injury, to repair damaged myofibers (Schultz, 1994; Goetsch, 2003).

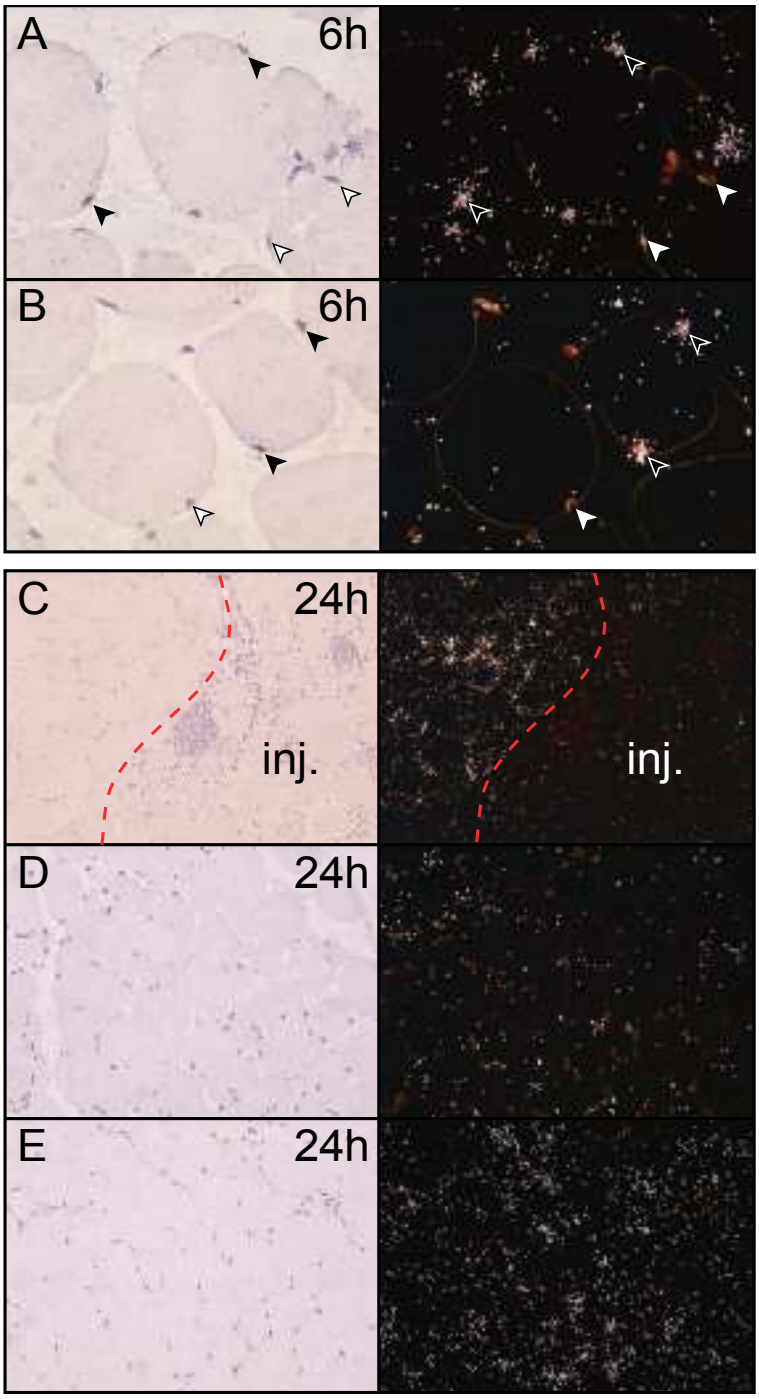

Figure 3.8 MKRP is expressed in the activated MPC of regenerating skeletal muscle. Using in situ hybridization. MKRP expression was evaluated morphologically at defined time periods following cardiotoxin-induced muscle injury. (A and B) Brightfield and darkfield images of skeletal muscle 6 hours following injury. Note robust signal associated with the activated MPC (white arrowheads). (C-E) Brightfield and darkfield images of skeletal muscle 24 hrs following injury. (C) Low magnification revealing the injured skeletal muscle and adjacent intact skeletal muscle (separated by a red line). (D and E) Higher magnification of panel C revealing an absence of MKRP expression in the injured, necrotic

muscle but robust expression in the activated, migrating MPC in the adjacent non-injured skeletal muscle.

In the later stages of regeneration, *in situ* hybridization analysis reveals that MKRP is expressed in regenerated skeletal muscle, but expression is restricted to immature, centrally nucleated myotubes, and is absent in in larger, more mature, peripherally nucleated myotubes (Figure 8). These data were supported by RT-PCR analysis of cultured C2/C12 cells undergoing differentiation (Figure 9). MKRP expression was absent in proliferating myoblasts, and only weakly expressed in 90% confluent myoblasts. MKRP expression was upregulated immediately after the induction of differentiation by the addition of low serum media, and peaked on the third day after differentiation. MKRP was still expressed after the formation of myotubes, but was downregulated from its peak expression on day 3. These data would support the hypothesis that MKRP was expressed in the early stages of satellite cell activation and may play a role in the migration and possibly the fusion of satellite cells in response to injury.

Discussion

Adult mammalian skeletal muscle has a unique ability to regenerate after injury, which is facilitated by a resident population of myogenenic progenitor cells termed satellite cells. Although previous studies have demonstrated that this regenerative capacity is both efficient and reproducible (Garry 1997; Garry, 2000; Goetsch, 2003), little is known about the molecular mechanisms regulating the function of satellite cells.

To investigate the mechanism of satellite cell regulation, we employed transcriptome analysis by microarray and RT-PCR, and *in situ* hybridization analysis. The microarray identified 2 transcripts upregulated during the acute stages of regeneration. A database search showed that one transcript was the murine homolog of filamin-c, the largest member of the filamin protein family, and the only filamin protein expressed only in skeletal and cardiac muscle (Van der Ven, 1999; Thompson, 2000). Filamin-c has been well characterized in humans, the protein localizes to the Z-disc in striated muscle, and has been shown to interact with other Z-disc proteins including myotilin (Salmikangas, 1999), N-RAP (Lu, 2003), calsarcin-2 (Frey, 2002), and KRP1 (Lu, 2003).

An alignment search using the BLAST alignment database indicated that the second transcript identified in the microarray was the mRNA of a novel, previously uncharacterized gene. This mRNA contained a kozak sequence preceding an open reading frame that coded for a protein belonging to the Kelch superfamily of proteins, and also containing a BTB/POZ domain, and a potential nuclear localization sequence (Kalderon, 1984). It also demonstrated strong homology to KRP1 another kelch protein known to interact with filamin-c (Lu, 2003).

KRP1 was first identified in rats, but also has a human homolog (Spence, 2000). KRP1 bound to actin and overexpression of the protein in 208f rat fibroblast cells resulted in pseudopod elongation, indicating that the protein played a role in cytoskeletal remodeling and migration (Spence, 2000). Other kelch family proteins including KLEIP (Hara, 2004), Mayven (Williams, 2005), klhl (Wu, 2004), KLHL15 (Yoshida, 2005), and mklhdc2 (Nehuas, 2006), have also been identified as actin binding partners, and involved with cellular migration.

In situ hybridization analysis of MKRP expression during embryogenesis and injury regeneration revealed high expression of MKRP in activated satellite cells migrating from uninjured tissue to an injured, necrotic region. These data support the hypothesis of a possible role for MKRP in satellite cell migration. *In situ* analysis also demonstrated that MKRP was upregulated in the later stages of embryogenesis, and restricted to the somites and developing skeletal muscle. In

the later stages of regeneration, MKRP expression appeared highest in centrally nucleated, newly regenerated myotubes, while only minimal expression was observed in older, more mature, peripherally nucleated myotubes.

The expression pattern of MKRP, and its sequence homology to other proteins known to participate in cytoskeletal remodeling and migration suggested the possibility that MKRP may play a role in the migration of satellite cells in response to injury, and also their ability to fuse with newly regenerated myotubes. To further characterize the activity of MKRP, we undertook assays to investigate its role in the differentiation and migration of cultured C2C12 cells, and to identify any phenotypical effects caused by the over expression or knockdown of MKRP.

Overexpression and Knockdown of MKRP by RNA Interference

Introduction

Overexpression of selected proteins in cell culture usinf conventional transfection strategies is one method to examine the role of the candidate protein, *in vitro.* To evaluate the effects of MKRP overexpression, and to observe its subcellular localization, I undertook the cloning of the full length of MKRP open reading frame (without the stop codon), by amplifying the mRNA fragment by PCR, and ligation into a vector containing the open reading frame for the Green Flourescent Protein (GFP). The MKRP sequence was ligated into the vector so that its sequence was in frame with the GFP sequence and under the regulation of a constitutive promoter. The two combined sequences created a protein with GFP attached to the N-terminus of MKRP. The fluorescent properties of GFP made it possible to evaluate the expression and localization of MKRP in cultured cells, by microscopy. After the successful cloning and transfection of MKRP, other fusion constructs were created by amplifying the mRNA sequences for the BTB, BACK, and Kelch domains, as well as the nuclear localization sequence, and ligation into the same GFP expression vector.

Because MKRP contained a sequence with strong homology to the nuclear localization sequence of the SV40 T-antigen protein (Kalderon, 1984), and other proteins containing a BTB domain function as transcription factors (Chen, 1995; Horlien, 1995; Mangelsdorf, 1995 for review), we hypothesized that MKRP may play a regulatory role in transcription, and the protein could be localized to the nucleus. To investigate the role of the functional domains of MKRP and evaluate the ability of the proposed nuclear localization sequence to affect nuclear transport, I amplified and cloned the BTB, BACK, and Kelch domains of MKRP and expressed them as fusion constructs with GFP, utilizing the same plasmid used to express full length MKRP-GFP. The functional domains were expressed with and without the nuclear localization sequence attached, and the nuclear localization sequence (NLS) by itself was also fused with GFP, to determine if that specific sequence alone was enough to affect nuclear transport. These constructs could also be used for protein binding assays, in the future.

Many strategies have been utilized in an effort to efficiently achieve down regulation of the expression of a specific gene, but most gave inadequate results for the the silencing of a gene in complex organisms. The first successful use of antisense RNA to silence a specific gene occurred in 1991, when researchers created transgenic *C. elegans* expressing RNA of the unc-22 and un-54 genes, in reverse orientation (Fire, 1991). The resulting transgenic worms demonstrated muscle defect phenotypes consistent with the loss of the function of the two targeted genes, and PCR analysis showed that the inverse RNA sequences were

being expressed at high levels. The success of these experiments with germline gene silencing encouraged other researchers to use antisense RNA to directly inhibit the expression of a gene in an adult worm by injecting the antisense RNA directly into the subject (Guo and kemphues, 1995). The success of this assay in silencing the expression of the par-1 gene in *C. elegans* began the utilization of RNA interference for gene silencing.

The original studies of Guo and Kemphues also revealed that a sense strand of RNA would give just as efficient a knockdown of targeted gene expression as an antisense strand (Guo and Kemphues, 1995). Future studies would demonstrate that a mixture of both sense and antisense RNA sequences would produce knockdown of a targeted gene at least 2 orders of magnitude stronger than injection of either strand alone (Fire, 1998).

Experiments in *Drosophila* demonstrated that cleavage of targeted RNA sequences was mediated by short RNA sequences, usually 21-22 nucleotides in length (Elbashir, 2001), and that these short segments were created by the cleavage of long sequences of double-stranded RNA by an enzyme from the RNase III family. This enzyme was identified as Dicer (Bernstein, 2001) an RNase III family member containing a helicase domain, and two RNase III domains.

After cleavage by Dicer, the short double stranded RNA segments serve as guides for the RNA induced silencing complex (RISC) protein (Hammond, 2000). An experiment using biotin labeled siRNA demonstrated that only the antisense sequence was utilized for targeting the RISC complex to the specific mRNA. By biotinylating either the sense or antisense strand of double stranded siRNAs and incubating the labeled products with cell extracts containing the target sequence, then filtering the extracts through an affinity column, it was shown that only the antisense strand interacted with the RISC complex, although both strands were necessary for efficient cleavage of the target (Martinez, 2002). This same study also demonstrated that modifications to the 5' end of the siRNA sequence would inhibit degradation by RISC, but modifications to the 3' end of the sequence did not interfere with RISC targeting activity. These data indicated that although double stranded RNA was necessary for efficient interference by siRNA, the doublestrand needed to be unwound after association with RISC, and that the mechanism may involve phosphorylation of the 5' end of the siRNA. Additional studies would demonstrate that the sense strand of the siRNA was cleaved by RISC with the association of the antisense strand with the RISC complex (Rand, 2005 and Matranga 2005).

Although the protein components of the RISC complex remain not fully defined, studies have shown that Argonaute2 is the protein required for RNAi activity (Rand 2004). By incubating an siRNA molecule that had been biotinylated at the 3' end with cell extracts, then filtering the extract through an affinity column,

researchers were able to purify the RISC complex. After a high salt wash, the affinity beads were incubated with trypsin, and the recovered proteins were analyzed by mass spectrometry. Argonaute2 was the only protein remaining after the high salt wash, although additional proteins were also present if the wash step was not performed. A database search identified the PIWI domain of Argonaute2 as having strong homology to the endonuclease V protein family, and the authors of the study hypothesized that this domain was responsible for the endonuclease activity of the RISC complex (Rand, 2004).

Initial studies utilizing RNAi were performed successfully in *C elegans* and *Drosophila*, but intial attempts to repeat these experiments in mammals resulted in the inhibition of protein expression, due to the interferon (IFN) response (Provost, 2002). This complication was removed by the use of synthetically produced 21-22 nucleotide siRNA molecules, instead of longer double stranded RNAs. By utilizing smaller RNA duplexes to begin, the experiment would bypass the Dicer cleavage of the larger RNA molecules and avoid the IFN response (Elbashir 2002).

The selection of a sequence for generating an efficient siRNA can involve multiple experimental trials. Many researchers will utilize several sequences targeted to different regions of the mRNA to find the sequence that delivers the strongest knockdown. Suggested guidelines for the selection of a sequence include avoiding the 5' untranslated region of the mRNA, as that region may

contain protein interaction and regulatory targets (Elbashir 2002). Also, the G/C content should ideally be less than 50% of the sequence, as a higher A/U content has been shown to be preferentially incorporated into the RISC complex (Khvorova 2003). Low internal thermodynamic stability may lead to more efficient cleavage of the sense strand by RISC. The presence of internal repeats in the sequence has also been shown to negatively impact the efficiency of siRNAs (Khvorova 2003). Specific nucleotide positions have also been shown to result in more efficient knockdown, including an A at nucelotides 3 and 19, and a U at nucleotide 10 in the sequence, and A, U, or C at position 13 (Reynolds, 2004). Also, the presence of G or C at nucleotide 19 has been demonstrated to have a notable negative effect on knockdown efficiency. Computer models have also been generated that will assess the optimal sequences for siRNA, based upon these criteria, and the predicted secondary structure of the target.

All knockdown of transcripts by siRNA is transient, and can vary in length based on the abundance of the target mRNA, and the stability of the transfected siRNA. To achieve a more prolonged silencing of target genes, researchers have recently utilized adenoviral vectors carrying siRNA expression cassettes. These viral vectors using a Polymerase II promoter to drive expression of the siRNA sequence and have been utilized in a variety of cell types (Xia, 2002, Shen, 2003).

These advances in the utilization of RNA interference, in particular the development of siRNA for use in mammalian systems, have generated a viable and less expensive alternative for the study of loss of gene function. Efficient knockdown of gene expression by siRNA can be performed in place of, or to complement, studies utilizing knockout animal models. The transient nature of RNAi also allows the investigator to reverse a phenotype by discontinuing the RNAi treatment, an option not available in transgenic models.

By using an siRNA strategy to knockdown expression of MKRP in cultured C2C12 myoblasts, our objective was to gain insight into a possible role for MKRP pertaining to the mechanisms of myoblast migration and differentiation. RT-PCR analysis had revealed that MKRP demonstrated a changing pattern of expression during injury regeneration, and the differentiation of cells grown in culture. If MKRP was required for differentiation, as was suggested by the upregulation of its expression immediately after the onset of differentiation, then we hypothesized that we would see a phenotypic change in differentiating cells when MKRP expression was inhibited. To test this hypothesis, I transfected cells with either siRNA oligos targeting the MKRP mRNA sequence, or with siRNA oligos targeting the green fluorescent protein (GFP). After transfection, the cells were shifted to low serum media to induce differentiation, and their ability to differentiate was evaluated using micrscopic techniques, based on the appearance and growth of myotubes in the culture plates.

In situ hybridization analyses of MKRP revealed expression of MKRP mRNA at high levels in migrating myogenic precursor cells within the first 48 hours after cardiotoxin injury. Because the closest homologue to MKRP had previously been linked to a possible migration mechanism (Spence, 2000), and other Kelch proteins had been shown to be involved in the migration of other cell types (Jiang, 2005), we hypothesized that MKRP could play a role in the migration of myogenic precursor cells. To test this theory, I proposed to transfect C2C12 cells with siRNA oligos targeting the MKRP mRNA sequence, and then evaluating the ability of those cells to migrate during a scratch/wound assay, in comparison to cells transfected with a nonsense oligo that did not target any known gene sequences. The the ability of the transfected cells to migrate would be evaluated based on the number of cells that were able to migrate into a wounded area generated by scratching the plate with a 1mm wide pipet tip.

Results

Cloning MKRP

To investigate the subcellular localization of the MKRP protein and the effect of overexpression of MKRP on differentiation and migration, I amplified the MKPR mRNA sequence by RT-PCR using the primers 5'-GAAGATCTTCCCTCGATACACAGACTTG-3' (forward), and 5'-CGGAATTCGCACTTGGTCAGGGCGAAG -3' (reverse) to amplify an 1820 bp mRNA segment of the mRNA. This segment contained the kozak sequence and ATG start codon, but terminated prior to the stop codon. The primers also created cut sites for the restriction enzymes EcoRI and BglII at the 5' and 3' ends respectively, allowing the segment to be ligated into the Clontech pEGFP-N1 expression vector, creating a fusion construct that expressed the 238 amino acid sequence of the green fluorescent protein at the amino terminus of MKRP. The MKRP-GFP construct was transfected into C2C12 myoblasts and the localization of the protein was visualized 24 hours later by fluorescence microscopy. The MKRP-GFP protein appeared to be excluded from the nucleus, and staining the transfected cells with Hoechst 33342 dye to mark the cell nucleus demonstrated that the GFP signal was absent from the nucleus in MKRP-GFP transfected cells, while in cells transfected with the empty GFP vector, GFP signal was ubiquitous.

After the addition of low serum media to induce differentiation, the MKRP-GFP protein remained excluded from the nucleus on the first day post-differentiation, but expression became perinuclear on the second day post differentiation. On the third day post-differentiation expression appeared to be completely nuclear.

A

B

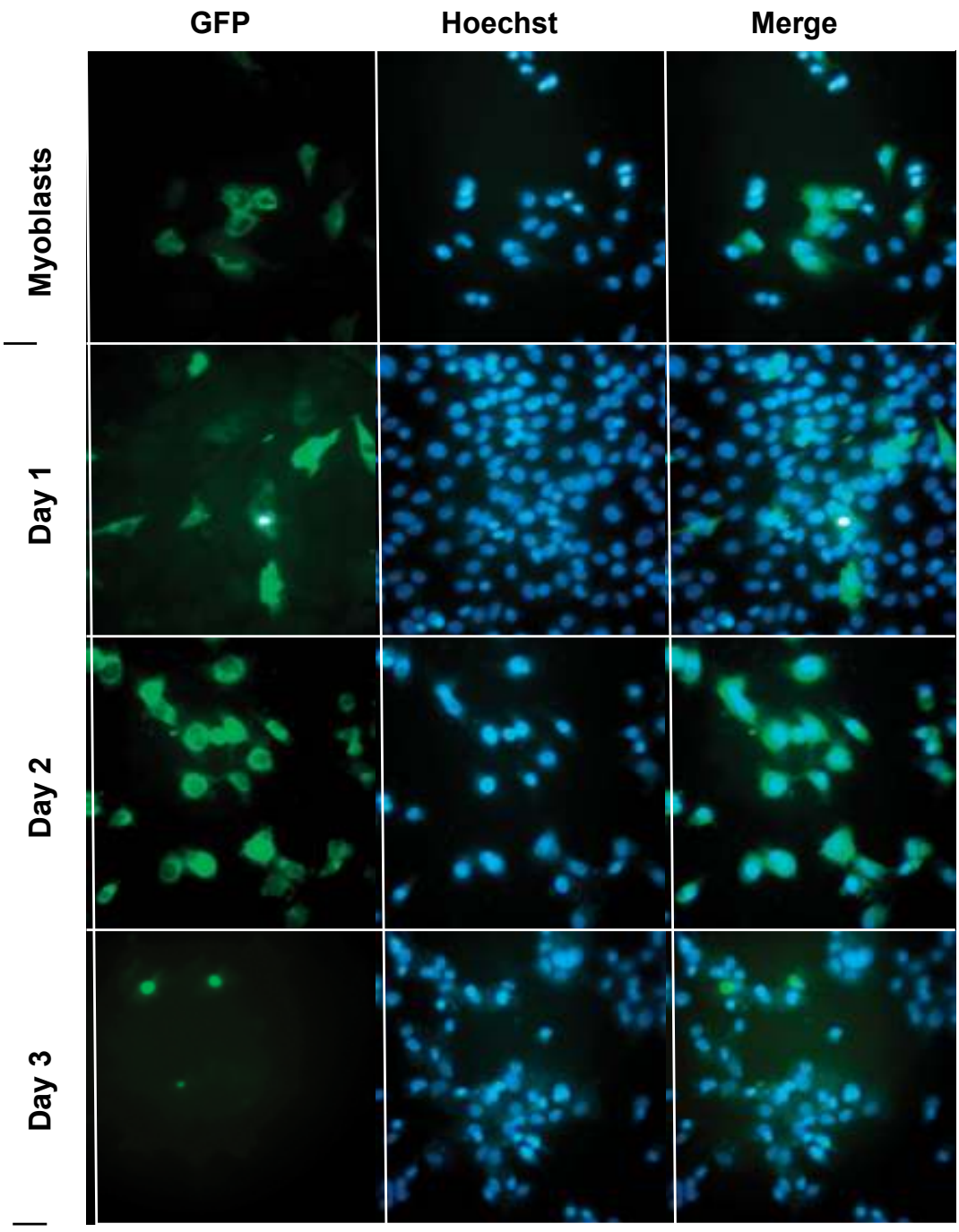

Figure 4.1 MKRP is localized to distinct cellular compartments. A) MKRP GFP fusion construct, GFP expressed at C-terminus of MKRP. B) C2C12 myoblasts were transfected with the MKRP-GFP fusion protein and evaluated in myoblasts and differentiated myotubes. Hoechst dye was used to define the nuclear compartment. Note nuclear exclusion of the MKRP-GFP fusion protein in myoblasts. The fusion protein is localized to the perinuclear region in Day 2 myotubes and is predominately localized to the nuclear compartment by Day 3 post differentiation.

TUNEL Assay

Extensive cell death was observed in the cells transfected with MKRP on the third day post-transfection, and no MKRP-GFP cells remained on the fourth day post-transfection. No myotubes expressing MKRP-GPF were ever observed. To investigate the possibility that the nuclear localization of MKRP-GFP was caused by the implosion of the cell during apoptotic cell death forcing the protein into the nucleus, I used a TUNEL assay to identify cells dying by apoptosis.

Terminal transferase dUTP nick end labeling (TUNEL) is an established method for detecting DNA fragmentation caused by apoptotic signaling cascades. The assay catalyzes the addition of dUTPs that are secondarily labeled with a fluorescent marker to the nicked ends of fragmented DNA (Gavrieli, 1992). Programmed cell death by apoptosis is characterized by a cell shrinkage due to the degradation and collapse of the cytoskeleton, and the fragmentation of DNA after the nucleus is ruptured (Lazebnik, 1993; Nagata, 2000). The TUNEL assay can determine if the translocation of MKRP-GFP to the nucleus is a function of a living cell, or caused by the collapse of the cell and rupture of the nuclear membrane. The presence of MKRP-GFP signal in TUNEL negative cells

indicates that the translocation of MKRP-GFP was not caused by apoptotic cell death (Figure 2).

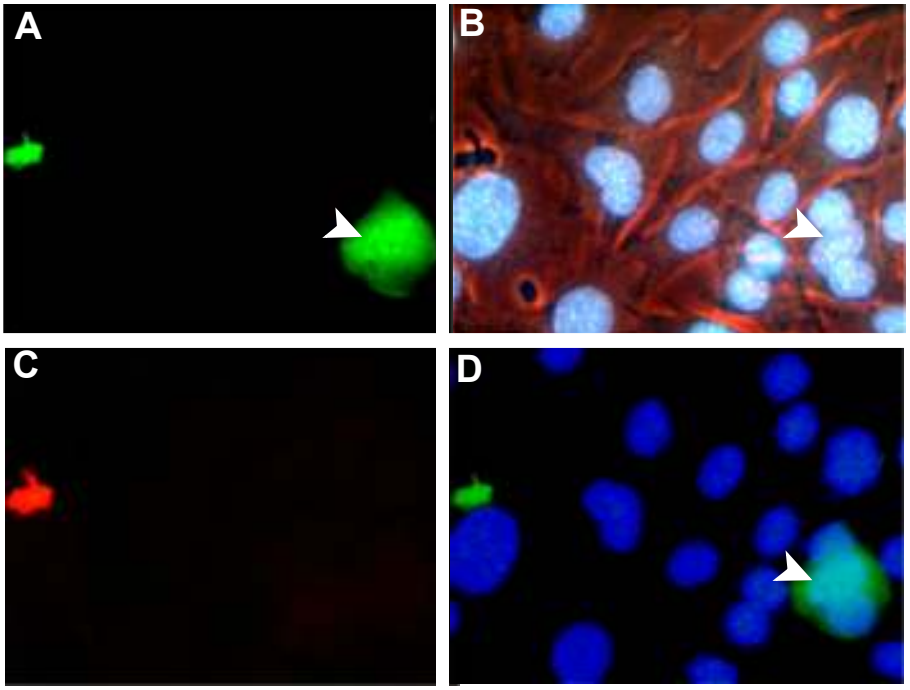

Figure 4.2 TUNEL assay. The TUNEL assay marks cells undergoing programmed cell death by apoptosis (red). The presence of green GFP signal in the nucleus of TUNEL negative cells indicates that the protein was transported into the nucleus, and not as the result of cellular collapse and the rupturing of the nuclear membrane. A) Cell expressing MKRP-GFP in its nucleus (nucleus marked by arrowheads) B) Nuclei marked by Hoechst dye (blue). C) TUNEL signal (red). Merger showing MKRP-expression in the nucleus of a TUNEL negative cell.

Functional domain fusion constructs

To investigate the effects of overexpression of specific domains of MKRP, I cloned the BTB, BACK and Kelch domains of MKRP into the GFP expression vector, both with and without the proposed nuclear localization sequence included (Figure 3). When the BTB-GFP construct was expressed in C2C12 cells, the protein appears to be ubiquitous throughtout the cell in myoblasts, but

was excluded from the nucleus in some cells after the onset of differentiation. On the third day post-differentiation, BTB-GFP was expressed predominantly in the nucleus in some cells, but not all (Figure 4).

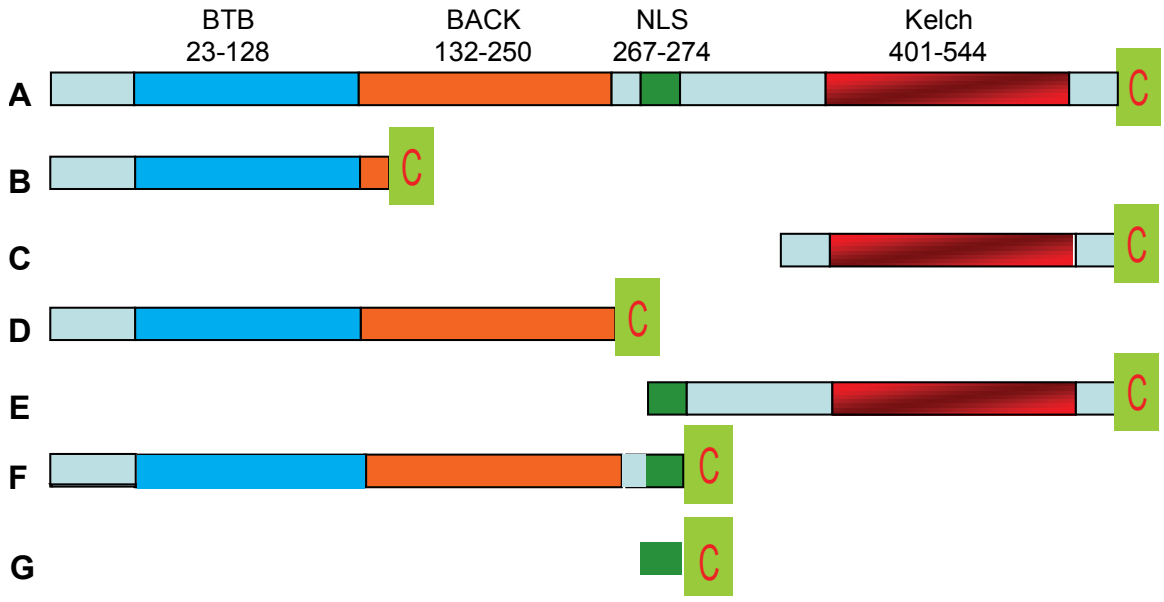

Figure 4.3 MKRP-GFP fusion constructs. Full length MKRP mRNA, without the stop codon, was cloned into a vector expressing GFP, creating a protein with GFP fused to MKRP at the carboxyl termini of MKRP, for protein localization and overexpression studies. The functional domains of MKRP were also individually fused to GFP for further analysis. A) Full length MKRP-GFP, the full length of the MKRP mRNA is expressed with GFP. B) The BTB domain with GFP, The BTB domain at the N-terminus of the protein is expressed alone, and fused to GFP. C) Kelch domain with GFP, The Kelch repeat domain and the C-terminal tail are expressed with GFP, and without the domains to the N-terminal side of the Kelch domain. D) The BTB and BACK domain fused to GFP. E) The nuclear localization sequence and the Kelch domain, with GFP. F) The BTB and BACK domains and the nuclear localization sequence were fused to GFP. G) The nuclear localization sequence alone, was fused to GFP without the surrounding domains.

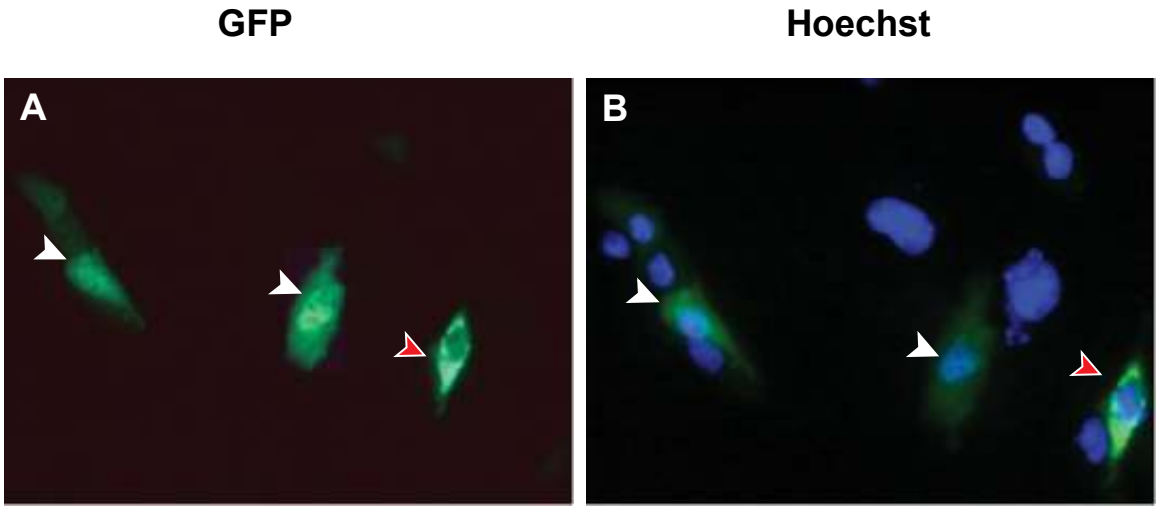

Figure 4.4 BTB-GFP is excluded from the nucleus in some cells after differentiation. The BTB-GFP construct was expressed ubiquitously throughout the cell in myoblasts (white arrowheads), but was excluded from the nucleus in some cells after the induction of differentiation (red arrowheads)

The Kelch-GFP fusion construct was excluded from the nucleus in both myoblasts and myotubes. After the onset of differentiation, the Kelch-GFP construct was localized to specific pockets surrounding the nucleus, but was never observed inside the nucleus. (Figure 5). Although excluded from the nucleus when expressed alone, Kelch-GFP was expressed primarily in the nucleus when the NLS was included (Figure 6). The NLS was also able to localize GFP to the nucleus when the sequence by itself was fused with GFP (Figure 7).

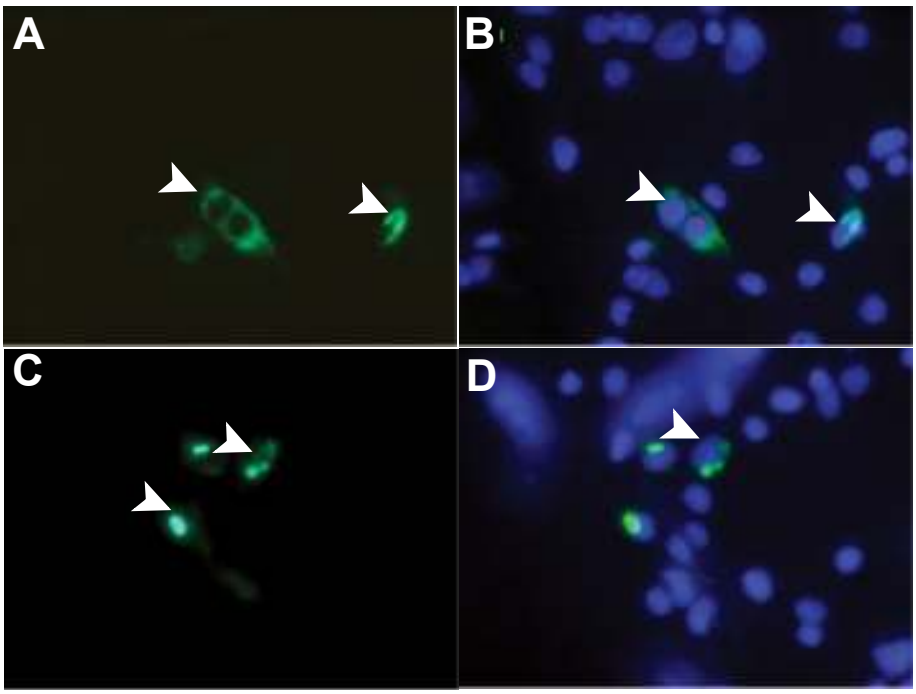

Figure 4.5 Kelch-GFP localizes to discrete pockets outside the nucleus. The Kelch-GFP construct was excluded from the nucleus before and after differentiation. Hoechst staining shows Kelch-GFP localizes outside the nucleus (arrowheads) in myoblasts (A and B) and in myotubes (C and D).

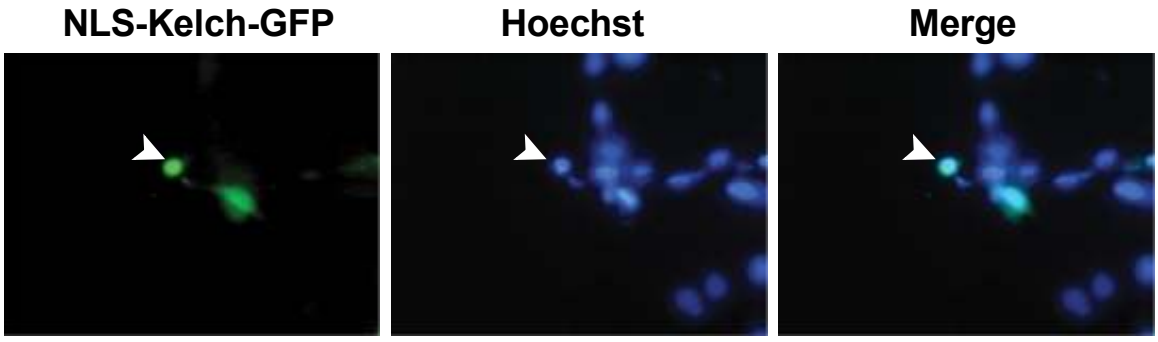

Figure 4.6 Kelch-GFP localizes to the nucleus when expressed with the NLS. The kelch domain and the nuclear localization sequence were clones in frame with GFP and expressed in C2C12 cells. The kelch domain was excluded from the nucleus when expressed by itself, but expression was primarily nuclear when expressed with the NLS.

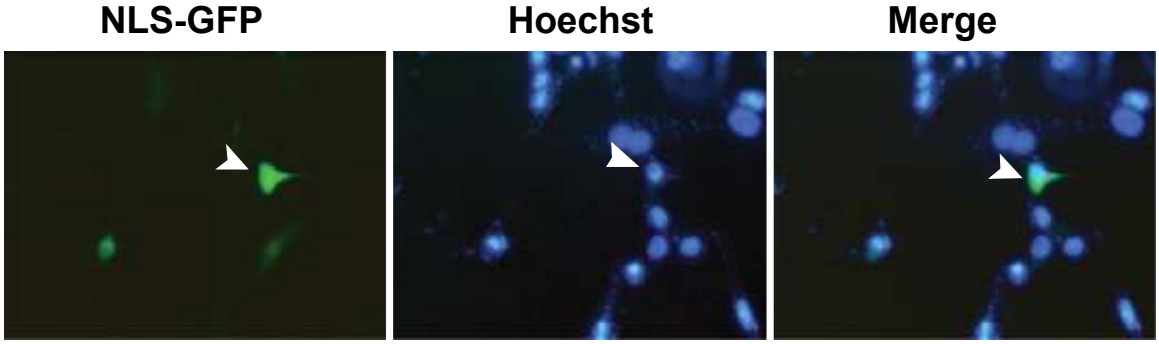

Figure 4.7 The NLS sequence alone is enough to promote nuclear localization of GFP. The NLS was fused in frame with the GFP sequence and transfected into C2C12 cells. GFP alone was expressed ubiquitously throughout the cell, but when expressed with the NLS it localized primarily to the nucleus (arrowheads).

siRNA knockdown of MKRP

To investigate the effect of MKRP knockdown on cell morphology, migration and differentiation, I utilized an siRNA knockdown assay. The primer 5'-GUGGACCUCCUUUGAGGCCUU-3 and its complementary strand were synthesized by the UT-Southwestern core facility and the 2 strands were annealed by an established protocol (see Materials and Methods). In the first assay, C2C12 cells were transfected with the MKRP-GFP construct and then 24 hours later transfected with the siRNA oligo, or were given transfection media without the oligo as a control. Flourescence microscopy revealed a clear

difference in the density of GFP signal between the cells transfected with oligo and those cells that received only the transfection media (Figure 8).

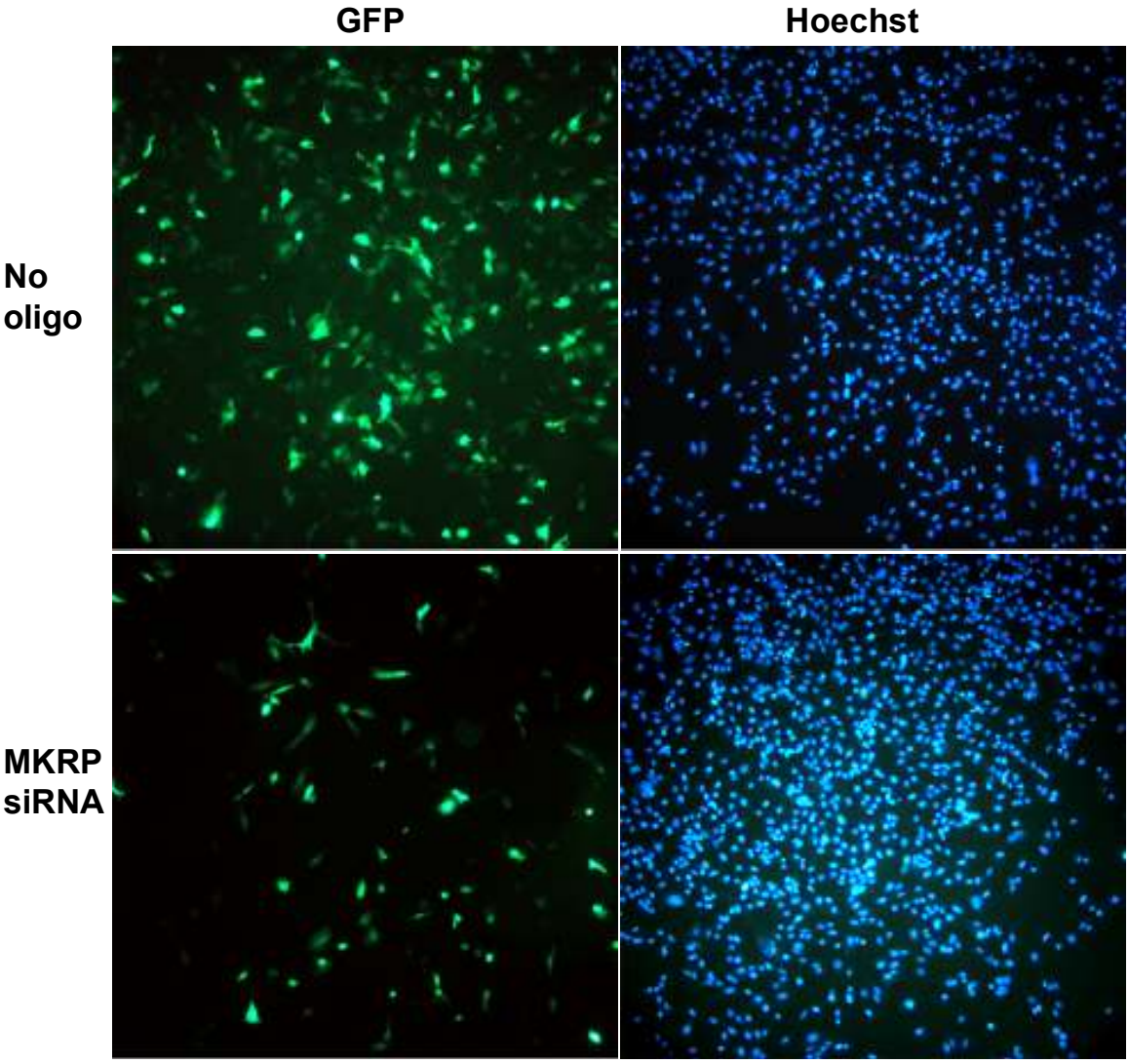

Figure 4.8 First experiment with MKRP siRNA oligo. C2C12 cells were transfected with MKRP-GFP and either siRNA oligos directed at MKRP, or transfection media with no oligo. Hoechst staining shows that the 2 plates were equally confluent, but the cells transfected with MKRP siRNA demonstrated a reduced level of GFP expression, indicating that the MKRP oligo had downregulated the expression of the MKRP-GFP transcript.

To quantify the extent of the knockdown achieved by the MKRP oligo, the MKRP-GFP plasmid was transfected into HEK293T cells, which do not express endogenous MKRP. After 24 hours, the cells were transfected with the MKRP

oligo, an oligo directed at GFP, a nonsense oligo, or no oligo. Cells were sorted by FACS on the basis of GFP expression. The cell populations that received the nonsense oligo or no oligo both contained slightly more than 40% GFP positive cells, while 21.61% of the cells transfected with the GFP oligo were GFP positive, and 22.57% of the cells receiving the MKRP oligo, still expressed GFP. These data showed that the MKRP oligo I was using was able to deliver an efficient knockdown of the target transcript (Figure 9).

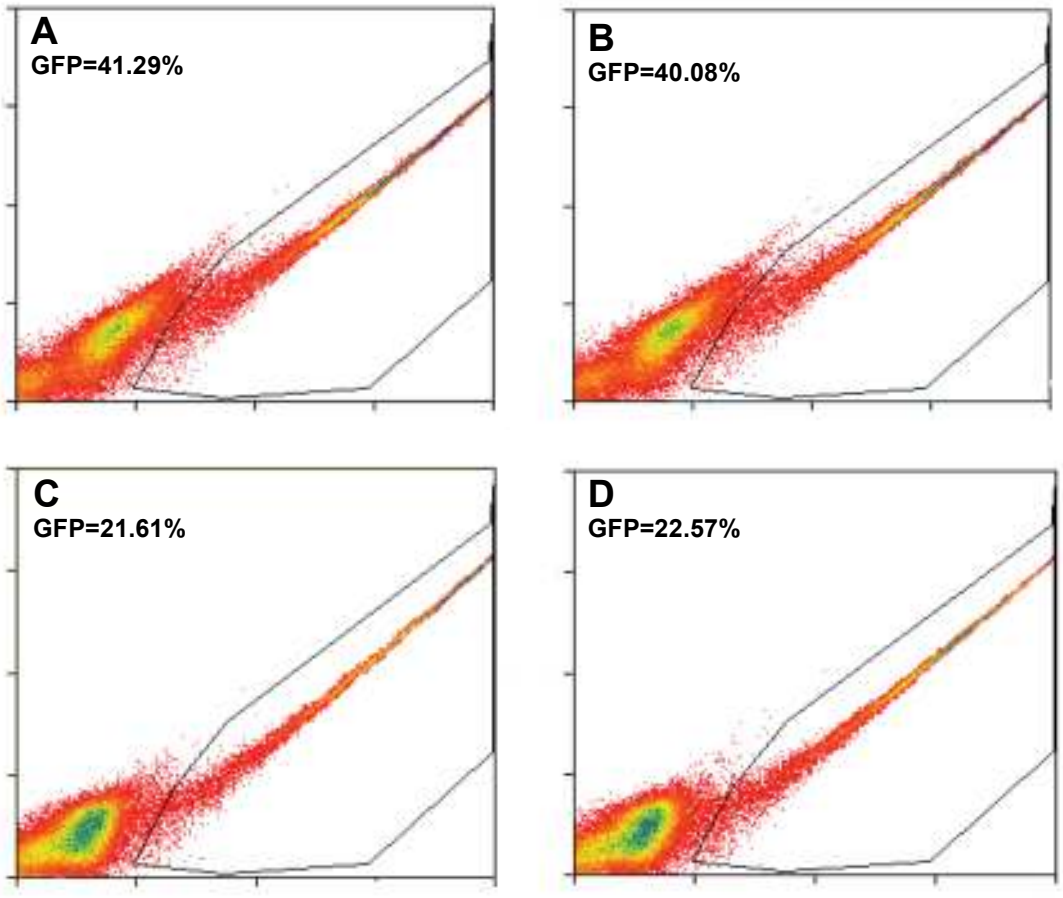

Figure 4.9 Facs analysis shows efficient knockdown of an MKRP-GFP construct by an MKRP siRNA oligo. Cells were transfected with equal amounts of an MKRP-GFP expression plasmid, and plasmid, and RNAi oligos directed at either GFP or MKRP, a nonsense oligo, or no oligo. A) Nonsense oligo. B) No oligo. C.) GFP Oligo. D) MKRP oligo. Both the GFP and MKRP RNAi oligos produced similar reduction in the number of GFP positive cells.

siRNA Titration curve

To determine the concentration of the oligo that achieved the most efficient knockdown of the transcript, I transfected HEK293T cells with equal amounts of MKRP-GFP, and decreasing concentrations of the MKRP siRNA oligo. Utilizing RT-PCR to evaluate levels of MKRP-GFP expression, I determined that a concentration of 1nM produced as strong a knockdown as 10 nM, and that at 0.5 nm knockdown was cleary diminished. Transfection with an oligo concentration of 0.1 nM produced no observable decrease in MKRP-GFP expression (Figure 10).

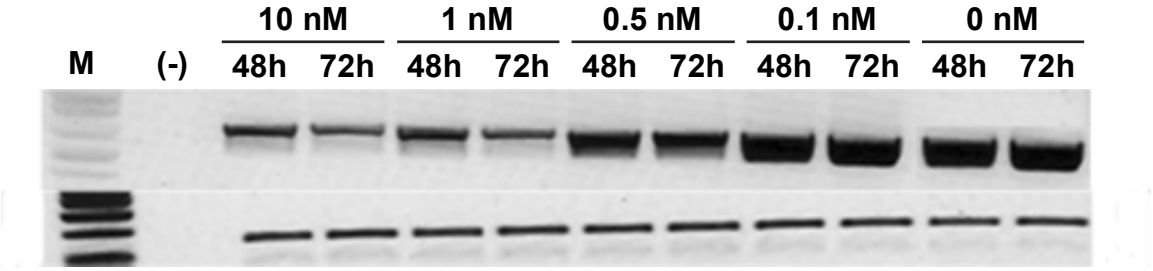

Figure 4.10 Knockdown of MKRP peaks at 72 hours. HEK293T cells were transfected with equal amounts of the MKRP-GFP construct, and decreasing concentrations of MRKP siRNA oligo, and harvested at 48 and 72 hours. 1 nM of oligo was sufficient to achieve efficient knockdown, and there was little to no gain in knockdown gained by increasing dosage to 10 nM. Knockdown was reduced or not observed in oligo concentrations lower than 1 nM.

MKRP siRNA delays differentiation

To evaluate the effect of a knockdown of MKRP expression on the differentiation of myogenic precursor cells, I transfected C2C12 cells with the MKRP siRNA oligo, or a nonsense oligo, and allowed them to differentiate. Twenty-four hours after transfection, cells were cultured in low serum media to induce differentiation. Cell samples were photographed and RNA was isolated prior to differentiation and days 1-5 post differentiation. A clear delay in differentiation was observed in the cells transfected with the MKRP siRNA oligo. Myotube formation was delayed in the MKRP oligo transfected cells (Figure 11), and when tubes did form they were clearly smaller than the mytubes forming in the cultures transfected with the nonsense oligo (Figure 12).

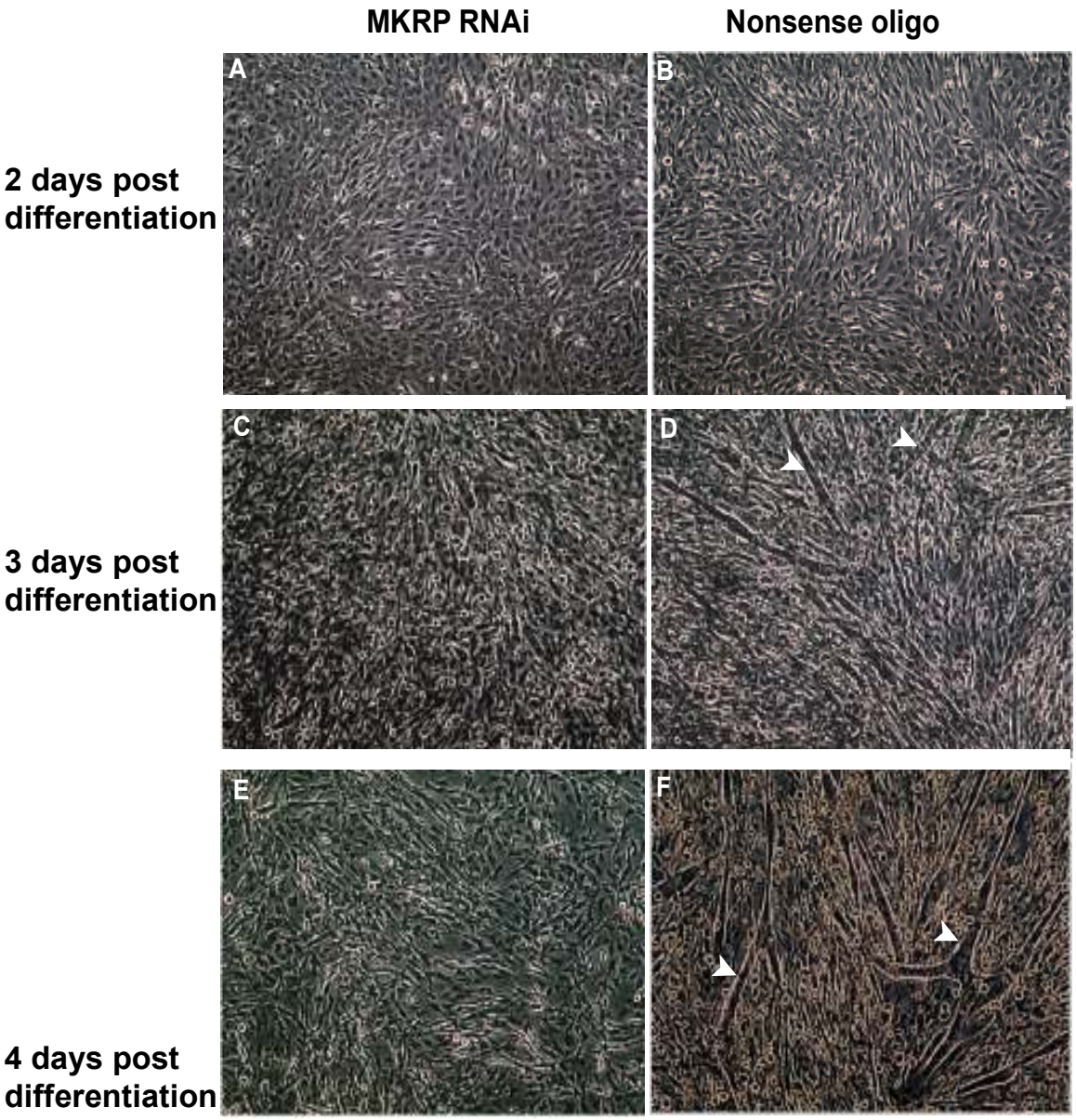

Figure 4.11 DIfferentiation is delayed in cells treated with an RNAi oligo specific for MKRP. A) MKRP RNAi treated cells 2 days post differentiation. B) Nonsense oligo treated cells 2 days post differentiation. C) MKRP RNAi treated cells 3 days post differentiation. D) Small myotubes evident in cells treated with a nonsense RNAi oligo at 3 days post differentiation (white arrowheads). E) Differentiated mytubes were absent at 4 days post differentiation in cells treated with MKRP RNAi oligo. F) Large myotubes were present in control cells at 4 days post differentiation

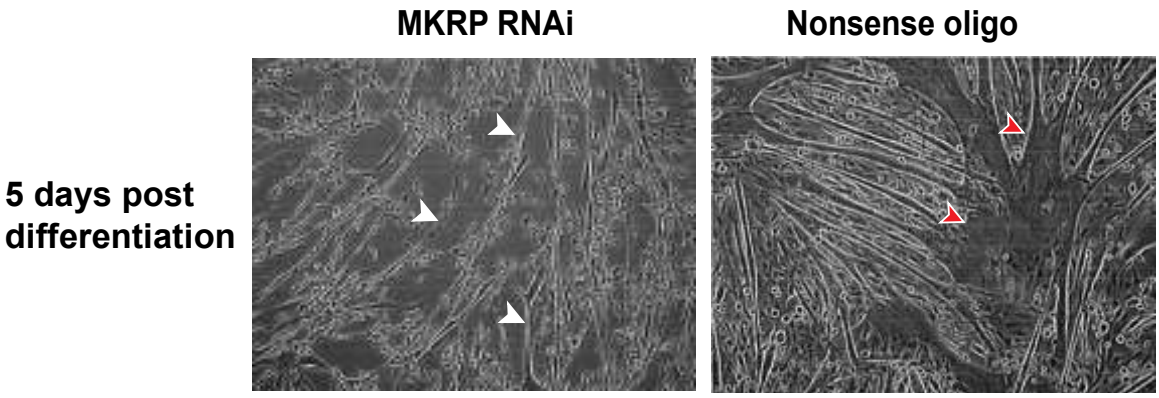

Figure 4.12 siRNA knockdown of MKRP results in delayed differentiation and reduced size in myotubes. Myotubes did not form in the cells treated with an siRNA oligo directed at MKRP until the fifth day post differentiation (white arrowheads), and were considerably smaller than myotubes in cells that received a nonsense oligo (red arrowheads).

Effects of siRNA on differentiation were specific to MKRP

To demonstrate the specifity of the effects of MKRP knockdown, two new oligos were designed and ordered from Ambion (see Materials and Methods), targeting a different location on the MKRP mRNA. Both oligos produced similar results when transfected into C2C12 cells and those cells were allowed to differentiate. Consistent with the transfection of the first oligo, a delay in formation and a decrease in the size of myotubes was observed in the cultures transfected with the two new oligos. In both cases, myotubes did not form after four days in differentiation media (Figure 13). These data support the hypothesis that the delay in differentiation was caused specifically by the knockdown of MKRP.

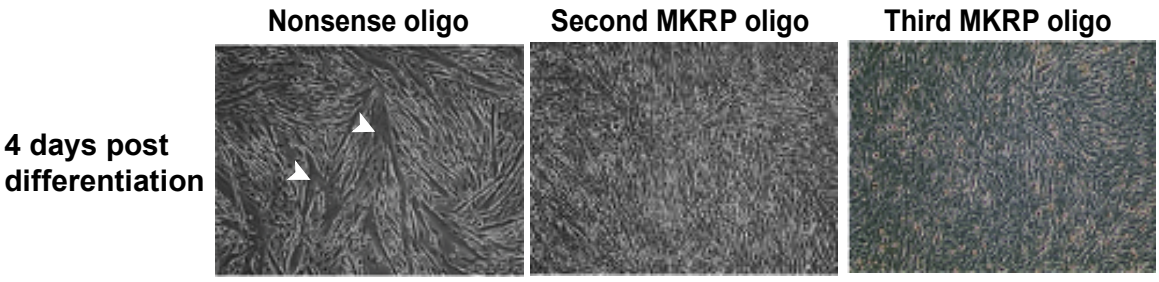

Figure 4.13 Multiple siRNA oligos specific for MKRP also delay differentiation. C2C12 cells were transfected with two different siRNA oligos specific for MKRP or with a nonsense oligo. Both of the new oligos yielded results consistent with the original siRNA assays. Differentiation was delayed in both cultures, myotubes failed to form by the 4th day post-differentiation. Large myotubes were observed in the cells that received the nonsense oligo (arrowheads).

To investigate the effect of MKRP knockdown on the migration capacity of myogenic precursor cells, I performed a wound assay, in which a confluent plate of cells that had been transfected with the MKRP siRNA oligo 24 hours earlier was scraped with a pipet tip to create a 1mm wide wounded area that was clear of cells. Migration was evaluated based on the density of cells that migrated into the wounded area 36 hours after wounding. Migration was clearly inhibited in the plates that received the MKRP siRNA oligo (Figure 13). Cells transfected with a GFP oligo, a nonsense oligo, and no oligo showed no visible affect on migration.

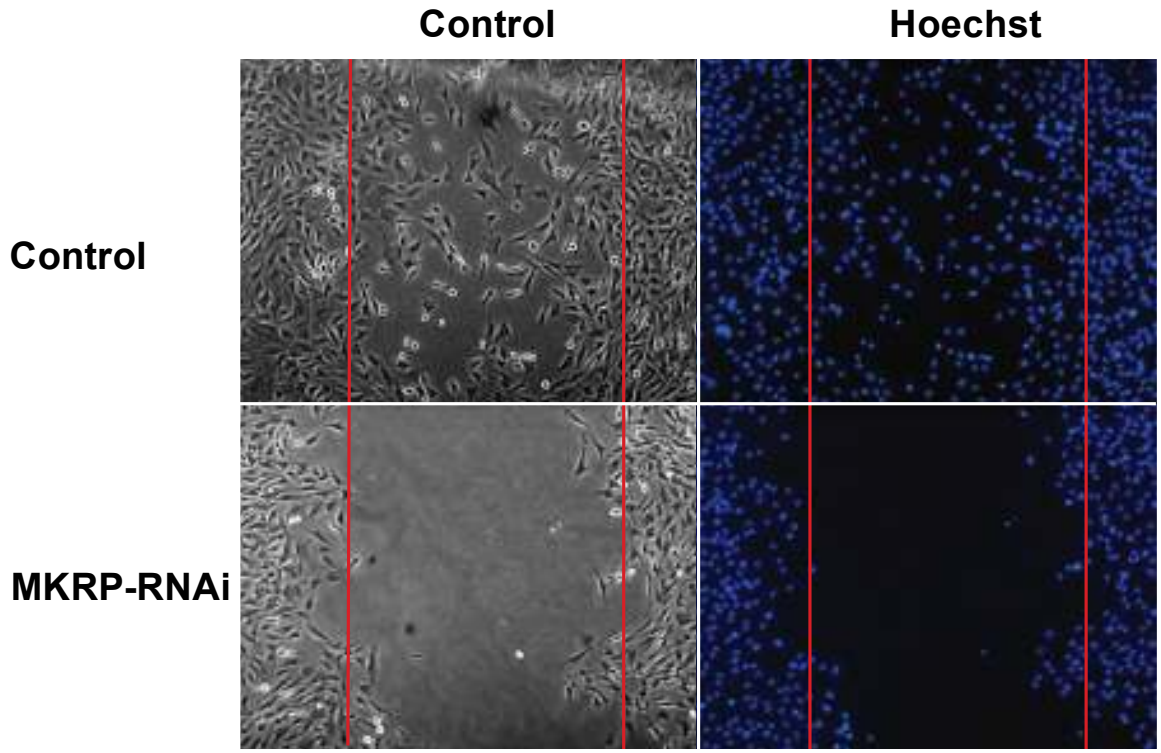

Figure 4.14 MKRP is required for the migration of myogenic progenitor cells. We utilized a conventional migration assay to evaluate the role of MKRP in cellular migration. Following the transfection of siRNA oligonucleotides that were specific for MKRP or GFP (control) a 1mm wide region of cells was denuded and analyzed at defined time periods for cellular migration. At all time periods (12, 24, 36, and 48 hrs) we observed decreased migration of C2C12 myoblasts that were transfected with an siRNA oligonucleotide that decreased MKRP mRNA. Quantification of these results showed a 10 fold reduction in the number of cells migrating into the 1mm wide wounded area in cells treated with MKRP siRNA.

Expression profile shows a delay in the expression of known myogenic genes after MKRP siRNA treatment.

The knockdown of MKRP resulted in the observance of a delay in the differentiation of myoblasts and the formation of myotubes. These data are supported by RT-PCR analysis of genes known to play a role in myogenesis. C2C12 cells were transfected with either the MKRP siRNA oligo, or a nonsense oligo, and induced to differentiate. RNA was extracted prior to differentiation, and for five days after the onset of differentiation. The expression of known

differentiation markers such as myoglobin (Mb), myogenin (Myog) and Mrf4 were delayed for varied lengths of time in cells following MKRP knockdown (Figure14).

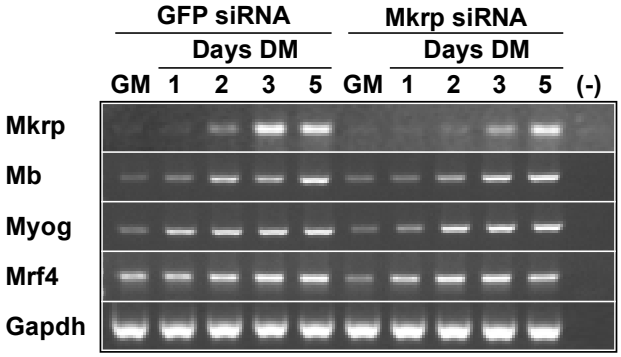

Figure 4.15 Expression profile of myogenic genes in MKRP siRNA treated cells. C2C12 cells were transfected with siRNA oligos directed at MKRP, or GFP, and given low serum media to induce differentiation. The expression of of MKRP was downregulated until the day 3 post differentiation, and the expression of differentiation markers myoglobin (Mb), myogenin (Myog), and Mrf4 were delayed in cells transfected with MKRP siRNA oligo. Gapdh was used as a loading control.

Discussion

Kelch proteins have many diverse functions, however interaction with the actin cytoskeleton is a feature common amongst several members of this protein family, including KRP1, the closest known homologue of MKRP (Spence, 2000). Because of the close structural similarity between MKRP and other proteins known to be involved in cytoskeletal remodeling, migration, and differentiation, we hypothesized that MKRP may have a similar role in myogenic progenitor cells. Microarray data, supported by RT-PCR, had previously demonstrated that MKRP was upregulated during the early stages of skeletal muscle regeneration, a period characterized by the activation, proliferation, and migration of satellite cells. *In situ* hybridization analysis also showed MKRP expression in activated satellite cells, migrating after injury. RT-PCR analysis in differentiating C2C12 cells showed MKRP expression was very low in myoblasts, but was induced at the onset of differentiation, and peaked on the third day post-differentiation. These data, taken together, suggested a possible role for MKRP in the differentiation and migration of myogenic progenitor cells.

To investigate the role of MKRP in the differentiation and migration of progenitor cells, I amplified the full length of MKRP mRNA and subcloned it into a vector

expressing GFP. The plasmid expressing the MKRP-GFP fusion protein was transfected into C2C12 myoblasts, and differentiation was induced by the addition of low serum media. The overexpression of MKRP did not appear to affect the ability of C2C12 cells to differentiate. Differentiation in the cultures transfected with the MKRP-GFP construct occurred in the same time fame as cells transfected with an empty vector. A high rate of cell death in the MKRP-GFP transfected cultures was observed, predominantly on the third day post-differentiation, which would correspond to the peak time period for expression of endogenous MKRP.

When MKRP-GFP was expressed in myoblasts, it was excluded from the nuclear compartment. This result was to be expected, endogenous MKRP would have a mass of approximately 75 kilodaltons (kd), while the addition of the GFP moiety at the C-terminus would create a fusion protein of approximately 100kd. It has been demonstrated previously that proteins larger that 60-70 kilodaltons are restricted in their ability to diffuse passively through the nuclear membrane (Paine, 1975; Peters, 1983, Feldherr, 1990). Diffusion can be affected by other factors such as shape and folding, hydrophobicity, and polarity, but mass greater than 60kd is an exclusionary factor. Both endogenous MKRP and the MKRP-GFP fusion protein would only be able to enter the nucleus at very slow rates, if at all, unless actively transported by a carrier such as Importin-α.

After the onset of differentiation, MKRP-GFP was first observed in a perinuclear position surrounding the nucleus, and then inside the nucleus on Day 3. A TUNEL assay demonstrated that this activity was not caused by the apoptotic death of the cell, and was likely to be the result of active transport.

Within the amino acid sequence of MKRP is an eight residue region of primarily basic amino acids that has strong homology to the canonical nuclear localization sequence (NLS) of the SV40 T-antigen (Kalderon, 1984). This sequence is flanked on both sides by serine and threonine residues, possible targets for regulation of the NLS by phosphorylation/dephosphorylation. To investigate the role of this sequence on the localization of MKRP, I generated fusion proteins expressing the functional domains of MKRP with GFP, and with our without the NLS.

The fusion protein linking the BTB domain to GFP was expressed ubiquitously throughout the cell. With a mass of 45kd, it was able to passively diffuse through the nuclear membrane. After the onset of differentiation, however, the fusion protein was excluded from the nucleus in some cells, and after the third day post-differentiation, it was expressed primarily in the nucleus in some cells. This activity was possibly due to the dimerization of BTB-GFP with endogenous MKRP, which was not expressed robustly until after the induction of differentiation. Dimerization is an activity common in BTB proteins (Perez-Torrado 2006, for review). Prior to differentiation, in the absence of endogenous

MKRP, the BTB-GFP construct would be free to diffuse throughout the cell, but after the expression of the endogenous MKRP, the BTB-GFP protein would interact with the larger endogenous protein, and it's localization would be directed by its binding partner.

When the Kelch domain was expressed with GFP, it never entered the nucleus. After differentiation, Kelch-GFP localized to discreet compartments surrounding the nucleus, similar to the perinuclear position exhibited by the full length protein on the second day post-differentiation. When the NLS was added to the N-terminus of the Kelch-GFP protein, the protein was observed in the nucleus on the third day post-differentiation.

A construct expressing the BTB and BACK domains with the NLS also was translocated to the nucleus. The final experiment was to express the NLS by itself with GFP, to determine if the eight residue sequence by itself was enough to direct the localization of GFP. Transfection of the NLS-GFP plasmid into C2C12 cells showed that GFP was primarily localized to the nucleus.

Although overexpression of MKRP did not appear to affect the ability of C2C12 cells to differentiate into myotubes, the knockdown of MKRP by siRNA clearly delayed the differentiation of myoblasts, and resulted in the formation of much smaller myotubes, indicating a possible impairment of cells ability to migrate or fuse with other cells.

Knockdown of MKRP also resulted in an inhibition of C2C12 cell's ability to migrate, as shown by the wound assay. Transfection with the MKRP-GFP construct, the empty GFP vector, or an siRNA oligo directed at GFP did not have any visible effect on the ability of C2C12 cells to migrate in the wound assay.

Migration, differentiation, and fusion are all functions that require remodeling of the actin cytoskeleton, an area involving Kelch protein family members in several different cell types, including myoblasts (Neuhaus, 2006).

Future directions

The GFP fusion constructs were generated with the intention of using them in protein binding assays, as well as the localization studies. Kelch and BTB domains have already demonstrated protein binding activity in several other known proteins. Prior studies have shown that all three domains, Kelch, BTB and BACK, play a role in the catalyzation of ubiquitination of Nrf2 by Keap1, by providing a scaffold for the ubiquitin ligase and it's substrate (Tong, 2006; Furukuwa, 2005). The three functional domains of MKRP could be used as bait in a yeast two-hybrid assay, or in pull down assays, to identify other interacting proteins. The full length MKRP construct has already been used as bait in a yeast two-hybrid screen, which will be discussed in the next chapter.

To verify the hypothesis that the subcellular localization of BTB-GFP was regulated by it's interaction with the full length endogenous MKRP through dimerization of the BTB domains, immunoprecipitation using an antibody directed at GFP could be used. After transfecting cells with the BTB-GFP plasmid, or the MKRP-GFP plasmid, and inducing differentiation, the cells would be lysed and extracts immunoprecipitated using the GFP antibody. Extracts would be run out on an SDS-PAGE gel, and the gel stained with Coomassie blue or Silver nitrate to visualize the protein bands. The appearance of a band at 75kd after immunoprecipitation would indicate that the BTB-GFP protein or MKRP-GFP had

pulled out endogenous MKRP. The negative control for this assay would be transfection and immunoprecipitation with a plasmid expressing MKRP without the BTB domain, which should not co-precipitate with the endogenous MKRP protein.

Overexpression of MKRP did not affect the ability of C2C12 cells to differentiate, but cell cultures were always given low serum media to induce differentiation at 24 hours after transfection. Knockdown assays with siRNA directed at MKRP showed that inhibition of MKRP expression resulted in a delay in differentiation and myotube formation. It would be possible to investigate the hypothesis that MKRP overexpression could induce or accelerate differentiation in cells without the stimulus of low serum media, with another transfection assay. By transfecting cells with either the MKRP-GFP construct or an empty GFP vector, and leaving them in growth media for four days, it would be possible to assess the ability of MKRP to induce or affect differentiation of myoblasts by observing the appearance of myotubes in the two cell cultures. If myotubes formed more rapidly in the cells transfected with MKRP-GFP, in the absence of low serum media, this would indicate that overexpression of MKRP could induce or accelerate differentiation of myoblasts.

The wound assay demonstrated that knockdown of MKRP by siRNA was able to inhibit the ability of C2C12 cells to migrate, but it does not quantify the degree or extent of that inhibition. It is possible to quantify cellular migration by utilizing

assays that employ two wells separated by a filter, one well containing the cells and the other containing a chemoattractant. Cells are allowed to migrate through the filter for a specific amount of time, and then labeled with a fluorescent dye. Cell number is quantified by FACS, or measurement of total fluorescence.

The role of MKRP and Calsarcin in the Calcineurin pathway

Introduction

Calcineurin is a calmodulin-dependant phosphatase that responds to calcium signaling in variety of tissue types. In skeletal muscle, calcineurin is activated an increase in calcium concentration, and after activation will dephosphorylate and activate the nuclear factor of activated T cell (NFAT) and myocyte enhancement factor-2 (MEF2) transcriptional pathways (Beals, 1997; Chin, 1998; Mao, 1999). Dephosphorylation by calcineurin allows NFATs to translocate from cytoplasm to nucleus, and initiate transcription of its target genes (Beals, 1997). Mammalian skeletal muscle expresses three forms of NFAT at different stages of differentiation, NFATc3 in myotubes, NFATc2 in newly fused, immature myotubes, and NFATc1 in mature myotubes (Abbott, 1998) and each isoform is translocated to the nucleus at the appropriate stage of differentiation. Forced expression of calcineurin in C2C12 myoblasts also resulted in the translocation of NFATc3 to the nucleus, but did not affect the localization of NFATc2 or NFATc3 (Delling 2000). Studies have shown that calcineurin signaling is required for the initiation of skeletal muscle differentiation (Friday, 2000), and that a constitively active form of calcineurin expressed in C2C12 cells induced rapid differentiation and myotube formation, and showed a preference for a slow-twitch muscle fiber type.

Calsarcin-2 has been shown to interact with calcineurin, and regulate its activity by sequestering it at the Z-line in skeletal muscle, and inhibiting its activation (Frey, 2000). A yeast two-hybrid screen performed by Dr. Haibin Xia in the Garry laboratory demonstrated that MKRP interacts with calsarcin-2, suggesting the possibility of a role for MKRP in the calcineurin pathway during development and injury regeneration. Dr. Xia also performed a co-immunoprecipitation assay using the full length of MKRP fused to a Flag tag to demonstrate that MKRP is able to interact with all three known calsarcin proteins, and that it's strongest interaction is with calsarcin-2 (Figure 1).

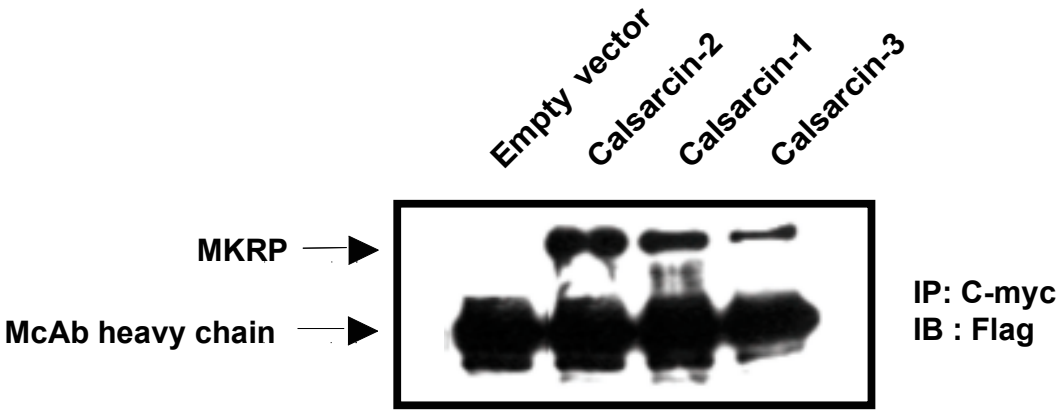

Figure 5.1 Coimmunoprecipitation of MKRP with calsarcins. C2C12 cells were transfected with Flag-MKRP and co-transfected with an empty vector, calsarcin-2-myc, calsarcin-1-myc or calsarcin-3-myc. Lysates were precipitated with C-myc McAb and immunoblottted by Flag McAb.

Dr. Xia hypothesized that MKRP may play a role in the ubiquitination and degradation of calsarcin-2 similar to the mechanism of the degradation of Nrf2 by Keap1 (Itoh, 2003; Zhang, 2004). To investigate this hypothesis, Dr. Xia cotransfected C2C12 cells with equal amounts of a flag tagged calsarcin-2 construct, and increasing concentrations of a plasmid expressing MKRP also fused with Flag. Western blotting of cell extracts showed a clear decrease in the levels of calsarcin-2-Flag protein in cell extracts relative to the increasing concentrations of MKRP-Flag expressed in cells (Figure 2).

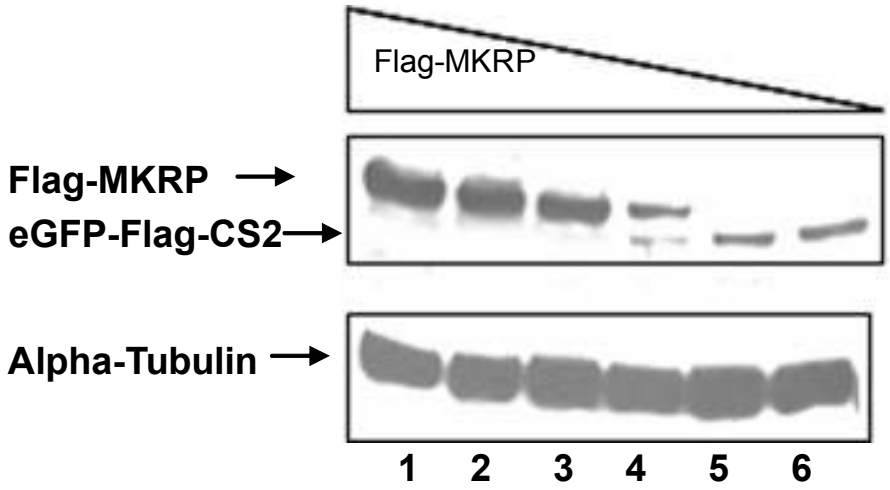

Figure 5.2 Coexpression with MKRP results in the degradation of Calsarcin-2. Cells were transfected with equal amounts (5µg) pf Flag-tagged Calsarcin-2 showed a decrease in Calsarcin-2 protein when co-transfected with increasing concentrations of Flag-tagged MKRP. Lanes: 1) 0 µg MKRP-Flag, 25 µg of empty vector. 2) 1 µg MKRP-FLag, 20 µg of empty vector. 3) 5µg of MKRP-Flag, 20 µg of empty vector. 4) 15 µg of MKRP-FLag, 10 µg of empty vector. 5) 20 µg of MKRP-FLag, 5 µg of empty vector. 6) 25 µg of MKRP-Flag

Taken together, these data suggest that MKRP could play a role in the differentiation of myogenic progenitor cells in development and injury

regeneration, through the regulation of the activation of calcineurin by the degradation of calsarcin-2 (Figure 3). Calcineurin is required for the initiation of differentiation (Friday, 2000) and activated calcineurin can induce differentiation and the accelerated formation of myotubes (Parsons, 2003), so I hypothesized that the loss of calsarcin-2 protein by degradation by MRKP initiates differentiation by allowing calcineurin to become activated, and dephosphorylate and activate its downstream transcription factors. This hypothesis was supported by RT-PCR data showing an inverse relationship between the expression of MKRP and the expression of calsarcin-2 during C2C12 differentiation. MKRP was absent in myoblasts but upregulated after differentiation, and reached a peak on the third day post differentiation. Calsarcin-2 was expressed in myoblasts, but downregulated after differentiation reaching its low point on the third day post differentiation (Figure 4).

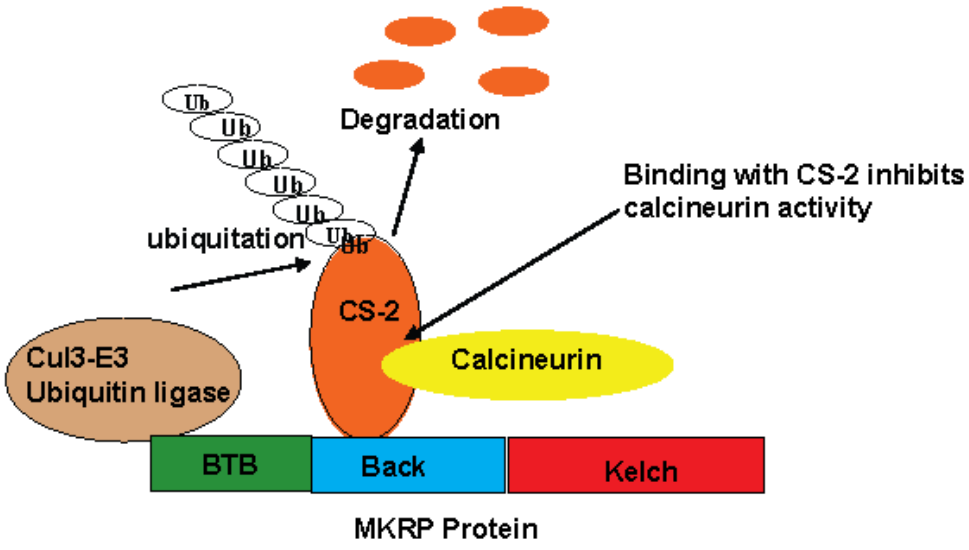

Figure 5.3 MKRP plays a regulatory role in the calcineurin pathway. MKRP provides the scaffold for ubiquitination of calsarcin-2 by a Cul3-E3 ubiquitin ligase. Calsarcin-2 binds calcineurin, rendering it inactive. Degradation of calsarcin-2, mediated by MKRP, releases calcineurin.

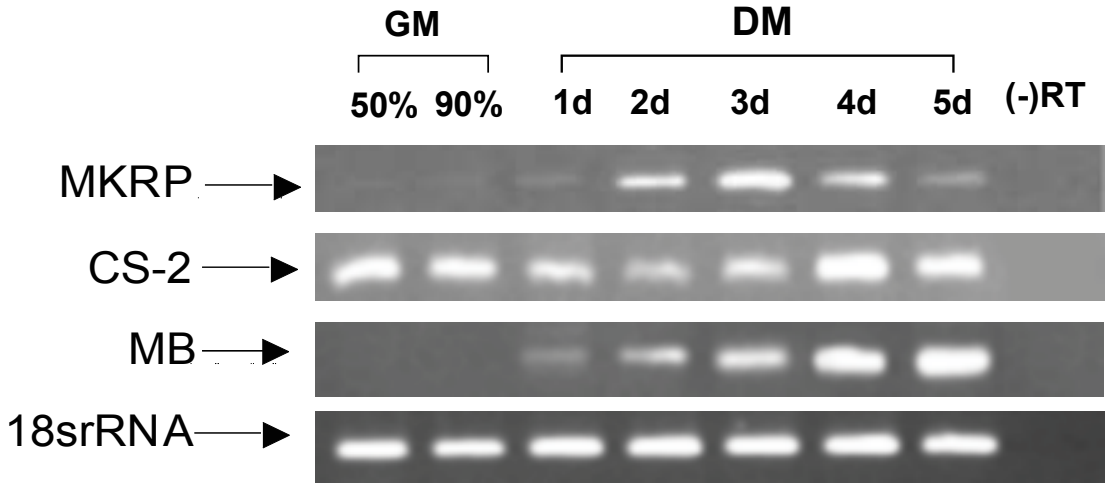

Figure 5.4 Expression of MKRP and calsarcin-2 in C2C12 myoblasts during differentiation. C2C12 myoblasts were cultured in growth media and then changed to low serum media to induce differentiation. Cells were harvested, RNA isolated at specific time periods and semiquantitative RT-PCR analysis was used to examine gene expression. Expression of MKRP was upregulated after the induction of differentiation followed by down regulation at 3 days post-differentiation. Conversely calsarcin-2 expression is present in myoblasts but downregulated after differention. Expression returned to pre-differentiation levels at 4 days post-differentiation. Myoglobin (Mb) expression, a marker for myotube fusion and the presence of mature myotubes, progressively increases after the removal of serum, indicating the progress of differentiation. 18s rRNA is used as a loading control.

A calsarcin-2 knockout mouse had been generated by Dr. Norbert Frye in the Eric Olson lab at Univ. of Texas-Southwestern, the first group to isolate calsarcin-2. However no studies had been performed on this mouse model to characterize the effect of the loss of calsarcin-2 expression *in vivo*. I hypothesized that the

loss of calsarcin-2 would cause a more rapid differentiation of satellite cells during injury regeneration, possibly leading to improved regeneration after injury. To investigate this hypothesis, I used a cardiotoxin injury model similar to that used in the identification of MKRP. Calsarcin-2-/- mice were injured to examine their regenerative capacity. I extracted myoblasts from calsarcin-2-/- animals and wild type littermates for microarray and RT-PCR analysis to create an expression profile.

Results

Calsarcin-2-/- mice showed improved regeneration after injury

The gastrocnemius muscle of 2 calsarcin-2-/- 2 month old males and two wild type littermates were injured by injection of 150 µl of cardiotoxin into each hindlimb. One calsarcin-2-/- and one wild type mouse were sacrificed at one week post injury, and the second pair were sacrificed at 2 weeks post injury. Skeletal muscle was harvested, fixed with PFA, and paraffin embedded for sectioning. H&E staining of embedded sections showed normal regeneration in each mouse at one week, but at 2 weeks, the calsarcin-2-/- demonstrated a much more rapid progression of regeneration. In the calsarcin-2-/- mouse sections, almost all regenerated cells had already become peripherally nucleated (Figure 5).

Due to the increased regenerative capacity in the calsarcin-2-/- mouse skeletal muscle samples after the first injury, there was a concern that the injury in the initial assays may not have been complete, or may have missed the gastrocnemius. To investigate this phenotype further and to make certain of a

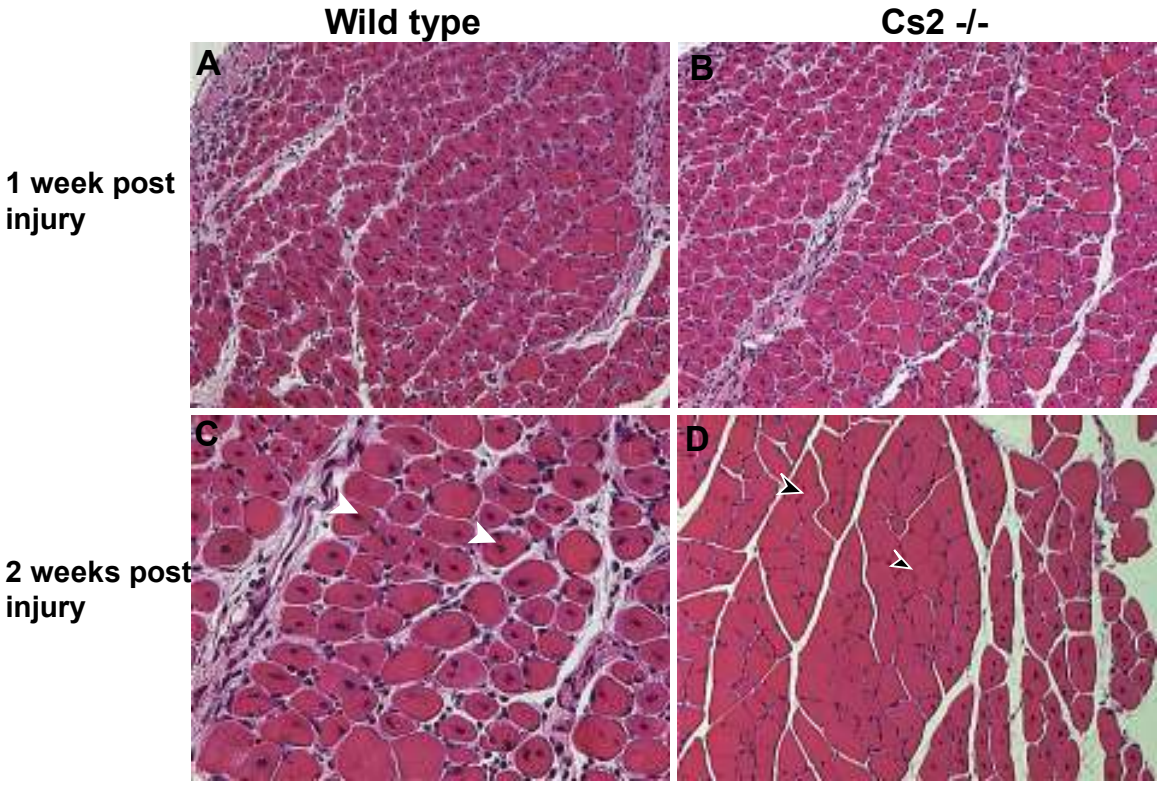

Figure 4.5 Improved regeneration after cardiotoxin injury observed in Calsarcin-2 knockout mice. Gastrocnemius muscles of wild type and CS-2 -/- mice were injured with 150 µl of cardiotxin, and tissues harvested at 1 week and 2 weeks post-injury. Similar regeneration is observed after 1 week in both (A) wild type and (B) CS2-/- mice. (C) Normal regeneration observed at 2 weeks post injury in wild type mice, muscle architecture is restored, and newly regenerated fibers remain centrally nucleated (white arrowheads). (D) Regenerated fibers in CS2-/- mice are peripherally nucleated (black arrowheads) at 2 weeks post injury.

thorough injury to the targeted tissue, I repeated the injury experiment with a calsarcin-2-/- two month old male mouse and a wild type littermate. In this experiment each hindlimb received 300 µl of cardiotoxin to ensure a severe injury occurred in each gastrocnemius. Tissues were harvested at two weeks post injury and fixed and sectioned as previously. The calsarcin-2-/- samples showed clear signs of injury and regeneration, with regenerating cells still centrally nucleated. However, regeneration in the calsarcin-2-/- samples clearly

surpassed regeneration in the wild type samples, which still showed evidence of severe injury including large fat deposits occupying areas where muscle cells had died by necrosis, but not regenerated. No similar fat deposits were observed in the calsarcin-2-/- tissues (Figure 6).

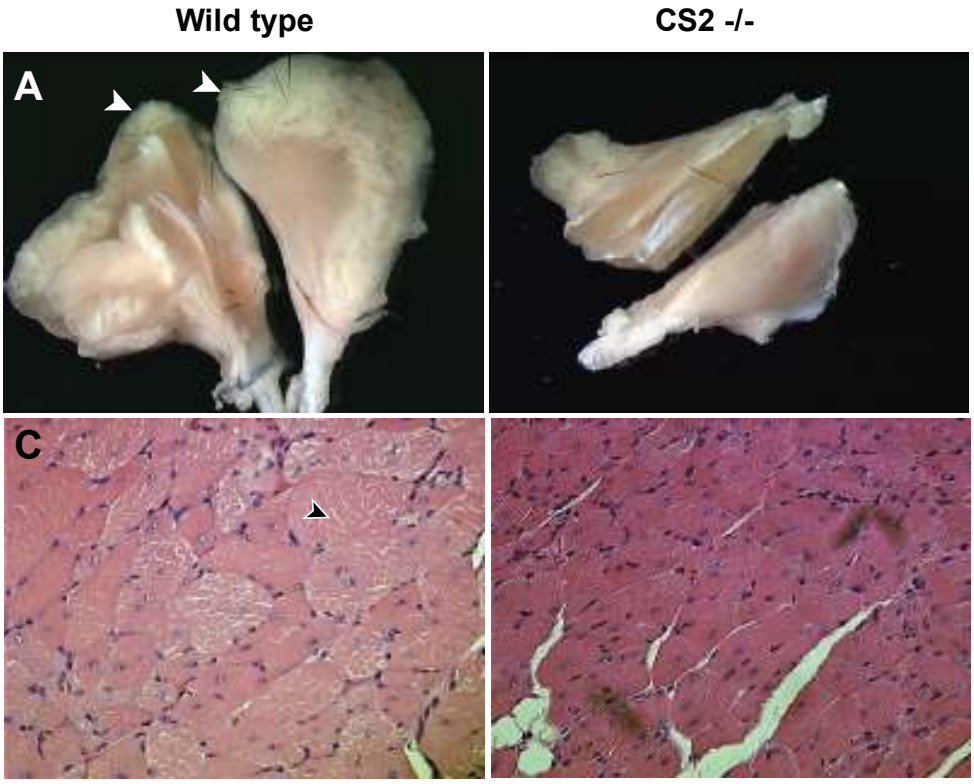

Figure 5.6 Improved regeneration observed after severe injury with cardiotoxin in Cs2 -/- mice. Gastrocnemius muscles of wild type and CS-2-/- mice were injured with 300 µl of cardiotoxin, and tissues harvested at 2 weeks post-injury. A) Gastrocnemius tissue harvested from wild type mice that recieved 300 µl of cardiotoxin contained large fibrotic regions. when harvested 2 weeks post-injury (white arrowheads). B) Tissue harvested from CS-2-/- mice that recieved 300 µl of cardiotoxin showed no fibrosis when harvested 2 weeks post injury. C) Wild type tissue 2 weeks post. D) CS-2 -/- muscle, 2 weeks post injury.

Brdu staining shows proliferating cells in both wild type and calsarcin-2-/- injured tissues.

The mice in the second injury assay were continually exposed to BrdU in their drinking water at a concentration of 8 µg/ml to label proliferating cells and newly regenerated fibers. Both samples showed heavy BrdU staining, with the wild type demonstrating very intense signaling in cells surrounding a number of small, unregenerated areas (Figure 7).

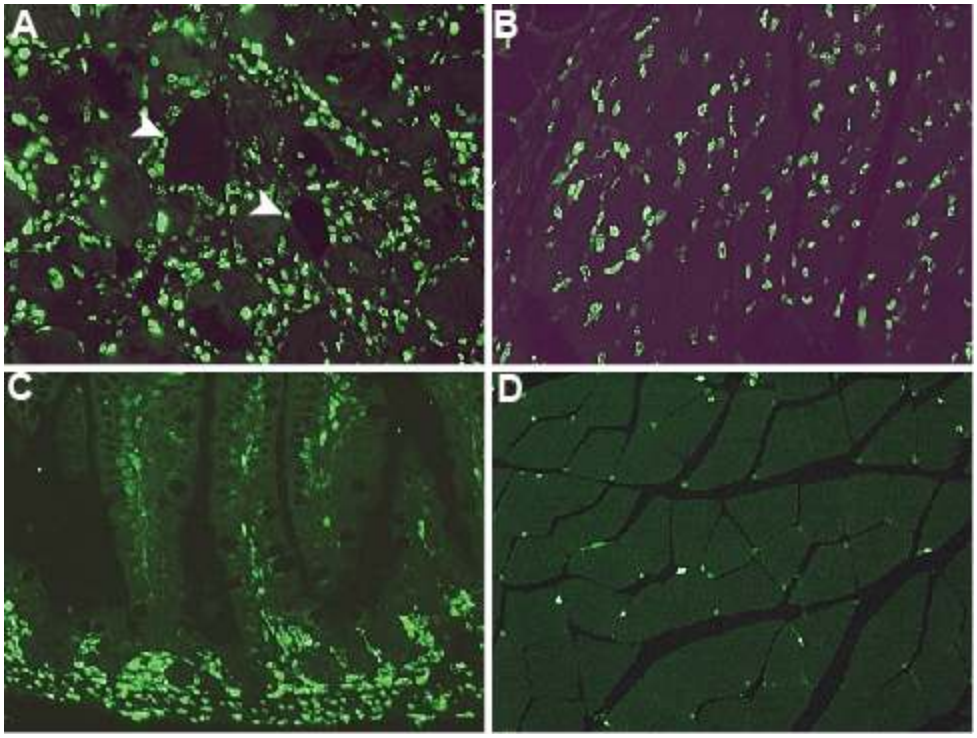

Figure 5.7 Brdu staining shows proliferating cells in wild type and calsarcin2-/- tissue after injury. A) Wild type skeletal muscle, 2 weeks post injury. Most intense expression surrounding areas lacking regeneration. B) Calsarcin-2-/- skeletal muscle, 2 weeks post injury. C) Gut epithelial cells. D) Uninjured wild type skeletal muscle.

Differentiation is accelerated in Calsarcin-2-/- myoblasts

To further investigate the effect of the loss of Calsarcin-2 on the differentiation of myogenic progenitor cells and the maturation of myotubes I isolated myoblasts from four day old calsarcin-2-/- neonates and wild type litter mates and grew them in culture. Differentiation was induced by the addition of low serum media. Cells were harvested for RNA isolation and pictures taken of the cultures prior to the addition of low serum media, and one day after differentiation, at the first appearance of myotubes. Both cultures were equally confluent prior to differentiation, and myotubes appeared earlier and grew larger in the Calsarcin-2-/- cultures (Figure 8).

Microarray

To analyze changes in levels of transcription in the calsarcin-2-/- model during the differentiation of myoblasts, total RNA isolated from 3 Calsarcin-2-/- and 3 wild type cell cultures, prior to and post differentiation, was amplified and cDNA was synthesized from RNA by reverse transcription. cRNA was then transcribed from cDNA templates, and labeled with biotin. The cRNA was hybridized to an Affymetrix microarray chip and scanned to compare changes in mRNA levels of specific transcripts. Student's *t*-tests were performed by Sean Goetsch of the Garry lab, and Dr. Cristi Galindo of the Harold Garner laboratory at Univ. of

Texas-Southwestern to identify significant differences ($P < 0.05$) in data obtained from wild type and Calsarcin-2-/- samples. Data are presented as means ± SE.

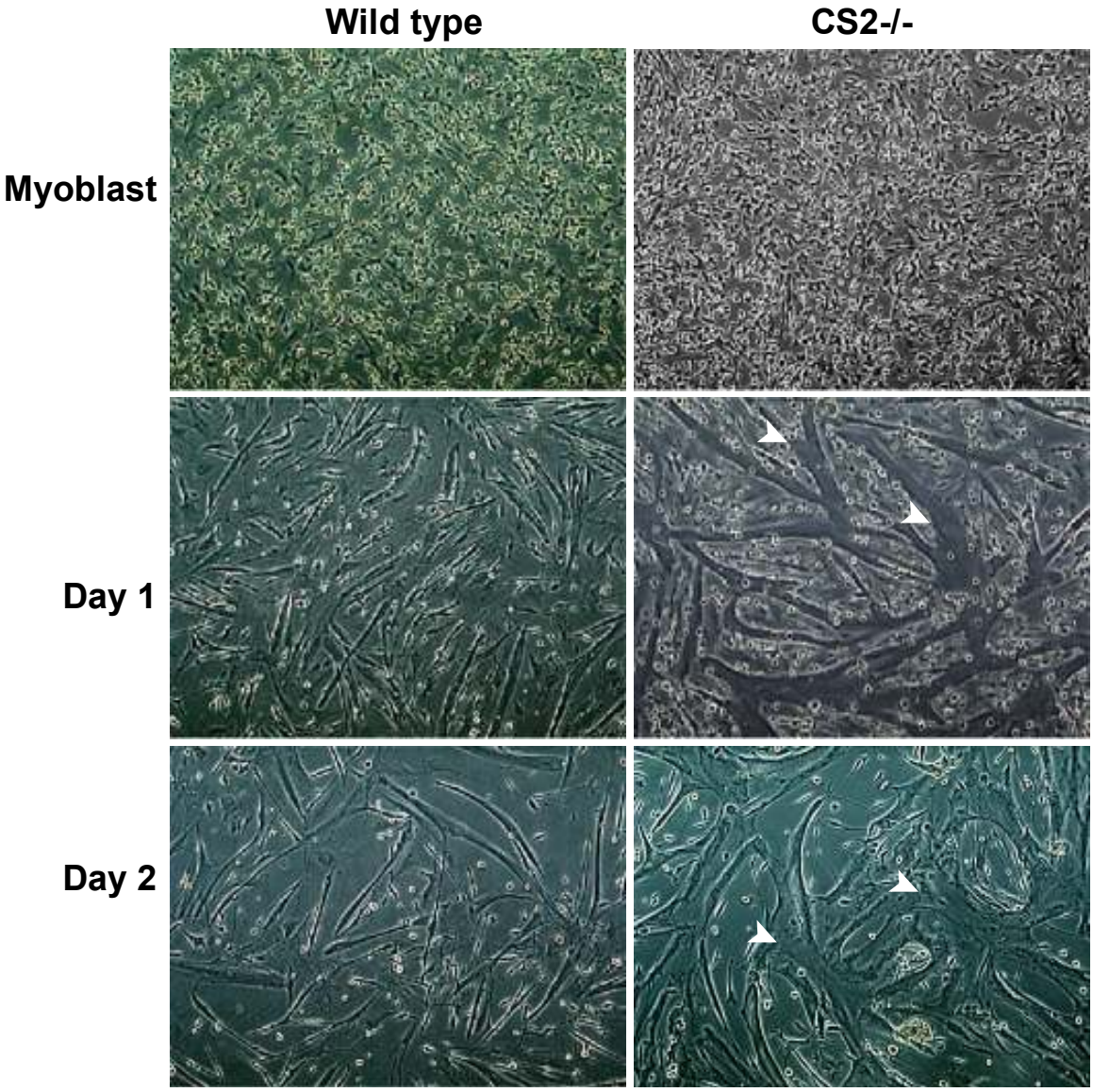

Figure 5.8 Accelerated differentiation in calsarcin-2-/- myoblasts. Myoblasts were isolated from 5-day old calsarcin-2-/- neonates and wild type littermates and plated in equal numbers. After the withdrawl of serum to induce differentiation, myotubes appeared first in the calsarcin-2-/- cells, and myotubes were larger and more mature in the calsarcin-2-/- cultures (arrowheads).

There was some notable disregulation in genes known to play significant roles in myogenesis, particularly Myf5, which was upregulated 5 fold in Calsarcin-2-/- myotubes (Table 1). Myod1 was downregulated in Calsarcin-2-/- myotubes, possibly indicating a more rapid exit from the cell cycle and progression to differentiation in the Calsarcin-2-/- cells. Mef2c, a dephosphorylation target of calcineurin, was downregulated 3.83 fold in the calsarcin-2-/- myoblasts.

Gene	Wild type blasts		CS2 -/- blasts		Fold change		Wild type myotubes		Cs2-/- myotubes		Fold change	
Mb	1233.4	P	1919.79	P	1.56	*	4120.62	P	5937.17	P	1.44	*
Kbtbd5	372.48	P	416.47	P	1.12		692.74	P	504.39	P	-1.37	*
Myog	4946.87	P	5739.94	P	1.16		8037.85	P	4614.56	P	-1.74	*
Myod1	3602.01	P	3757.06	P	1.04		3456.45	P	2279.12	P	-1.52	*
Mef2c	87.58	P	127.77	P	1.46		198.09	P	51.73	P	-3.83	*
Myf6	31.24	A	60.46	A	1.94		80.12	M	129.96	A	1.62	
Nfatc3	545.99	P	563.38	P	1.03		503.13	P	767.47	P	1.53	*
Myf5	645.55	P	804.99	P	1.25	*	160.52	P	817.09	P	5.09	*

Table 5.1 Myogenic genes disregulated in Calsarcin2-/- cells. Several genes known to play a role in myogenesis were disregulated in the Calsarcin2-/- cells, including Myf5, Mef2, and Nfatc3. MKRP (Kbtbd5) was also disregulated after differentiation in Calsarcin2-/- cells. Calsarcin-2 (Myoz1) and Calcineurin (Ppp3ca) were not present at significant levels in myoblasts or myotubes, in this assay.

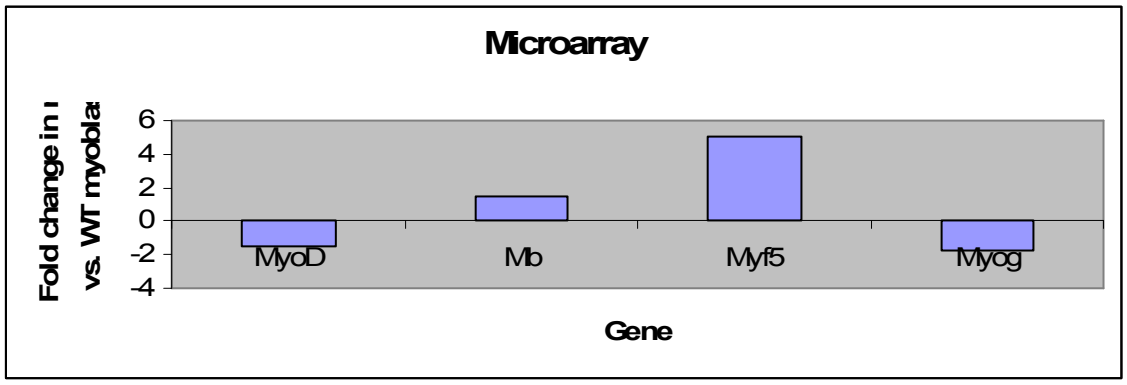

The microarray compares the expression level of 45,000 transcripts. For purposes of thiy analysis, I considered significant dysregulation to be anything greater than 1.5 fold. 1,700 transcripts that demonstrated disregulation during wild type differentiation (comparison of wild type myoblasts and wild type myotubes) were also significantly disregulated between wild type and Calsarcin-2-/- myotubes. A literature search of those 1,700 transcripts showed that 74 were involved in cell migration, cell adhesion, differentiation, or cytoskeletal remodeling (Table 2), functions that could be related to MKRP or Kelch family proteins. Seven of the disregulated genes were involved in cell cycle progression, another key element of the progression from the proliferation cycle to differentiation. Twelve of the identified transcripts were previously characterized transcriptional regulators, including Mef2C, a downstream target of calcineurin, and Foxg1, a Fox family protein related to other genes being characterized in our laboratory.

NAME	Function	A	B	C	D
Dishevelled associated activator of morphogenesis 2 (Daam2)	Actin cytoskeleton organization and biogenesis	2.3			-2.3
Dishevelled associated activator of morphogenesis 2 (Daam2)	Actin cytoskeleton organization and biogenesis	2.3			-2.0
Synaptopodin 2 (Synpo2)	Actin organization and cell motility	-3.9	-3.9	-3.9	-3.9
Neighbor of Punc E11 (Nope)	Cell adhesion	1.5	2.8		2.1
Procollagen, type VIII, alpha 1 (Col8a1)	Cell adhesion	2.0			-2.1
Procollagen, type VIII, alpha 1 (Col8a1)	Cell adhesion	2.1	-1.6		-2.9
Procollagen, type III, alpha 1 (Col3a1)	Cell adhesion	2.1			-2.7
Thrombospondin 2 (Thbs2)	Cell adhesion	2.1			-2.3

Pleckstrin homology domain containing, family H (with MyTH4 domain) member 1 (Plekhh1)	Cell adhesion	2.2	5.4	1.5	3.7
Procollagen, type VIII, alpha 1 (Col8a1)	Cell adhesion	2.2	-1.6		-2.7
Lectin, galactose binding, soluble 9 (Lgals9)	Cell adhesion	2.3			-2.8
Procollagen, type IV, alpha 1 (Col4a1)	Cell adhesion	2.3			-2.4
Thrombospondin 2 (Thbs2)	Cell adhesion	2.4	1.5	-1.6	-2.7
Procollagen, type VI, alpha 2 (Col6a2)	Cell adhesion	2.5			-2.3
Procollagen, type V, alpha 3 (Col5a3)	Cell adhesion	2.6			-2.0
Mesothelin (Msln)	Cell adhesion	2.7	3.0	1.9	2.2
Fibulin 2 (Fbln2)	Cell adhesion	2.8	1.6	-1.7	-2.9
Transmembrane glycoprotein cadherin-10 (Cdh10)	Cell adhesion	3.1	1.7	-1.6	-3.0
Procollagen, type III, alpha 1 (Col3a1)	Cell adhesion	3.2	-2.5		-7.0
Procollagen, type VI, alpha 3 (Col6a3)	Cell adhesion	4.1			-5.0
Procollagen, type V, alpha 1 (Col5a1)	Cell adhesion	4.1	1.5		-3.1
Procollagen, type VI, alpha 2 (Col6a2)	Cell adhesion	4.1	1.5		-3.2
Fibulin 2 (Fbln2)	Cell adhesion	4.3		-1.8	-5.5
Procollagen, type V, alpha 1 (Col5a1)	Cell adhesion	4.4			-3.8
Dermatopontin (Dpt)	Cell adhesion	4.8	1.7		-3.2
Procollagen, type VI, alpha 1 (Col6a1)	Cell adhesion	5.5	2.2		-3.4
Fibulin 5 (Fbln5)	Cell adhesion	6.1	2.8		-3.1
Procollagen, type I, alpha 1 (Col1a1)	Cell adhesion	6.6	2.7		-3.1
Procollagen, type IV, alpha 5 (Col4a5)	Cell adhesion	15.9	6.6		-2.7
Epidermal growth factor-containing fibulin-like extracellular matrix protein 1 (Efemp1)	Cell adhesion	44.6	6.7	-2.3	-15.3
Synaptopodin 2 (Synpo2)	Cell adhesion and motility	7.6			-4.5
EGF-like repeats and discordin I-like domains 3 (Edil3)	Cell adhesion; development	2.0	5.3		2.1
F11 receptor (F11r)	Cell adhesion; epithelial cell differentiation	2.3			-2.0
Amine oxidase, copper containing 3 (Aoc3)	Cell adhesion; inflammatory response	3.9			-5.1
Glycoprotein (transmembrane) nmb (Gpnmb)	Cell adhesion; negative regulation of cell proliferation	3.9		2.8	
Scavenger receptor class B, member 2 (Scarb2)	Cell adhesion; signal transduction	1.5	2.8		2.5
Peripheral myelin protein, 22	Cell cycle arrest; synaptic	2.1	-2.3		-5.0

kDa (Pmp22)	transmission; peripheral nervous system development; negative regulation of cell proliferation				
Cell cycle progression 1 (Ccpg1)	Cell cycle regulation	2.5	4.1		2.0
Calcium/calmodulin-dependent protein kinase II alpha (Camk2a)	Cell cycle regulation	2.6	-1.6		-3.5
High mobility group box protein (Sox2)	Cell fate specification; establishment and/or maintenance of chromatin architecture; transcription regulation	2.0	6.6	-1.7	2.0
Enabled homolog (Enah)	Cell motility; actin filament organization; nervous system development	2.0	-1.6		-2.8
Enabled homolog (Enah)	Cell motility; actin filament organization; nervous system development	2.1			-2.8
Enabled homolog (Enah)	Cell motility; actin filament organization; nervous system development	2.5	-3.8		-6.9
Plateletendothelial cell adhesion molecule (Pecam)	Cell motility; cell adhesion; Rho protein signal transduction; cell recognition	2.8			-2.3
LIM domain only 7 (Lmo7)	Cell-cell adhesion	2.2	-2.9		-4.4
Tensin 1 (Tns1)	Cell-substrate junction assembly; cell migration	2.1			-2.8
Tensin 1 (Tns1)	Cell-substrate junction assembly; cell migration	2.5			-3.0
Tensin 1 (Tns1)	Cell-substrate junction assembly; cell migration	3.0			-3.1
CXC chemokine MIP-2gamma precursor (Cxcl14)	Chemotaxis; inflammation	1.5	-2.3	5.0	
Small inducible cytokine A7 (ScyA7) (Ccl7)	Chemotaxis; inflammation	2.6			-3.2
Small inducible cytokine A9 (ScyA9, Mip-1 gamma)	Chemotaxis; inflammation	3.5	-7.3	3.4	-7.6
Small inducible cytokine A9 (ScyA9, Mip-1 gamma)	Chemotaxis; inflammation	3.7	-6.4	3.7	-6.3
Chemokine (C-C motif) ligand 6 (Ccl6)	Chemotaxis; inflammation	4.0		2.1	-2.5
Small inducible cytokine A2 precursor (Scya2) (Ccl2) (MCP-1)	Chemotaxis; inflammation	4.3		-1.7	-9.6
Proline-serine-threonine phosphatase-interacting protein 1 (Pstpip1)	Cytokinesis; cell adhesion	2.4			-2.3
Palladin, cytoskeletal associated protein (Palld)	Cytoskeleton organization and biogenesis	2.1	-1.7		-3.4
Keratin 19 (Krt19)	Cytoskeleton organization and biogenesis	2.1			-2.9
Palladin, cytoskeletal associated protein (Palld)	Cytoskeleton organization and biogenesis	2.2			-3.0
Actin binding LIM protein family, member 3 (Ablim3)	Cytoskeleton organization and biogenesis	2.3			-2.4
Myosin IF (Myo1f)	Cytoskeleton organization and	2.5	-1.9	2.5	-1.9

	biogenesis				
Actin binding LIM protein family, member 3 (Ablim3)	Cytoskeleton organization and biogenesis	2.6	-1.9	1.8	-2.7
Proline-serine-threonine phosphatase-interacting protein 2 (Pstpip2)	Cytoskeleton organization and biogenesis	5.0	4.0	2.2	1.7
Sema domain, immunoglobulin domain (Ig), short basic domain, secreted, (semaphorin) 3D (Sema3d)	Development; cell differentiation	4.3	1.8		-2.8
Alpha-spectrin 1, erythroid (Spna1)	Hemopoiesis; regulation of cell shape; barbed-end actin filament capping; G-protein coupled receptor protein signaling pathway	3.8	1.7		-2.2
Nuclear distribution gene E-like (Ndel1)	Microtubule cytoskeleton organization and biogenesis; neuron migration; inner mass cell proliferation	2.2	-2.1	2.1	-2.2
Tubulin, beta 6 (Tubb6)	Microtubule-based movement; transport	1.5	-4.8		-6.6
Tubulin, alpha 1 (Tuba1)	Microtubule-based movement; transport	1.5	-3.4		-4.9
Tubulin, alpha 4 (Tuba4)	Microtubule-based movement; transport	4.2			-4.4
Tubulin, alpha 4 (Tuba4)	Microtubule-based movement; transport	5.0			-4.5
Follistatin-like (Fstl1)	Muscle cell proliferation and migration	2.7			-3.1
Follistatin-like (Fstl1)	Muscle cell proliferation and migration	2.8			-3.0
LIM domain and actin binding 1 (Lima1)	Negative regulation of actin filament depolymerization; ruffle organization and biogenesis; actin filament bundle formation	2.0	-1.8		-3.3
Double cortin and calcium/calmodulin-dependent protein kinase-like 1 (Dcamkl1)	Neuron migration; development	3.1	-1.5		-4.0
Double cortin and calcium/calmodulin-dependent protein kinase-like 1 (Dcamkl1)	Neuron migration; development	4.9			-4.0
Double cortin and calcium/calmodulin-dependent protein kinase-like 1 (Dcamkl1)	Neuron migration; development	5.9	2.1		-2.0
S100 calcium binding protein A4 (S100a4)	Regulation of cell adhesion and motility	3.0			-2.7
WNT1 inducible signaling pathway protein 1 (Wisp1)	Regulation of cell growth; cell adhesion; Wnt receptor signaling pathway	2.6	-1.6		-3.7
WNT1 inducible signaling pathway protein 1 (Wisp1)	Regulation of cell growth; cell adhesion; Wnt receptor signaling pathway	2.7	-1.7		-4.0
Nephroblastoma overexpressed gene (Nov)	Regulation of cell growth; cell morphogenesis	2.4			-2.6
Cysteine rich protein 61 (Cyr61)	Regulation of cell growth;	2.2	-2.1		-5.0

	patterning of blood vessels; chemotaxis; cell adhesion				
Cysteine rich protein 61 (Cyr61)	Regulation of cell growth; patterning of blood vessels; chemotaxis; cell adhesion	2.2	-2.2		-5.3
CD24a antigen (CD24a)	Regulation of differentiation	2.0	1.7	-1.7	-2.1
B-cell src-homology tyrosine kinase (Frk)	Regulation of progression through cell cycle	2.2			-2.1
B-cell src-homology tyrosine kinase (Frk)	Regulation of progression through cell cycle	2.4			-2.0
c-Fos induced growth factor (Figf)	Regulation of progression through cell cycle; angiogenesis; cell lproliferation	3.4	1.9		-2.1
c-Fos induced growth factor (Figf)	Regulation of progression through cell cycle; angiogenesis; cell lproliferation	3.8	1.7		-2.7
Growth arrest and DNA-damage-inducible 45 gamma (Gadd45g)	Regulation of progression through cell cycle; DNA repair; MAPK activation	2.8	-1.9		-5.0
Pleiotrophin (Ptn)	Regulation of progression through cell cycle; ossification; transmembrane receptor protein tyrosine phosphatase signaling pathway; nervous system development	5.3			-3.9
Pleiotrophin (Ptn)	Regulation of progression through cell cycle; ossification; transmembrane receptor protein tyrosine phosphatase signaling pathway; nervous system development	49.9	4.7		-10.3
Myosin binding protein H (Mybph)	Regulation of striated muscle contraction; cell adhesion	3.0			-2.6
Procollagen, type I, alpha 2 (Col1a2)	Skeletal development; cell adhesion	2.5			-3.0
Procollagen, type I, alpha 2 (Col1a2)	Skeletal development; cell adhesion	3.0	2.1	-1.6	-2.3
Procollagen, type I, alpha 2 (Col1a2)	Skeletal development; cell adhesion	4.3	1.8	-1.6	-3.9
Collagen pro-alpha-1 type I chain (Col1a1)	Skeletal development; cell adhesion	4.8	3.4	-1.6	-2.3
T-box 18 (Tbx18)	Somitogenesis; positive regulation of mesenchymal cell proliferation; transcription regulation; cell proliferation and differentiation	3.2			-2.4
Zinc finger protein 14 (Zfp14)	Transcription regulation	1.5	2.7		2.2
TAF15 RNA polymerase II, TATA box binding protein (TBP)-associated factor (Taf15)	Transcription regulation	2.2	-2.1	4.5	
Estrogen-related receptor gamma (Esrrg)	Transcription regulation	2.9	4.7		2.2
LIM and cysteine-rich domains 1 (Lmcd1)	Transcription regulation	3.2	-1.9	1.7	-3.5
Ankyrin repeat and SOCS box-containing protein 15 (Asb15)	Transcription regulation	4.6	10.9		2.3

PRKC, apoptosis, WT1, regulator (Pawr)	Transcription regulation; apoptosis; negative regulation of B cell proliferation	2.8	2.1	-1.5	-2.0
D site albumin promoter binding protein (Dbp)	Transcription regulation; circadian rhythm	2.4	7.5		4.1
Friend leukemia integration 1 (Fli1)	Transcription regulation; circulation; organ morphogenesis	3.1	-1.8	1.7	-3.3
Early B-cell factor 2 (Ebf2)	Transcription regulation; development	2.1			-2.4
Early B-cell factor 2 (Ebf2)	Transcription regulation; development	2.6			-2.9
Myocyte enhancer factor 2C (Mef2c)	Transcription regulation; development	2.8	-1.5	2.7	-1.5
Homeo box A1 (Hoxa1)	Transcription regulation; development	4.5			-3.3
GATA binding protein 6 (Gata6)	Transcription regulation; development; microtubule-based movement	2.3			-2.1
Homeo box D9 (Hoxd9)	Transcription regulation; development; organ morphogenesis	1.5	2.7		2.0
Forkhead box G1 (Foxg1)	Transcription regulation; dorsal/ventral pattern formation	2.5		-2.1	-6.5
Muscle, skeletal, receptor tyrosine kinase (Musk)	Transcription regulation; microtubule-based movement; neuromuscular junction development; receptor clustering	2.6	4.5	1.5	2.6
Retinoblastoma-like 2 (Rbl2)	Transcription regulation; negative regulation of progression through cell cycle	2.5	2.0	2.0	1.6
PYD and CARD domain containing (Pycard)	Transcription regulation; proteolysis; induction of apoptosis; inflammatory response; negative regulation of progression through cell cycle; positive regulation of caspase activity; positive regulation of interleukin-1 beta secretion	2.1	-2.2	2.3	-2.1

Table 5.2 Differentiation related transcripts disregulated between Calsarcin-2-/- and wild type myotubes. Microarray analysis of the expression profile of Calsarcin-2-/- myoblasts during differentiation showed significant disregulation in several transcripts related to cell migration and cytoskeletal remodeling, and in twelve transcription factors including Mef2C, a known downstream target of calcineurin. Column A) The fold change in expression of specific genes as wild type myoblasts differentiate into myotubes. Column B) The fold change in expression of specific genes in Calsarcin-2-/- myoblasts as they differentiate into myotubes. Column C) The difference in expression levels of specific genes between wild type and Calsarcin-2-/- myoblasts, expressed as fold change. Column D) The difference in expression levels of specific genes between wild type and Calsarcin-2-/- myotubes, expressed as fold change.

Discussion

The hypothesis that the loss of Calsarcin-2 results in accelerated regeneration and more rapid differentiation of myoblasts is supported by the results of my investigations. The initial injury assay showed the rapid regeneration of skeletal muscle lacking Calsarcin-2, and these data were confirmed by a second, more severe injury, in which the Calsarcin-2-/- tissue clearly regenerated more rapidly and more completely than the injury in its wild type counterpart. The differentiation assay also showed that myotubes formed more rapidly in cultures of Calsarcin-2-/- myoblasts, in comparison to wild type myoblasts. The microarray analysis showed an upregulation of myoglobin (Mb), an established marker for differentiation, in the Calsarcin-2-/- cells. These data taken together support the hypothesis that myoblasts which do not express Calsarcin-2 are able to differentiate and regenerate from injury more rapidly, possibly through the constitutive signaling of calcineurin, an established interacting partner with Calsarcin-2.

All of the assays in this study should be repeated when more Calsarcin-2-/- mice are available. Seven different time points should be used for the injury assays, comparable to the time points used in the original assay that identified MKRP. Injured tissue should also be harvested for RNA isolation at those same time

points for microarray analysis and RT-PCR to generate a more complete expression profile.

The myoblast isolation and microarray analysis also need to be performed again with more time points, which is also contingent on the availability and breeding capacity of the Calsarcin-2-/- mouse colony. The Calsarcin-2-/- mice have been very poor breeders with very small litters that are often cannabilized by the parents, making it difficult to produce enough cells for the assay, and those cells that are isolated have not grown or proliferated well in culture.

The available data support the hypothesis that MKRP plays an important role in the differentiation and migration of myogenic precursor cells, through its interaction with Calsarcin-2 and a possible connection to the calcineurin pathway, but more extensive assays need to be performed to characterize this proposed mechanism.

References

Abbott KL, Friday BB, Thaloor D, Murphy TJ, Pavlath GK., Activation and cellular localization of the cyclosporine A-sensitive transcription factor NF-AT in skeletal muscle cells.
Mol Biol Cell. 1998 Oct;9(10):2905-16.

Adams J, Kelso R, Cooley L., The kelch repeat superfamily of proteins: propellers of cell function.
Trends Cell Biol. 2000 Jan;10(1):17-24.

Adi S, Cheng ZQ, Zhang PL, Wu NY, Mellon SH, Rosenthal SM., Opposing early inhibitory and late stimulatory effects of insulin-like growth factor-I on myogenin gene transcription.
J Cell Biochem. 2000 Jun 12;78(4):617-26.

Albagli O, Dhordain P, Deweindt C, Lecocq G, Leprince D., The BTB/POZ domain: a new protein-protein interaction motif common to DNA- and actin-binding proteins.
Cell Growth Differ. 1995 Sep;6(9):1193-8.

Allen RE, Sheehan SM, Taylor RG, Kendall TL, Rice GM., Hepatocyte growth factor activates quiescent skeletal muscle satellite cells in vitro.
J Cell Physiol. 1995 Nov;165(2):307-12.

Andermarcher E, Surani MA, Gherardi E., Co-expression of the HGF/SF and c-met genes during early mouse embryogenesis precedes reciprocal expression in adjacent tissues during organogenesis.
Dev Genet. 1996;18(3):254-66.

Armand O, Boutineau AM, Mauger A, Pautou MP, Kieny M., Origin of satellite cells in avian skeletal muscles.
Arch Anat Microsc Morphol Exp. 1983;72(2):163-81.

Beals CR, Clipstone NA, Ho SN, Crabtree GR., Nuclear localization of NF-ATc by a calcineurin-dependent, cyclosporin-sensitive intramolecular interaction.
Genes Dev. 1997 Apr 1;11(7):824-34.

Benson DA, Karsch-Mizrachi I, Lipman DJ, Ostell J, Wheeler DL., GenBank: update.
Nucleic Acids Res. 2004 Jan 1;32(Database issue):D23-6.

Bernstein E, Caudy AA, Hammond SM, Hannon GJ., Role for a bidentate ribonuclease in the initiation step of RNA interference.
Nature. 2001 Jan 18;409(6818):363-6.

Berry MJ, Banu L, Chen YY, Mandel SJ, Kieffer JD, Harney JW, Larsen PR., Recognition of UGA as a selenocysteine codon in type I deiodinase requires sequences in the 3' untranslated region.
Nature. 1991 Sep 19;353(6341):273-6.

Bittner RE, Schofer C, Weipoltshammer K, Ivanova S, Streubel B, Hauser E, Freilinger M, Hoger H, Elbe-Burger A, Wachtler F., Recruitment of bone-marrow-derived cells by skeletal and cardiac muscle in adult dystrophic mdx mice.
Anat Embryol (Berl). 1999 May;199(5):391-6.

Bladt F, Riethmacher D, Isenmann S, Aguzzi A, Birchmeier C., Essential role for the c-met receptor in the migration of myogenic precursor cells into the limb bud.
Nature. 1995 Aug 31;376(6543):768-71.

Bober E, Franz T, Arnold HH, Gruss P, Tremblay P., Pax-3 is required for the development of limb muscles: a possible role for the migration of dermomyotomal muscle progenitor cells.
Development. 1994 Mar;120(3):603-12.

Bodine SC, Stitt TN, Gonzalez M, Kline WO, Stover GL, Bauerlein R, Zlotchenko E, Scrimgeour A, Lawrence JC, Glass DJ, Yancopoulos GD., Akt/mTOR pathway is a crucial regulator of skeletal muscle hypertrophy and can prevent muscle atrophy in vivo.
Nat Cell Biol. 2001 Nov;3(11):1014-9.

Bork P, Doolittle RF., Drosophila kelch motif is derived from a common enzyme fold.
J Mol Biol. 1994 Mar 11;236(5):1277-82.

Bougis PE, Marchot P, Rochat H., Characterization of elapidae snake venom components using optimized reverse-phase high-performance liquid chromatographic conditions and screening assays for alpha-neurotoxin and phospholipase A2 activities.
Biochemistry. 1986 Nov 4;25(22):7235-43.

Brand-Saberi B, Ebensperger C, Wilting J, Balling R, Christ B., The ventralizing effect of the notochord on somite differentiation in chick embryos.
Anat Embryol (Berl). 1993 Sep;188(3):239-45.

Braun T, Bober E, Buschhausen-Denker G, Kohtz S, Grzeschik KH, Arnold HH., Differential expression of myogenic determination genes in muscle cells: possible autoactivation by the Myf gene products.
EMBO J. 1989 Dec 1;8(12):3617-25. Erratum in: EMBO J 1989 Dec;8(13):4358.

Braun T, Arnold HH., The four human muscle regulatory helix-loop-helix proteins Myf3-Myf6 exhibit similar hetero-dimerization and DNA binding properties.
Nucleic Acids Res. 1991 Oct 25;19(20):5645-51.

Braun T, Rudnicki MA, Arnold HH, Jaenisch R., Targeted inactivation of the muscle regulatory gene Myf-5 results in abnormal rib development and perinatal death.
Cell. 1992 Oct 30;71(3):369-82.

Braun T, Bober E, Rudnicki MA, Jaenisch R, Arnold HH., MyoD expression marks the onset of skeletal myogenesis in Myf-5 mutant mice.
Development. 1994 Nov;120(11):3083-92.

Brohmann H, Jagla K, Birchmeier C., The role of Lbx1 in migration of muscle precursor cells.
Development. 2000 Jan;127(2):437-45.

Caldwell CJ, Mattey DL, Weller RO., Role of the basement membrane in the regeneration of skeletal muscle.
Neuropathol Appl Neurobiol. 1990 Jun;16(3):225-38.

Camargo FD, Green R, Capetanaki Y, Jackson KA, Goodell MA., hematopoietic stem cells generate skeletal muscle through myeloid intermediates.
Nat Med. 2003 Dec;9(12):1520-7.

Carlson BM., Regeneration research in the Soviet Union.
Anat Rec. 1968 Apr;160(4):665-74.

Carlson BM., Regeneration of the completely excised gastrocnemius muscle in the frog and rat from minced muscle fragments.
J Morphol. 1968 Aug;125(4):447-72.

Carlson BM., The regeneration of a limb muscle in the axolotl from minced fragments.
Anat Rec. 1970 Mar;166(3):423-34.

Carlson BM., The effects of rotation and positional change of stump tissues upon morphogenesis of the regenerating axolotl limb.
Dev Biol. 1975 Dec;47(2):269-91.

Carlson BM, Foster AH, Bader DM, Hnik P, Vejsada R., Restoration of full mass in nerve-intact muscle grafts after delayed reinnervation.
Experientia. 1983 Feb 15;39(2):171-2.

Carredano E, Westerlund B, Persson B, Saarinen M, Ramaswamy S, Eaker D, Eklund H., The three-dimensional structures of two toxins from snake venom throw light on the anticoagulant and neurotoxic sites of phospholipase A2.
Toxicon. 1998 Jan;36(1):75-92.

Carroll SL, Herrera AH, Horowits R., Targeting and functional role of N-RAP, a nebulin-related LIM protein, during myofibril assembly in cultured chick cardiomyocytes.
J Cell Sci. 2001 Dec;114(Pt 23):4229-38.

Chen W, Zollman S, Couderc JL, Laski FA., The BTB domain of bric a brac mediates dimerization in vitro.
Mol Cell Biol. 1995 Jun;15(6):3424-9.

Chien KY, Chiang CM, Hseu YC, Vyas AA, Rule GS, Wu W., Two distinct types of cardiotoxin as revealed by the structure and activity relationship of their

interaction with zwitterionic phospholipid dispersions.
J Biol Chem. 1994 May 20;269(20):14473-83.

Chin ER, Olson EN, Richardson JA, Yang Q, Humphries C, Shelton JM, Wu H, Zhu W, Bassel-Duby R, Williams RS., calcineurin-dependent transcriptional pathway controls skeletal muscle fiber type.
Genes Dev. 1998 Aug 15;12(16):2499-509.

Chiou SH, Raynor RL, Zheng B, Chambers TC, Kuo JF., Cobra venom cardiotoxin (cytotoxin) isoforms and neurotoxin: comparative potency of protein kinase C inhibition and cancer cell cytotoxicity and modes of enzyme inhibition.
Biochemistry. 1993 Mar 2;32(8):2062-7.

Cornelison DD, Wold BJ., Single-cell analysis of regulatory gene expression in quiescent and activated mouse skeletal muscle satellite cells.
Dev Biol. 1997 Nov 15;191(2):270-83.

Cossu G, Kelly R, Tajbakhsh S, Di Donna S, Vivarelli E, Buckingham M., Activation of different myogenic pathways: myf-5 is induced by the neural tube and MyoD by the dorsal ectoderm in mouse paraxial mesoderm.
Development. 1996 Feb;122(2):429-37.

Cuff JA, Barton GJ., Application of multiple sequence alignment profiles to improve protein secondary structure prediction.
Proteins. 2000 Aug 15;40(3):502-11.

De Angelis L, Berghella L, Coletta M, Lattanzi L, Zanchi M, Cusella-De Angelis MG, Ponzetto C, Cossu G., Skeletal myogenic progenitors originating from embryonic dorsal aorta coexpress endothelial and myogenic markers and contribute to postnatal muscle growth and regeneration.
J Cell Biol. 1999 Nov 15;147(4):869-78.

Delling U, Tureckova J, Lim HW, De Windt LJ, Rotwein P, Molkentin JD., A calcineurin-NFATc3-dependent pathway regulates skeletal muscle differentiation and slow myosin heavy-chain expression.
Mol Cell Biol. 2000 Sep;20(17):6600-11.

Dhume A, Lu S, Horowits R., Targeted disruption of N-RAP gene function by RNA interference: a role for N-RAP in myofibril organization.
Cell Motil Cytoskeleton. 2006 Aug;63(8):493-511.

DiBello PR, Withers DA, Bayer CA, Fristrom JW, Guild GM., The Drosophila Broad-Complex encodes a family of related proteins containing zinc fingers.
Genetics. 1991 Oct;129(2):385-97.

Dietrich S, Abou-Rebyeh F, Brohmann H, Bladt F, Sonnenberg-Riethmacher E, Yamaai T, Lumsden A, Brand-Saberi B, Birchmeier C., The role of SF/HGF and c-Met in the development of skeletal muscle.
Development. 1999 Apr;126(8):1621-9.

Doyonnas R, LaBarge MA, Sacco A, Charlton C, Blau HM., Hematopoietic contribution to skeletal muscle regeneration by myelomonocytic precursors.
Proc Natl Acad Sci U S A. 2004 Sep 14;101(37):13507-12.

Dubovskii PV, Lesovoy DM, Dubinnyi MA, Utkin YN, Arseniev AS., Interaction of the P-type cardiotoxin with phospholipid membranes.
Eur J Biochem. 2003 May;270(9):2038-46.

Dufton MJ, Hider RC., Conformational properties of the neurotoxins and cytotoxins isolated from Elapid snake venoms.
CRC Crit Rev Biochem. 1983;14(2):113-71

Dufton MJ, Eaker D, Hider RC., Conformational properties of phospholipases A2. Secondary-structure prediction, circular dichroism and relative interface hydrophobicity.
Eur J Biochem. 1983 Dec 15;137(3):537-44.

Echeverri K, Clarke JD, Tanaka EM., In vivo imaging indicates muscle fiber dedifferentiation is a major contributor to the regenerating tail blastema.
Dev Biol. 2001 Aug 1;236(1):151-64.

Eggler AL, Liu G, Pezzuto JM, van Breemen RB, Mesecar AD., Modifying specific cysteines of the electrophile-sensing human Keap1 protein is insufficient to disrupt binding to the Nrf2 domain Neh2.
Proc Natl Acad Sci U S A. 2005 Jul 19;102(29):10070-5.

Eichinger L, Bomblies L, Vandekerckhove J, Schleicher M, Gettemans J., A novel type of protein kinase phosphorylates actin in the actin-fragmin complex.
EMBO J. 1996 Oct 15;15(20):5547-56.

Elbashir SM, Lendeckel W, Tuschl T., RNA interference is mediated by 21- and 22-nucleotide RNAs.
Genes Dev. 2001 Jan 15;15(2):188-200.

Elbashir SM, Harborth J, Weber K, Tuschl T., Analysis of gene function in somatic mammalian cells using small interfering RNAs.
Methods. 2002 Feb;26(2):199-213.

Epstein JA, Shapiro DN, Cheng J, Lam PY, Maas RL., Pax3 modulates expression of the c-Met receptor during limb muscle development.
Proc Natl Acad Sci U S A. 1996 Apr 30;93(9):4213-8.

Faulkner G, Pallavicini A, Comelli A, Salamon M, Bortoletto G, Ievolella C, Trevisan S, Kojic' S, Dalla Vecchia F, Laveder P, Valle G, Lanfranchi G., FATZ, a filamin-, actinin-, and telethonin-binding protein of the Z-disc of skeletal muscle.
J Biol Chem. 2000 Dec 29;275(52):41234-42.

Feldherr CM, Akin D., The permeability of the nuclear envelope in dividing and nondividing cell cultures.
J Cell Biol. 1990 Jul;111(1):1-8.

Feng YX, Levin JG, Hatfield DL, Schaefer TS, Gorelick RJ, Rein A,. Suppression of UAA and UGA termination codons in mutant murine leukemia viruses.
J Virol. 1989 Jun;63(6):2870-3.

Ferrari G, Cusella-De Angelis G, Coletta M, Paolucci E, Stornaiuolo A, Cossu G, Mavilio F., Muscle regeneration by bone marrow-derived myogenic progenitors.
Science. 1998 Mar 6;279(5356):1528-30. Erratum in: Science 1998 Aug 14;281(5379):923.

Fink E, Fortin D, Serrurier B, Ventura-Clapier R, Bigard AX., Recovery of contractile and metabolic phenotypes in regenerating slow muscle after notexin-induced or crush injury.
J Muscle Res Cell Motil. 2003;24(7):421-9.

Fire A, Albertson D, Harrison SW, Moerman DG., Production of antisense RNA leads to effective and specific inhibition of gene expression in C. elegans muscle.
Development. 1991 Oct;113(2):503-14.

Fire A, Xu S, Montgomery MK, Kostas SA, Driver SE, Mello CC., Potent and specific genetic interference by double-stranded RNA in Caenorhabditis elegans.
Nature. 1998 Feb 19;391(6669):806-11.

Fletcher JE, Jiang MS, Gong QH, Yudkowsky ML, Wieland SJ., Effects of a cardiotoxin from Naja naja kaouthia venom on skeletal muscle: involvement of calcium-induced calcium release, sodium ion currents and phospholipases A2 and C.
Toxicon. 1991;29(12):1489-500.

Frey N, Richardson JA, Olson EN., Calsarcins, a novel family of sarcomeric calcineurin-binding proteins.
Proc Natl Acad Sci U S A. 2000 Dec 19;97(26):14632-7.

Frey N, Olson EN., Calsarcin-3, a novel skeletal muscle-specific member of the calsarcin family, interacts with multiple Z-disc proteins.
J Biol Chem. 2002 Apr 19;277(16):13998-4004.

Frey N, Barrientos T, Shelton JM, Frank D, Rutten H, Gehring D, Kuhn C, Lutz M, Rothermel B, Bassel-Duby R, Richardson JA, Katus HA, Hill JA, Olson EN, Mice lacking calsarcin-1 are sensitized to calcineurin signaling and show accelerated cardiomyopathy in response to pathological biomechanical stress.
Nat Med. 2004 Dec;10(12):1336-43.

Friday BB, Horsley V, Pavlath GK., Calcineurin activity is required for the initiation of skeletal muscle differentiation.
J Cell Biol. 2000 May 1;149(3):657-66.

Furukawa M, He YJ, Borchers C, Xiong Y., Targeting of protein ubiquitination by BTB-Cullin 3-Roc1 ubiquitin ligases.
Nat Cell Biol. 2003 Nov;5(11):1001-7. Epub 2003 Oct 5

Furukawa M, Xiong Y., BTB protein Keap1 targets antioxidant transcription factor Nrf2 for ubiquitination by the Cullin 3-Roc1 ligase.
Mol Cell Biol. 2005 Jan;25(1):162-71.

Gamel AJ, Brand-Saberi B, Christ B., Halves of epithelial somites and segmental plate show distinct muscle differentiation behavior in vitro compared to entire somites and segmental plate.
Dev Biol. 1995 Dec;172(2):625-39.

Garry DJ, Yang Q, Bassel-Duby R, Williams RS., Persistent expression of MNF identifies myogenic stem cells in postnatal muscles.
Dev Biol. 1997 Aug 15;188(2):280-94.

Garry DJ, Meeson A, Elterman J, Zhao Y, Yang P, Bassel-Duby R, Williams, S,. Myogenic stem cell function is impaired in mice lacking the forkhead/winged helix protein MNF.
Proc Natl Acad Sci U S A. 2000 May 9;97(10):5416-21.

Gavrieli Y, Sherman Y, Ben-Sasson SA., Identification of programmed cell death in situ via specific labeling of nuclear DNA fragmentation.
J Cell Biol. 1992 Nov;119(3):493-501.

Geyer R, Wee S, Anderson S, Yates J, Wolf DA., BTB/POZ domain proteins are putative substrate adaptors for cullin 3 ubiquitin ligases.
Mol Cell. 2003 Sep;12(3):783-90.

Gierer A, Berking S, Bode H, David CN, Flick K, Hansmann G, Schaller H, Trenkner E., Regeneration of hydra from reaggregated cells.
Nat New Biol. 1972 Sep 27;239(91):98-101.

Goetsch SC, Hawke TJ, Gallardo TD, Richardson JA, Garry DJ., Transcriptional profiling and regulation of the extracellular matrix during muscle regeneration.
Physiol Genomics. 2003 Aug 15;14(3):261-71.

Gontier Y, Taivainen A, Fontao L, Sonnenberg A, van der Flier A, Carpen O, Faulkner G, Borradori L., The Z-disc proteins myotilin and FATZ-1 interact with each other and are connected to the sarcolemma via muscle-specific filamins.
J Cell Sci. 2005 Aug 15;118(Pt 16):3739-49. Epub 2005 Aug 2.

Guo S, Kemphues KJ., par-1, a gene required for establishing polarity in C. elegans embryos, encodes a putative Ser/Thr kinase that is asymmetrically distributed.
Cell. 1995 May 19;81(4):611-20.

Gussoni E, Soneoka Y, Strickland CD, Buzney EA, Khan MK, Flint AF, Kunkel LM, Mulligan RC., Dystrophin expression in the mdx mouse restored by stem cell transplantation.
Nature. 1999 Sep 23;401(6751):390-4.

Gros J, Manceau M, Thome V, Marcelle C., A common somitic origin for embryonic muscle progenitors and satellite cells.
Nature. 2005 Jun 16;435(7044):954-8. Epub 2005 Apr 20.

Gross MK, Moran-Rivard L, Velasquez T, Nakatsu MN, Jagla K, Goulding M., Lbx1 is required for muscle precursor migration along a lateral pathway into the limb.
Development. 2000 Jan;127(2):413-24.

Grounds, M.D., K.L. Garrett, M.C. Lai, W.E. Wright and M.W. Beilharz, Identification of muscle precursor cells in vivo by use of MyoD1 and myogenin probes. *Cell Tissue Res.* **267** (1992), pp. 99–104.

Halpert J, Eaker D., Amino acid sequence of a presynaptic neurotoxin from the venom of Notechis scutatus scutatus (Australian tiger snake).
J Biol Chem. 1975 Sep 10;250(17):6990-7.

Hammond SM, Bernstein E, Beach D, Hannon GJ., An RNA-directed nuclease mediates post-transcriptional gene silencing in Drosophila cells.
Nature. 2000 Mar 16;404(6775):293-6.

Hauser MA, Horrigan SK, Salmikangas P, Torian UM, Viles KD, Dancel R, Tim RW, Taivainen A, Bartoloni L, Gilchrist JM, Stajich JM, Gaskell PC, Gilbert JR, Vance JM, Pericak-Vance MA, Carpen O, Westbrook CA, Speer MC., Myotilin is mutated in limb girdle muscular dystrophy 1A.
Hum Mol Genet. 2000 Sep 1;9(14):2141-7.

Hara T, Ishida H, Raziuddin R, Dorkhom S, Kamijo K, Miki T., Novel kelch-like protein, KLEIP, is involved in actin assembly at cell-cell contact sites of Madin-Darby canine kidney cells.
Mol Biol Cell. 2004 Mar;15(3):1172-84.

Harris JB, Karlsson E, Thesleff S., Effects of an isolated toxin from Australian tiger snake (Notechis scutatus scutatus) venom at the mammalian neuromuscular junction.
Br J Pharmacol. 1973 Jan;47(1):141-6.

Hawke TJ, Garry DJ., Myogenic satellite cells: physiology to molecular biology.
J Appl Physiol. 2001 Aug;91(2):534-51.

Heslop L, Morgan JE, Partridge TA., Evidence for a myogenic stem cell that is exhausted in dystrophic muscle.
J Cell Sci. 2000 Jun;113 (Pt 12):2299-308.

Hock RS, Davis G, Speicher DW., Purification of human smooth muscle filamin and characterization of structural domains and functional sites.
Biochemistry. 1990 Oct 9;29(40):9441-51.

Hodges SJ, Agbaji AS, Harvey AL, Hider RC., Cobra cardiotoxins. Purification, effects on skeletal muscle and structure/activity relationships [published errtum appears in Eur J Biochem 1988 Feb 1;171(3):727]
Eur J Biochem. 1987 Jun 1;165(2):373-83.

Horlein AJ, Naar AM, Heinzel T, Torchia J, Gloss B, Kurokawa R, Ryan A, Kamei Y, Soderstrom M, Glass CK, et al., Ligand-independent repression by the thyroid hormone receptor

mediated by a nuclear receptor co-repressor.
Nature. 1995 Oct 5;377(6548):397-404.

Horsley V, Jansen KM, Mills ST, Pavlath GK., IL-4 acts as a myoblast recruitment factor during mammalian muscle growth.
Cell. 2003 May 16;113(4):483-94.

Houzelstein D, Auda-Boucher G, Cheraud Y, Rouaud T, Blanc I, Tajbakhsh S, Buckingham ME, Fontaine-Perus J, Robert B., The homeobox gene Msx1 is expressed in a subset of somites, and in muscle progenitor cells migrating into the forelimb.
Development. 1999 Jun;126(12):2689-701.

Houzelstein D, Cohen A, Buckingham ME, Robert B.,Insertional mutation of the mouse Msx1 homeobox gene by an nlacZ reporter gene.
Mech Dev. 1997 Jul;65(1-2):123-33.

Iten LE, Bryant SV., Stages of tail regeneration in the adult newt, Notophthalmus viridescens.
J Exp Zool. 1976 Jun;196(3):283-92.

Itoh K, Chiba T, Takahashi S, Ishii T, Igarashi K, Katoh Y, Oyake T, Hayashi N, Satoh K, Hatayama I, Yamamoto M, Nabeshima Y., An Nrf2/small Maf heterodimer mediates the induction of phase II detoxifying enzyme genes through antioxidant response elements.
Biochem Biophys Res Commun. 1997 Jul 18;236(2):313-22.

Itoh K, Wakabayashi N, Katoh Y, Ishii T, Igarashi K, Engel JD, Yamamoto M., Keap1 represses nuclear activation of antioxidant responsive elements by Nrf2 through binding to the amino-terminal Neh2 domain.
Genes Dev. 1999 Jan 1;13(1):76-86

Itoh K, Wakabayashi N, Katoh Y, Ishii T, O'Connor T, Yamamoto M., Keap1 regulates both cytoplasmic-nuclear shuttling and degradation of Nrf2 in response to electrophiles.
Genes Cells. 2003 Apr;8(4):379-91..

Jackson TA, Richer JK, Bain DL, Takimoto GS, Tung L, Horwitz KB., The partial agonist activity of antagonist-occupied steroid receptors is controlled by a novel hinge domain-binding coactivator L7/SPA and the corepressors N-CoR or SMRT.
Mol Endocrinol. 1997 Jun;11(6):693-705.

Jarvinen M, Sorvari T., Healing of a crush injury in rat striated muscle. 1. Description and testing of a new method of inducing a standard injury to the calf muscles.
Acta Pathol Microbiol Scand [A]. 1975 Mar;83(2):259-65.

Jiang S, Avraham HK, Park SY, Kim TA, Bu X, Seng S, Avraham S., Process elongation of oligodendrocytes is promoted by the Kelch-related actin-binding protein Mayven.
J Neurochem. 2005 Mar;92(5):1191-203.

Jones DS, Nemoto F, Kuchino Y, Masuda M, Yoshikura H, Nishimura S., The effect of specific mutations at and around the gag-pol gene junction of Moloney murine leukaemia virus.
Nucleic Acids Res. 1989 Aug 11;17(15):5933-45.

Jostes B, Walther C, Gruss P., The murine paired box gene, Pax7, is expressed specifically during the development of the nervous and muscular system.
Mech Dev. 1990 Dec;33(1):27-37.

Kablar B, Krastel K, Ying C, Asakura A, Tapscott SJ, Rudnicki MA., MyoD and Myf-5 differentially regulate the development of limb versus trunk skeletal muscle.
Development. 1997 Dec;124(23):4729-38.

Kablar B, Krastel K, Ying C, Tapscott SJ, Goldhamer DJ, Rudnicki MA., Myogenic determination occurs independently in somites and limb buds.
Dev Biol. 1999 Feb 15;206(2):219-31.

Kalderon D, Richardson WD, Markham AF, Smith AE., Sequence requirements for nuclear location of simian virus 40 large-T antigen.
Nature. 1984 Sep 6-11;311(5981):33-8.

Karlsson E, Eaker D, Ryden L., Purification of a presynaptic neurotoxin from the venom of the australian tiger snake Notechis scutatus scutatus.
Toxicon. 1972 Jun;10(4):405-13.

Khvorova A, Reynolds A, Jayasena SD., Functional siRNAs and miRNAs exhibit strand bias.
Cell. 2003 Oct 17;115(2):209-16.

Kim IF, Mohammadi E, Huang RC., Isolation and characterization of lPP, a novel human gene encoding an actin-binding, kelch-like protein.
Gene. 1999 Mar 4;228(1-2):73-83.

Kobayashi A, Kang MI, Okawa H, Ohtsuji M, Zenke Y, Chiba T, Igarashi K, Yamamoto M., Oxidative stress sensor Keap1 functions as an adaptor for Cul3-based E3 ligase to regulate proteasomal degradation of Nrf2.
Mol Cell Biol. 2004 Aug;24(16):7130-9.

Kumar TK, Jayaraman G, Lee CS, Arunkumar AI, Sivaraman T, Samuel D, Yu C., Snake venom cardiotoxins-structure, dynamics, function and folding.
J Biomol Struct Dyn. 1997 Dec;15(3):431-63.

LaBarge MA, Blau HM., Biological progression from adult bone marrow to mononucleate muscle stem cell to multinucleate muscle fiber in response to injury.
Cell. 2002 Nov 15;111(4):589-601.

Lassar AB, Davis RL, Wright WE, Kadesch T, Murre C, Voronova A, Baltimore D, Weintraub H., Functional activity of myogenic HLH proteins requires hetero-oligomerization with

E12/E47-like proteins in vivo.
Cell. 1991 Jul 26;66(2):305-15.

Lazebnik YA, Cole S, Cooke CA, Nelson WG, Earnshaw WC., Nuclear events of apoptosis in vitro in cell-free mitotic extracts: a model system for analysis of the active phase of apoptosis.
J Cell Biol. 1993 Oct;123(1):7-22.

Lee CC, Craigen WJ, Muzny DM, Harlow E, Caskey CT., Cloning and expression of a mammalian peptide chain release factor with sequence similarity to tryptophanyl-tRNA synthetases.
Proc Natl Acad Sci U S A. 1990 May;87(9):3508-12.

Li X, Zhang D, Hannink M, Beamer LJ., Crystal structure of the Kelch domain of human Keap1.
J Biol Chem. 2004 Dec 24;279(52):54750-8.

Lo DC, Allen F, Brockes JP., Reversal of muscle differentiation during urodele limb regeneration.
Proc Natl Acad Sci U S A. 1993 Aug 1;90(15):7230-4.

Lu S, Carroll SL, Herrera AH, Ozanne B, Horowits R., New N-RAP-binding partners alpha-actinin, filamin and Krp1 detected by yeast two-hybrid screening: implications for myofibril assembly.
J Cell Sci. 2003 Jun 1;116(Pt 11):2169-78.

Luo G, Herrera AH, Horowits R., Molecular interactions of N-RAP, a nebulin-related protein of striated muscle myotendon junctions and intercalated disks.
Biochemistry. 1999 May 11;38(19):6135-43.

Mangelsdorf DJ, Thummel C, Beato M, Herrlich P, Schutz G, Umesono K, Blumberg B, Kastner P, Mark M, Chambon P, Evans RM., The nuclear receptor superfamily: the second decade.
Cell. 1995 Dec 15;83(6):835-9.

Mansouri A, Stoykova A, Torres M, Gruss P., Dysgenesis of cephalic neural crest derivatives in Pax7-/- mutant mice.
Development. 1996 Mar;122(3):831-8.

Mao Z, Wiedmann M., Calcineurin enhances MEF2 DNA binding activity in calcium-dependent survival of cerebellar granule neurons.
J Biol Chem. 1999 Oct 22;274(43):31102-7.

Matranga C, Tomari Y, Shin C, Bartel DP, Zamore PD.,Passenger-strand cleavage facilitates assembly of siRNA into Ago2-containing RNAi enzyme complexes.
Cell. 2005 Nov 18;123(4):607-20.

MAURO A., Satellite cell of skeletal muscle fibers.
J Biophys Biochem Cytol. 1961 Feb;9:493-5.

Martin CM, Meeson AP, Robertson SM, Hawke TJ, Richardson JA, Bates S, Goetsch SC, Gallardo TD, Garry DJ., Persistent expression of the ATP-binding cassette transporter, Abcg2, identifies cardiac SP cells in the developing and adult heart.
Dev Biol. 2004 Jan 1;265(1):262-75.

Martin P., Wound healing--aiming for perfect skin regeneration.
Science. 1997 Apr 4;276(5309):75-81.

Martinez J, Patkaniowska A, Urlaub H, Luhrmann R, Tuschl T., Single-stranded antisense siRNAs guide target RNA cleavage in RNAi.
Cell. 2002 Sep 6;110(5):563-74.

McCullagh KJ, Calabria E, Pallafacchina G, Ciciliot S, Serrano AL, Argentini C, Kalhovde JM, Lomo T, Schiaffino S., NFAT is a nerve activity sensor in skeletal muscle and controls activity-dependent myosin switching.
Proc Natl Acad Sci U S A. 2004 Jul 20;101(29):10590-5.

McMahon M, Thomas N, Itoh K, Yamamoto M, Hayes JD., Redox-regulated turnover of Nrf2 is determined by at least two separate protein domains, the redox-sensitive Neh2 degron and the redox-insensitive Neh6 degron.
J Biol Chem. 2004 Jul 23;279(30):31556-67.

Megeney LA, Kablar B, Garrett K, Anderson JE, Rudnicki MA., MyoD is required for myogenic stem cell function in adult skeletal muscle.
Genes Dev. 1996 May 15;10(10):1173-83.

Megeney LA, Kablar B, Perry RL, Ying C, May L, Rudnicki MA., Severe cardiomyopathy in mice lacking dystrophin and MyoD.
Proc Natl Acad Sci U S A. 1999 Jan 5;96(1):220-5.

Michel RN, Dunn SE, Chin ER., Calcineurin and skeletal muscle growth.
Proc Nutr Soc. 2004 May;63(2):341-9.

Morrison JI, Loof S, He P, Simon A., Salamander limb regeneration involves the activation of a multipotent skeletal muscle satellite cell population.
J Cell Biol. 2006 Jan 30;172(3):433-40.

Muir AR, Kanji AH, Allbrook D. The structure of the satellite cells in skeletal muscle.
J Anat. 1965 Jul;99(Pt 3):435-44.

Musaro A, Rosenthal N., Maturation of the myogenic program is induced by postmitotic expression of insulin-like growth factor I.
Mol Cell Biol. 1999 Apr;19(4):3115-24.

Musaro A, McCullagh KJ, Naya FJ, Olson EN, Rosenthal N., IGF-1 induces skeletal myocyte hypertrophy through calcineurin in association with GATA-2 and NF-ATc1.
Nature. 1999 Aug 5;400(6744):581-5.

Musaro A, McCullagh K, Paul A, Houghton L, Dobrowolny G, Molinaro M, Barton ER, Sweeney HL, Rosenthal N., Localized Igf-1 transgene expression sustains hypertrophy and

regeneration in senescent skeletal muscle.
Nat Genet. 2001 Feb;27(2):195-200.

Nagata S., Apoptotic DNA fragmentation.
Exp Cell Res. 2000 Apr 10;256(1):12-8.

Neuhaus P, Jaschinsky B, Schneider S, Neuhaus H, Wolter A, Ebelt H, Braun T., Overexpression of Kelch domain containing-2 (mKlhdc2) inhibits differentiation and directed migration of C2C12 myoblasts.
Exp Cell Res. 2006 Oct 1;312(16):3049-59.

Nicolas N, Gallien CL, Chanoine C., Analysis of MyoD, myogenin, and muscle-specific gene mRNAs in regenerating Xenopus skeletal muscle.
Dev Dyn. 1996 Sep;207(1):60-8.

Oustanina S, Hause G, Braun T., Pax7 directs postnatal renewal and propagation of myogenic satellite cells but not their specification.
EMBO J. 2004 Aug 18;23(16):3430-9.

Padmanabhan B, Scharlock M, Tong KI, Nakamura Y, Kang MI, Kobayashi A, Matsumoto T, Tanaka A, Yamamoto M, Yokoyama S., Purification, crystallization and preliminary X-ray diffraction analysis of the Kelch-like motif region of mouse Keap1.
Acta Crystallograph Sect F Struct Biol Cryst Commun. 2005 Jan 1;61(Pt 1):153-5

Paine PL, Moore LC, Horowitz SB., Nuclear envelope permeability.
Nature. 1975 Mar 13;254(5496):109-14.

Parsons SA, Wilkins BJ, Bueno OF, Molkentin JD., Altered skeletal muscle phenotypes in calcineurin Aalpha and Abeta gene-targeted mice.
Mol Cell Biol. 2003 Jun;23(12):4331-43.

Perez-Torrado R, Yamada D, Defossez PA., Born to bind: the BTB protein-protein interaction domain.
Bioessays. 2006 Dec;28(12):1194-202.

Peters R., Nuclear envelope permeability measured by fluorescence microphotolysis of single liver cell nuclei.
J Biol Chem. 1983 Oct 10;258(19):11427-9.

Pfaff M, Liu S, Erle DJ, Ginsberg MH., Integrin beta cytoplasmic domains differentially bind to cytoskeletal proteins.
J Biol Chem. 1998 Mar 13;273(11):6104-9.

Pintard L, Willis JH, Willems A, Johnson JL, Srayko M, Kurz T, Glaser S, Mains PE, Tyers M, Bowerman B, Peter M., The BTB protein MEL-26 is a substrate-specific adaptor of the CUL-3 ubiquitin-ligase.
Nature. 2003 Sep 18;425(6955):311-6.

Provost P, Silverstein RA, Dishart D, Walfridsson J, Djupedal I, Kniola B, Wright A, Samuelsson B, Radmark O, Ekwall K., Dicer is required for chromosome segregation and gene

silencing in fission yeast cells.
Proc Natl Acad Sci U S A. 2002 Dec 24;99(26):16648-53.

Provost P, Dishart D, Doucet J, Frendewey D, Samuelsson B, Radmark O., Ribonuclease activity and RNA binding of recombinant human Dicer.
EMBO J. 2002 Nov 1;21(21):5864-74.

Rand TA, Ginalski K, Grishin NV, Wang X., Biochemical identification of Argonaute 2 as the sole protein required for RNA-induced silencing complex activity.
Proc Natl Acad Sci U S A. 2004 Oct 5;101(40):14385-9.

Rand TA, Petersen S, Du F, Wang X., Argonaute2 cleaves the anti-guide strand of siRNA during RISC activation.
Cell. 2005 Nov 18;123(4):621-9.

Reddi AH, Role of morphogenetic proteins in skeletal tissue engineering and regeneration.
Nat Biotechnol. 1998 Mar;16(3):247-52.

Relaix F, Rocancourt D, Mansouri A, Buckingham M., Divergent functions of murine Pax3 and Pax7 in limb muscle development.
Genes Dev. 2004 May 1;18(9):1088-105.

Reynolds A, Leake D, Boese Q, Scaringe S, Marshall WS, Khvorova A., Rational siRNA design for RNA interference.
Nat Biotechnol. 2004 Mar;22(3):326-30.

Robinson DN, Smith-Leiker TA, Sokol NS, Hudson AM, Cooley L., Formation of the Drosophila ovarian ring canal inner rim depends on cheerio.
Genetics. 1997 Apr;145(4):1063-72.

Rudnicki MA, Braun T, Hinuma S, Jaenisch R., Inactivation of MyoD in mice leads to up-regulation of the myogenic HLH gene Myf-5 and results in apparently normal muscle development.
Cell. 1992 Oct 30;71(3):383-90.

Rudnicki MA, Schnegelsberg PN, Stead RH, Braun T, Arnold HH, Jaenisch R., MyoD or Myf-5 is required for the formation of skeletal muscle.
Cell. 1993 Dec 31;75(7):1351-9.

Serrano AL, Murgia M, Pallafacchina G, Calabria E, Coniglio P, Lomo T, Schiaffino S., Calcineurin controls nerve activity-dependent specification of slow skeletal muscle fibers but not muscle growth.
Proc Natl Acad Sci U S A. 2001 Nov 6;98(23):13108-13.

Salmikangas P, Mykkanen OM, Gronholm M, Heiska L, Kere J, Carpen O., Myotilin, a novel sarcomeric protein with two Ig-like domains, is encoded by a candidate gene for limb-girdle muscular dystrophy.
Hum Mol Genet. 1999 Jul;8(7):1329-36.

Sanders MC, Way M, Sakai J, Matsudaira P., Characterization of the actin cross-linking properties of the scruin-calmodulin complex from the acrosomal process of Limulus sperm.
J Biol Chem. 1996 Feb 2;271(5):2651-7.

Sanes JR, Marshall LM, McMahan UJ., Reinnervation of muscle fiber basal lamina after removal of myofibers. Differentiation of regenerating axons at original synaptic sites.
J Cell Biol. 1978 Jul;78(1):176-98.

Satokata I, Maas R., Msx1 deficient mice exhibit cleft palate and abnormalities of craniofacial and tooth development.
Nat Genet. 1994 Apr;6(4):348-56.

Schafer BW, Czerny T, Bernasconi M, Genini M, Busslinger M., Molecular cloning and characterization of a human PAX-7 cDNA expressed in normal and neoplastic myocytes.
Nucleic Acids Res. 1994 Nov 11;22(22):4574-82

Schafer K, Braun T., Early specification of limb muscle precursor cells by the homeobox gene Lbx1h.
Nat Genet. 1999 Oct;23(2):213-6.

Schafer K, Braun T., Early specification of limb muscle precursor cells by the homeobox gene Lbx1h.
Nat Genet. 1999 Oct;23(2):213-6.

Schierbeek A,. The collected letters of Antoni van Leeuwenhoek; an appeal to the scientific world.Antonie Van Leeuwenhoek. 1953;19(3):181-8

Schmid MF, Agris JM, Jakana J, Matsudaira P, Chiu W., Three-dimensional structure of a single filament in the Limulus acrosomal bundle: scruin binds to homologous helix-loop-beta motifs in actin.
J Cell Biol. 1994 Feb;124(3):341-50.

Schneider JW, Gu W, Zhu L, Mahdavi V, Nadal-Ginard B., Reversal of terminal differentiation mediated by p107 in Rb-/- muscle cells.
Science. 1994 Jun 3;264(5164):1467-71.

Schon A, Bock A, Ott G, Sprinzl M, Soll D., The selenocysteine-inserting opal suppressor serine tRNA from E. coli is highly unusual in structure and modification.
Nucleic Acids Res. 1989 Sep 25;17(18):7159-65.

Schupbach T, Wieschaus E., Female sterile mutations on the second chromosome of Drosophila melanogaster. I. Maternal effect mutations.
Genetics. 1989 Jan;121(1):101-17.

Seale P, Sabourin LA, Girgis-Gabardo A, Mansouri A, Gruss P, Rudnicki MA., Pax7 is required for the specification of myogenic satellite cells.
Cell. 2000 Sep 15;102(6):777-86.

Shelton JM, Lee MH, Richardson JA, Patel SB., Microsomal triglyceride transfer protein expression during mouse development.
J Lipid Res. 2000 Apr;41(4):532-7.

Shen C, Buck AK, Liu X, Winkler M, Reske SN., Gene silencing by adenovirus-delivered siRNA.
FEBS Lett. 2003 Mar 27;539(1-3):111-4.

Sherwood RI, Christensen JL, Weissman IL, Wagers AJ., Determinants of skeletal muscle contributions from circulating cells, bone marrow cells, and hematopoietic stem cells.
Stem Cells. 2004;22(7):1292-304.

Sherwood RI, Christensen JL, Conboy IM, Conboy MJ, Rando TA, Weissman IL, Wagers AJ., Isolation of adult mouse myogenic progenitors: functional heterogeneity of cells within and engrafting skeletal muscle.
Cell. 2004 Nov 12;119(4):543-54.

Snow MH., Myogenic cell formation in regenerating rat skeletal muscle injured by mincing. I. A fine structural study.
Anat Rec. 1977 Jun;188(2):181-99.

Snow MH., Myogenic cell formation in regenerating rat skeletal muscle injured by mincing. II. An autoradiographic study.
Anat Rec. 1977 Jun;188(2):201-17.

Soltysik-Espanola M, Rogers RA, Jiang S, Kim TA, Gaedigk R, White RA, Avraham H, Avraham S.. Characterization of Mayven, a novel actin-binding protein predominantly expressed in brain.
Mol Biol Cell. 1999 Jul;10(7):2361-75.

Song K, Wang Y, Sassoon D., Expression of Hox-7.1 in myoblasts inhibits terminal differentiation and induces cell transformation.
Nature. 1992 Dec 3;360(6403):477-81.

Spence HJ, Johnston I, Ewart K, Buchanan SJ, Fitzgerald U, Ozanne BW., Krp1, a novel kelch related protein that is involved in pseudopod elongation in transformed cells.
Oncogene. 2000 Mar 2;19(10):1266-76.

Steinbacher S, Hof P, Eichinger L, Schleicher M, Gettemans J, Vandekerckhove J, Huber R, Benz J., The crystal structure of the Physarum polycephalum actin-fragmin kinase: an atypical protein kinase with a specialized substrate-binding domain.
EMBO J. 1999 Jun 1;18(11):2923-9.

Stogios PJ, Prive GG., The BACK domain in BTB-kelch proteins.
Trends Biochem Sci. 2004 Dec;29(12):634-7.

Strauss EG, Rice CM, Strauss JH., Sequence coding for the alphavirus nonstructural proteins is interrupted by an opal termination codon.
Proc Natl Acad Sci U S A. 1983 Sep;80(17):5271-5.

Suzuki M, Sunaga N, Shames DS, Toyooka S, Gazdar AF, Minna JD., RNA interference-mediated knockdown of DNA methyltransferase 1 leads to promoter demethylation and gene re-expression in human lung and breast cancer cells.
Cancer Res. 2004 May 1;64(9):3137-43.

Tajbakhsh S, Buckingham ME., Mouse limb muscle is determined in the absence of the earliest myogenic factor myf-5.
Proc Natl Acad Sci U S A. 1994 Jan 18;91(2):747-51.

Takada F, Vander Woude DL, Tong HQ, Thompson TG, Watkins SC, Kunkel LM, Beggs AH., Myozenin: an alpha-actinin- and gamma-filamin-binding protein of skeletal muscle Z lines.
Proc Natl Acad Sci U S A. 2001 Feb 13;98(4):1595-600. Epub 2001 Feb 6.

Takafuta T, Wu G, Murphy GF, Shapiro SS., Human beta-filamin is a new protein that interacts with the cytoplasmic tail of glycoprotein Ibalpha.
J Biol Chem. 1998 Jul 10;273(28):17531-8.

Tanaka EM, Brockes JP., A target of thrombin activation promotes cell cycle re-entry by urodele muscle cells.
Wound Repair Regen. 1998 Jul-Aug;6(4):371-81.

Tapscott SJ, Davis RL, Thayer MJ, Cheng PF, Weintraub H, Lassar AB., MyoD1: a nuclear phosphoprotein requiring a Myc homology region to convert fibroblasts to myoblasts.
Science. 1988 Oct 21;242(4877):405-11.

Thompson TG, Chan YM, Hack AA, Brosius M, Rajala M, Lidov HG, McNally EM, Watkins S, Kunkel LM., Filamin 2 (FLN2): A muscle-specific sarcoglycan interacting protein.
J Cell Biol. 2000 Jan 10;148(1):115-26.

Thornton CS., Limb regeneration and survival of prolactin treated hypophysectomized adult newts.
J Morphol. 1968 Nov;126(3):365-71.

T'Jampens D, Devriendt L, De Corte V, Vandekerckhove J, Gettemans J., Selected BTB/POZ-kelch proteins bind ATP.
FEBS Lett. 2002 Apr 10;516(1-3):20-6.

Tong KI, Katoh Y, Kusunoki H, Itoh K, Tanaka T, Yamamoto M., Keap1 recruits Neh2 through binding to ETGE and DLG motifs: characterization of the two-site molecular recognition model.
Mol Cell Biol. 2006 Apr;26(8):2887-900.

van den Bosch H, Postema NM, de Haas GH, van Deenen LL., On the positional specificity of phospholipase A from pancreas.
Biochim Biophys Acta. 1965 Jun 1;98(3):657-9.

van der Ven PF, Wiesner S, Salmikangas P, Auerbach D, Himmel M, Kempa S, Hayess K, Pacholsky D, Taivainen A, Schroder R, Carpen O, Furst DO., Indications for a novel muscular dystrophy pathway. gamma-filamin, the muscle-specific filamin isoform, interacts with myotilin.
J Cell Biol. 2000 Oct 16;151(2):235-48.

van der Ven PF, Obermann WM, Lemke B, Gautel M, Weber K, Furst DO., Characterization of muscle filamin isoforms suggests a possible role of gamma-filamin/ABP-L in sarcomeric Z-disc formation.
Cell Motil Cytoskeleton. 2000 Feb;45(2):149-62.

Vracko R, Benditt EP., Basal lamina: the scaffold for orderly cell replacement. Observations on regeneration of injured skeletal muscle fibers and capillaries.
J Cell Biol. 1972 Nov;55(2):406-19.

Waite M, van Deenen LL., Hydrolysis of phospholipids and glycerides by rat-liver preparations.
Biochim Biophys Acta. 1967 Jun 6;137(3):498-517.

Wakabayashi N, Itoh K, Wakabayashi J, Motohashi H, Noda S, Takahashi S, Imakado S, Kotsuji T, Otsuka F, Roop DR, Harada T, Engel JD, Yamamoto M., Keap1-null mutation leads to postnatal lethality due to constitutive Nrf2 activation.
Nat Genet. 2003 Nov;35(3):238-45.

Wakabayashi N, Dinkova-Kostova AT, Holtzclaw WD, Kang MI, Kobayashi A, Yamamoto M, Kensler TW, Talalay P., Protection against electrophile and oxidant stress by induction of the phase 2 response: fate of cysteines of the Keap1 sensor modified by inducers.
Proc Natl Acad Sci U S A. 2004 Feb 17;101(7):2040-5

Warn RM, Gutzeit HO, Smith L, Warn A., F-actin rings are associated with the ring canals of the Drosophila egg chamber.
Exp Cell Res. 1985 Apr;157(2):355-63.

Weiner AM, Weber K., A single UGA codon functions as a natural termination signal in the coliphage q beta coat protein cistron.
J Mol Biol. 1973 Nov 15;80(4):837-55

Weintraub H, Tapscott SJ, Davis RL, Thayer MJ, Adam MA, Lassar AB, Miller AD., Activation of muscle-specific genes in pigment, nerve, fat, liver, and fibroblast cell lines by forced expression of MyoD.
Proc Natl Acad Sci U S A. 1989 Jul;86(14):5434-8.

Williams SK, Spence HJ, Rodgers RR, Ozanne BW, Fitzgerald U, Barnett SC., Role of Mayven, a kelch-related protein in oligodendrocyte process formation.
J Neurosci Res. 2005 Sep 1;81(5):622-31

Woloshin P, Song K, Degnin C, Killary AM, Goldhamer DJ, Sassoon D, Thayer MJ., inhibits myoD expression in fibroblast x 10T1/2 cell hybrids.
Cell. 1995 Aug 25;82(4):611-20.

Wolpert L, Hicklin J, Hornbruch A.,Positional information and pattern regulation in regeneration of hydra.
Symp Soc Exp Biol. 1971;25:391-415.

Wu YL, Gong Z., A novel zebrafish kelchlike gene klhl and its human ortholog KLHL display conserved expression patterns in skeletal and cardiac muscles.
Gene. 2004 Aug 18;338(1):75-83.

Xia H, Mao Q, Paulson HL, Davidson BL., siRNA-mediated gene silencing in vitro and in vivo.
Nat Biotechnol. 2002 Oct;20(10):1006-10.

Xu L, Wei Y, Reboul J, Vaglio P, Shin TH, Vidal M, Elledge SJ, Harper JW., BTB proteins are substrate-specific adaptors in an SCF-like modular ubiquitin ligase containing CUL-3.
Nature. 2003 Sep 18;425(6955):316-21.

Xue F, Cooley L., Kelch encodes a component of intercellular bridges in Drosophila egg chambers.
Cell. 1993 Mar 12;72(5):681-93.

Yoshida K., Identification and characterization of a novel kelch-like gene KLHL15 in silico.
Oncol Rep. 2005 Jun;13(6):1133-7.

Zheng N, Schulman BA, Song L, Miller JJ, Jeffrey PD, Wang P, Chu C, Koepp DM, Elledge SJ, Pagano M, Conaway RC, Conaway JW, Harper JW, Pavletich NP., Structure of the Cul1-Rbx1-Skp1-F boxSkp2 SCF ubiquitin ligase complex.
Nature. 2002 Apr 18;416(6882):703-9.

Zhang DD, Hannink M., Distinct cysteine residues in Keap1 are required for Keap1-dependent ubiquitination of Nrf2 and for stabilization of Nrf2 by chemopreventive agents and oxidative stress.
Mol Cell Biol. 2003 Nov;23(22):8137-51.

Zhang DD, Lo SC, Cross JV, Templeton DJ, Hannink M., Keap1 is a redox-regulated substrate adaptor protein for a Cul3-dependent ubiquitin ligase complex.
Mol Cell Biol. 2004 Dec;24(24):10941-53.

Zhang DD, Lo SC, Sun Z, Habib GM, Lieberman MW, Hannink M., Ubiquitination of Keap1, a BTB-Kelch substrate adaptor protein for Cul3, targets Keap1 for degradation by a proteasome-independent pathway.
J Biol Chem. 2005 Aug 26;280(34):30091-9.